



**THE MECHANISM AND KINETICS OF 2-t-BUTYLANTHRAQUINONE
REDUCTION BY HYDROGEN SULFIDE IN NON-AQUEOUS SOLVENTS**

**ARTHUR LAKES LIBRARY
COLORADO SCHOOL OF MINES
GOLDEN, CO 80401**

by

Elsa A. Krisanti

ProQuest Number: 10796536

All rights reserved

INFORMATION TO ALL USERS

The quality of this reproduction is dependent upon the quality of the copy submitted.

In the unlikely event that the author did not send a complete manuscript and there are missing pages, these will be noted. Also, if material had to be removed, a note will indicate the deletion.



ProQuest 10796536

Published by ProQuest LLC (2019). Copyright of the Dissertation is held by the Author.

All rights reserved.

This work is protected against unauthorized copying under Title 17, United States Code
Microform Edition © ProQuest LLC.

ProQuest LLC.
789 East Eisenhower Parkway
P.O. Box 1346
Ann Arbor, MI 48106 – 1346

T-4308

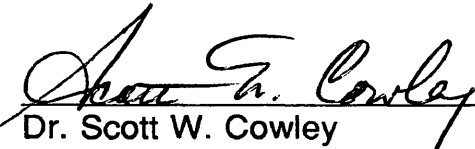
A thesis submitted to the Faculty and the Board of Trustees of the Colorado School of Mines in partial fulfillment of the requirements for the degree of Doctor of Philosophy (Applied Chemistry).

Golden, Colorado

Date December 23, 1992

Signed: 


Elsa A. Krisanti

Approved: 

Dr. Scott W. Cowley
Thesis Advisor

Golden, Colorado

Date Jan. 8, 1993



Dr. Steven R. Daniel
Department Head and Professor
Applied Chemistry

ABSTRACT

The conversion of hydrogen sulfide into elemental sulfur and hydrogen has been developed in the HYSULFSM process¹. This process has advantages not found in other processes used today. In this process, the valuable hydrogen will be recovered, corrosion problems can be prevented, and the operating conditions are mild.

There are two stages in the HYSULFSM process. In the first stage, hydrogen sulfide is oxidized by a quinone type molecule to form elemental sulfur, and in the second stage the hydrogen is produced by oxidizing the hydroquinone molecule back to quinone. To optimize and commercialize the process, the rate of quinone conversion and sulfur polymerization should be increased. The problems in the first stage should be solved if the fundamental chemistry of this process is known. Unfortunately, the reaction mechanisms in the first stage are still unknown. However, some experiments have produced useful information about these mechanisms.

Experiments have been conducted to investigate the effects of H₂S pressure, reaction temperature and solvent on the kinetic data of quinone

¹ SM = Service Mark of Marathon Oil Company

conversion and sulfur polymerization. Electron and proton transfer during the reaction in the first stage was investigated by a voltammetric technique. To obtain further information about the reaction mechanisms, the intermediate species and the charge transfer complex formation were also investigated.

The experimental data shows that quinone reduction is initiated by a one-electron transfer, but this electron transfer is affected by several variables. The overall reaction mechanisms, including quinone reduction and sulfur polymerization, are complicated.

TABLE OF CONTENTS

ABSTRACT	iii
ACKNOWLEDGMENTS	viii
Chapter 1	INTRODUCTION	1
Chapter 2	PROBLEM STATEMENT	4
Chapter 3	BACKGROUND	6
3.1	H ₂ S Conversion Methods Used Today	6
3.2	The Dry Oxidation Processes	7
3.2.1	The Iron Oxide Process	7
3.2.2	The Claus Process	9
3.3	The Liquid Oxidation Processes	10
3.3.1	The Stretford™ Process	11
3.4	The HYSULF SM Process	12
3.5	Quinone Chemistry	13
3.5.1	Quinones in Non-aqueous Solvents	17
3.5.2	Quinones in Aqueous Solvents	22
3.6	Sulfanes	23
3.6.1	Sulfanes Preparation from Aqueous Polysulfide Solutions	23
3.6.2	Polysulfane Preparation from Anhydrous Polysulfides	25
3.6.3	Polysulfane Preparation by Cathodic Reduction of SO ₂	26
3.6.4	Polysulfane Preparation via Condensation Reactions	26
3.6.5	Chemistry of Sulfanes	27
3.6.6	Hydrogen Sulfide	30
Chapter 4	EXPERIMENTAL	32
4.1	Solvents	32
4.2	Solubility of TBAQ	32
4.3	Reaction Mixture Preparation	34
4.4	Sulfur Recovery Technique	34

4.5	Mini and Microreactors	35
4.6	NMR Tube Reactor	36
4.7	Analytical Methods	40
4.7.1	Nuclear Magnetic Resonance	41
4.7.2	Ultraviolet-Visible Spectroscopy	42
4.7.3	Cyclic Voltammetry	43
Chapter 5	RESULT AND DISCUSSION	47
5.1	NMR Analysis	47
5.1.1	The Effect of H ₂ S Pressure on TBAQ Conversion	47
5.1.2	The Effect of H ₂ S Pressure on the TBAQ Reduction Rate Constant	53
5.1.3	The Effect of Temperature on TBAQ Conversion	55
5.1.4	The Effect of Temperature on the TBAQ Reduction Rate Constant	55
5.1.5	Reaction Mechanism	57
5.1.6	The Effect of Temperature on Sulfur Formation	62
5.1.7	The Effect of H ₂ S Pressure on Sulfur Formation	65
5.1.8	The Role of Solvent on TBAQ Conversion	65
5.1.9	The Formation of Sulfanes as Intermediate Species in TBAQ Reduction and Sulfur Polymerization	76
5.2	Cyclic Voltammetry	79
5.2.1	Reaction Mechanisms in Cyclic Voltammetry	79
5.2.2	Aprotic Solvent Effect	82
5.2.3	The Effect of Protic Agents: Phenol and Butanol	90
5.2.4	The Effect of Protic Agent: Benzoic Acid	93
5.2.5	In situ Generation of Protonated Intermediates	99
5.2.6	The Effect of the Protic agent : Benzenethiol	105
5.2.7	Correlation of Redox Potentials with HOMO and LUMO Energy Levels	109
5.3	Ultraviolet and Visible Spectroscopy Analysis	116
5.3.1	Ultraviolet Spectra of TBAQ in Various Solvents	116
5.3.2	Identification of Charge Transfer Complex between Bisulfide Anion and Amide Solvents	117
Chapter 6	CONCLUSIONS	120
6.1	Role of Solvents	120
6.2	Overall TBAQ Reduction Kinetics	121
6.3	Overall Sulfur Formation Kinetics	122
6.4	Detailed Reaction Mechanisms	122

Chapter 7	RECOMMENDATIONS	124
7.1	Role of HS ⁻ and Solvents in TBAQ Reduction	124
7.2	Mechanism of Sulfane Formation	125
7.3	Effect of Substituent on TBAQ Reduction Rate	126
	REFERENCES CITED	127
	APPENDIX A Experimental Procedure	A-1
	APPENDIX B NMR Data	B-1
	APPENDIX C Cyclic Voltammetry Data	C-1

Chapter 1

INTRODUCTION

Hydrogen sulfide removal from natural gas or from gases produced by the petroleum industries typically involves air oxidation of hydrogen sulfide into elemental sulfur and water. The Claus process is a common dry oxidation process and yields sulfur in good quantity (*Kohl and Riesenfeld, 1985*). Unfortunately, this process has some limitations :

- a) it requires a high ratio of hydrogen sulfide to carbon dioxide in the feed gas;
- b) it requires precise air flow control;
- c) to reduce emission of sulfur compounds to the atmosphere, it requires the removal of residual sulfur compounds, such as carbonyl sulfide and carbon disulfide, from the Claus plant tail gas;
- d) valuable hydrogen is lost as water

The conversion of hydrogen sulfide into sulfur and water via liquid phase oxidation, such as in the Stretford™ process¹ (*Kohl and Riesenfeld, 1985*), is also common. The limitations of this process are :

¹TM = Trade Mark of North West Gas and Clayton Aniline Company Ltd.

- a) it requires periodic removal of side reaction products, such as thiosulfate, sulfate and thiocyanate, from the oxidant liquid solution;
- b) pollution problems from the disposal of thiocyanate, thiosulfate and sulfate;
- c) contamination by bacterial growth;
- d) plugging problems because of sticky sulfur;
- e) corrosion of carbon steel equipment from use of an aqueous medium;
- f) loss of valuable hydrogen as water.

The direct conversion of hydrogen sulfide into hydrogen and sulfur would reduce the cost of gas purification by yielding an additional valuable product, hydrogen. Unfortunately, the direct conversion of hydrogen sulfide to hydrogen and sulfur normally demands severe reaction conditions. The reaction is endothermic and is thermodynamically unfavorable at temperatures below 1527 °C (1779.8 K). The presence of a catalyst, such as a transition metal sulfide, is required to improve the reaction rate at temperatures below 977 °C (1249.8 K) (*Raymont, 1975*).

Recently the HYSULFSM process was reported to use a less corrosive aprotic medium and mild conditions to recover hydrogen and sulfur from hydrogen sulfide (*Plummer, 1987*). The process has two stages. In the first stage, at a reaction temperature of about 57.2 °C (330.3 K), hydrogen sulfide reacts with a quinone to form the corresponding hydroquinone and solid sulfur. In the second stage, at a

temperature range of 237.8 °C (510.9 K) to 323.9 °C (597 K), the hydroquinone is catalytically dehydrogenated to regenerate the quinone and make hydrogen.

Although the HYSULFSM process looks promising, a better understanding of the fundamental chemistry is required if the process is to be commercialized. Since the reaction mechanisms for the quinone reduction and the sulfur polymerization steps are still unknown, the role of the aprotic organic solvent needs to be better defined. The goals of this study are to improve the rate of quinone reduction and sulfur formation in the first stage. These goals should be achieved by understanding the reaction mechanisms and using this information to choose the optimum quinone and solvent combination, and the best operating conditions.

Chapter 2

PROBLEM STATEMENT

There are still some important questions to be answered before the first stage of the HYSULFSM process can become a viable option. These questions are:

- a) how can the quinone reduction rate be increased ?
- b) how can the sulfur yield be improved ?
- c) what role does the organic solvent play in the reaction rate ?
- d) and what are the reaction mechanisms in the first stage ?

This thesis will address these questions, which concern the first stage of the process. The quinone reduction rate and the sulfur yield can be influenced by variables such as the hydrogen sulfide pressure, the reaction temperature, and the solvent properties. A study of the influence of these variables provides information about the best operating conditions for the first stage of the process. The reaction will be studied in a glass stirred-tank reactor which can be sampled at specified times during the progress of the reaction.

Spectroscopic analysis of the reactants and products by NMR and UV-visible spectroscopy will provide important information about the reaction kinetics. Cyclic voltammetry, NMR and UV-visible spectroscopy will be used to obtain detailed information about the reaction mechanisms by identifying the important

intermediates and charge-transfer complexes involved.

Chapter 3

BACKGROUND

3.1 H₂S Conversion Methods Used Today

There are many methods for removing hydrogen sulfide from sour natural gases and sour crude petroleum. The selection of the gas-treating process is affected by many factors such as the volume of gas to be processed, the temperature, the pressure, the hydrogen sulfide (H₂S) content, the selectivity required, the types of impurities present, the concentration of the impurities, and the air-pollution regulations and specifications required (*West, 1983*).

There are two steps for treating gases in order to remove H₂S. In the first step, the dilute H₂S present in sour gas is absorbed by a solvent involving chemical reactions or physical interactions; examples are the Selexol and the Purisol processes (*Kohl and Riesenfeld, 1985*), and then the concentrated H₂S is recovered from the solvent.

The absorption processes are normally used to remove acid gases from sour gas streams found in the natural gas or petroleum refining industries. Sour gas is any gas stream which contains acid gas components. The ones most common in natural gases are CO₂, H₂S and COS. Alkanolamines are widely used as acid-gas absorbents. The amine and H₂S undergo a chemical reaction to form

a soluble salt ($R_3NH^+ HS^-$). This salt can be decomposed at higher temperatures to reform the amine and H_2S . Two amines which have proved to be important for commercial purposes are monoethanolamine (MEA) and diethanolamine (DEA).

In the second step of acid gas treating processes, H_2S is oxidized into elemental sulfur and water, and the sulfur is removed by filtration or centrifugation. This step is found in the sulfur recovery unit which treats the H_2S -rich gas stream from the acid gas removal unit (*Gary and Handwerk, 1984*). The two oxidation processes most commonly used are the dry oxidation process and the liquid phase oxidation process.

3.2 The Dry Oxidation Processes

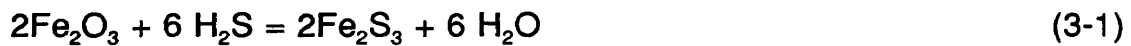
These processes are selective for H_2S removal and have no effect on other gaseous impurities that may be present.

3.2.1 The Iron Oxide Process

One of the earliest methods used in the dry oxidation process is the iron oxide-gas purification process (*West, 1983*). In this process, H_2S is removed completely by reaction with hydrated ferric oxide as the oxidizing agent, to form ferric sulfide. Upon exposure to atmospheric oxygen, ferric sulfide is oxidized to elemental sulfur and ferric oxide. The cycle can be repeated several times until the elemental sulfur covers most of the surface of the oxide and fills most of the

interstices between the oxide particles. In this condition, the purifying material loses its activity and causes a pressure drop through the bed. After removal of the sulfur and regeneration of the iron oxide, the oxide may be recycled in the process.

The iron oxide process are represented by the following reactions (*Kohl and Riesenfeld, 1985*):



The optimum condition for iron oxide regeneration is at a temperature of approximately 38°C (310.9 K) at a pH of 8.0 or higher. A large number of side reactions may occur, depending on the operating conditions. Variables that affect the reaction are temperature, moisture content, and the pH of the purifying material.

The iron oxide process is recommended for desulfurization of high pressure gases containing less than 20 grains H₂S/100 scf (0.4838 g H₂S/m³). Its widest application is in the treatment of gases where complete removal of H₂S is essential. Some of the disadvantages of this process are that the plants are large; large amounts of iron oxides must be handled; varying iron oxide activity must be accounted for; pressure decreases must be accounted for through a series of oxide boxes; and the formation of hydrates must be dealt with. Some of the

advantages are selectivity toward H₂S and mercaptans; good efficiency for H₂S removal; and low sensitivity to pressure.

3.2.2 The Claus Process

The Claus process is one of the most widely used processes for recovery of sulfur from pure gaseous H₂S or from acid gas streams containing H₂S in high concentration (*Kohl and Riesenfeld, 1985*). The Claus process yields a good quality of sulfur and thus is an important source of this valuable basic chemical. This process has undergone several modifications and has been extended to other processes such as the Sulfreen Process or the AMOCO Cold Bed Adsorption Process (*West, 1983*).

The removal of H₂S from the gas can be described by the following reaction sequence (*Kohl and Riesenfeld, 1985*)



In this dry oxidation process, oxygen is used as an oxidizing agent. The basic chemical reactions in the Claus process are represented by equations (3-3),

(3-4), and (3-6). The first two reactions take place in the thermal stage (reaction furnace) and equation (3-6) occurs in the catalytic stage (catalytic converters). Natural bauxite or alumina pellets or balls are used as the catalyst. The temperature at the thermal stage is above 538°C (810.9 K), and the catalytic stage has an upper temperature below 371°C (644.2 K) and a lower temperature that must remain above the sulfur dew point.

Lower temperatures at the catalytic stage can increase the conversion. However, there are limitations on the degree of H₂S conversion using this method. First, the presence of water vapor in the reaction gases can cause corrosion from the aqueous condensate and plugging of the equipment with solid sulfur. Second, a number of side reactions occur, due to the presence of carbon dioxide and light hydrocarbons.

Deactivation of the catalyst causes serious problems in the Claus process, especially at low combustion temperatures. This deactivation can be caused by the deposition of carbonaceous material, the gradual accumulation of sulfate, or by the condensation of sulfur on the catalyst.

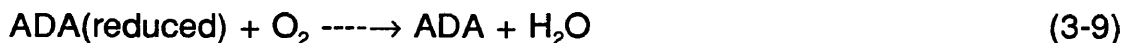
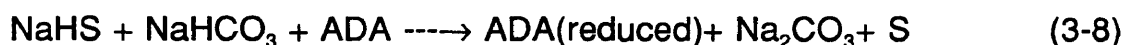
3.3 The Liquid Oxidation Processes

The liquid oxidation processes are used for the treatment of gases with a relatively low concentration of H₂S and a high concentration of carbon dioxide. The oxidation of H₂S to elemental sulfur is achieved by agents that are dissolved

or suspended in aqueous or nonaqueous solution (*Kohl and Riesenfeld, 1985*). The liquid phase oxidation process has the same chemical reactions as the dry oxidation process. Most of the compounds used as oxidizing agents are used in regenerative systems.

3.3.1 The Stretford™ Process

There are some processes widely used in industry, that use organic compounds as catalysts or oxidizing agents. One of these processes is the Stretford™ process (*Kohl and Riesenfeld, 1985*). In this process anthraquinone disulfonic acid (ADA) is used as an oxidizing agent for H₂S. An aqueous solution of sodium carbonate and sodium bicarbonate is used as a solvent for the quinone and H₂S. The chemical steps in this process can be represented by the following equations (*Kohl and Riesenfeld, 1985*):



As H₂S is oxidized to sulfur, the oxidizing agent (ADA) is reduced to the hydroquinone. Some of the limitations on the use of this process in commercial installations are: very large liquid circulation volume and high power consumption;

slow rate of elemental sulfur formation; and partial decarbonation of the solution before recycling to the absorber. Additives have been tested in order to improve this process. These additives increase the solution capacity for H₂S absorption and promote the rate of H₂S conversion to elemental sulfur. Alkali vanadates were found to promote the reduction of H₂S to elemental sulfur.

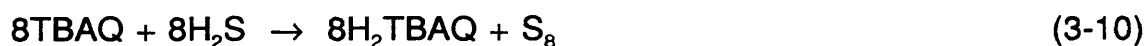
Under some conditions, side reactions occur in the process. It was found that the solution may absorb more H₂S than the vanadate can oxidize, causing vanadium to precipitate as a black complex vanadium-oxygen-sulfur compound. It was also found that this process had some disadvantages because of bacterial growth. The sulfur produced was sticky and adhered to all surfaces, causing plugging problems. Another problem was corrosion of carbon steel equipment.

3.4 The HYSULFSM Process

As mentioned in the previous section, the current H₂S removal processes still face many problems. Researchers are still trying to solve the most serious problems, such as the loss of valuable hydrogen, precise air rate control, removal of trace sulfur compounds from the spent air and the upper limit on the ratio of carbon dioxide to H₂S.

Recently, a new process has been proposed which recovers both the hydrogen and sulfur from H₂S in nonaqueous medium (*Plummer, 1987*). The basic chemistry of this process is related to the StretfordTM Process (*Kohl and*

Riesenfeld, 1985) in that quinones are used as oxidizing agents. However, the similarity ends there, because water is replaced by polar non-aqueous solvents. 2-tert-Butylanthraquinone (TBAQ) was selected as the H₂S oxidant because of its high solubility in polar aprotic solvents. The overall process consists of the two stages shown below.



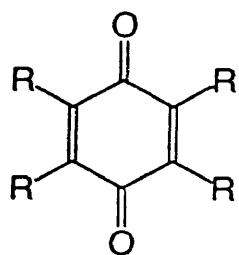
The first stage is the reaction of H₂S with TBAQ to form elemental sulfur and 2-tert-butylidihydroxyanthracene (H₂TBAQ). The second stage is the catalytic dehydrogenation of H₂TBAQ to form TBAQ and hydrogen (H₂). This research will address only the chemistry of the first stage, equation (3-10).

There are still some problems in the HYSULFSM process such as the slow rate of quinone reduction and the slow sulfur polymerization rate. Since little is known about the fundamental reaction chemistry, this research must be performed if the process is to be commercialized.

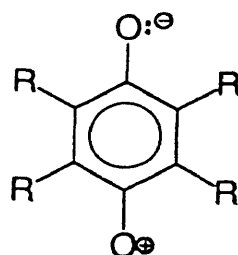
3.5 Quinone Chemistry

Quinones are six-member ring compounds that have carbonyl groups conjugated with a carbon-carbon double bond and have potential to form aromatic.

There is little aromatic character in quinones structures. Quinones can be represented by quinonoid (I) and benzenoid (II) resonance structures as illustrated below (*Gleicher, 1974*):

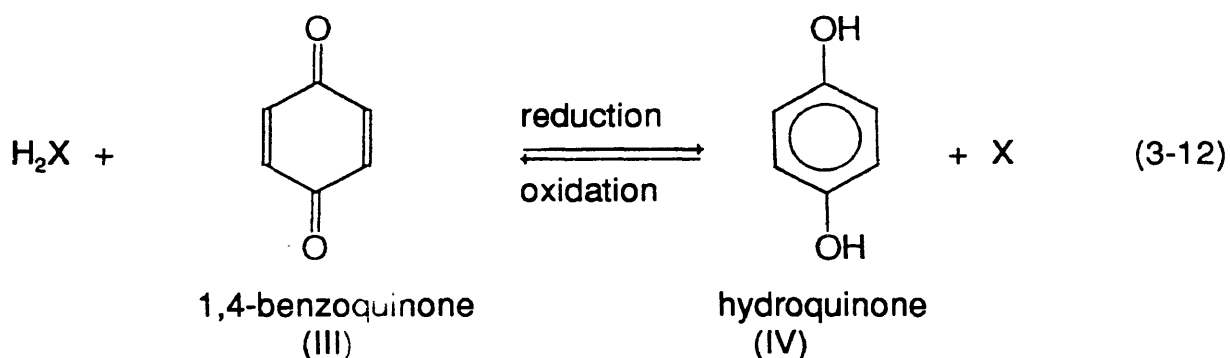


quinonoid
(I)



benzenoid
(II)

The oldest and best known example of a quinone is 1,4-benzoquinone (III). This quinone and 1,4-benzenediol (hydroquinone, IV) form a reversible reduction/oxidation equilibrium or redox couple. Quinones are excellent oxidants while being themselves reduced.

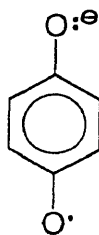


The most widely used oxidants are 1,4-benzoquinone, and 2,3,5,6-tetrachloro-1,4-benzoquinone (chloranil) (*Finley, 1978*).

Based on the ability of quinones to undergo reduction and oxidation, these compounds have been studied extensively in electrochemistry. Using controlled potential techniques, where the voltage is applied to the electrode cells and the resulting current is measured, the reduction potential of quinones in the electrochemical cell can be determined.

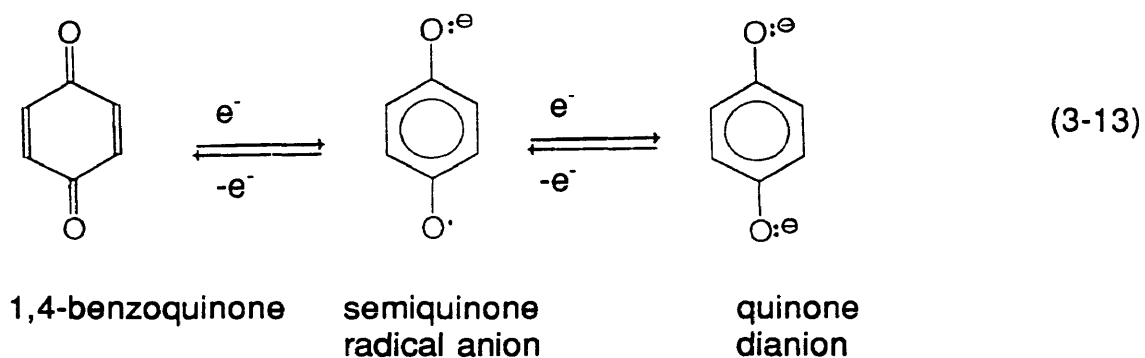
The reduction process of unsubstituted complex quinones has been the subject of investigation for years. Early work in electrochemistry (*Gleicher, 1974*) indicated that the electron-donating substituents on the quinone ring lower the reduction potential and that electron-withdrawing groups raise it.

In electrode processes, quinones can accept an electron to form radical anions. This intermediate between the quinone dianion and 1,4-benzoquinone is known as a semiquinone. The quinone system has an unpaired electron, and thus has a radical character. The molecule is usually represented with a negative charge on one oxygen and the odd electron on the other.



semiquinone

An electrochemical study (*Wawzonek, 1956*) reported that the reduction of quinones in anhydrous solvents, such as acetonitrile and dimethylformamide, proceeds first to the semiquinone anion and then to the quinone dianion.



The effect of proton donors or protic solvents on the simple quinone-hydroquinone couples has been widely studied (*Chambers, 1974*). The reversible oxidation and reduction as half reaction in the electrochemical cell is presented below :



where Q and QH_2 represent the quinone and the hydroquinone species, respectively. The electrode potential of these half reactions will obey the Nernst equation:

$$E = E^\circ + \frac{RT}{2F} \ln \left(\frac{a_Q}{a_{QH_2}} \right) + \frac{RT}{2F} \ln a_{H^+}^2 \quad (3-15)$$

where E = applied potential in the electrode cell

E° = standard potential of the system

R = gas constant ($8.314 \text{ Joule}\cdot\text{mol}^{-1}\cdot\text{K}^{-1}$)

T = absolute temperature (K)

F = Faraday constant ($9.648 \times 10^4 \text{ C}\cdot\text{mol}^{-1}$)

The Nernst equation is applied to the points on the surface of working electrode, since a_Q , a_{QH_2} and a_{H^+} are activities of quinone, hydroquinone and proton, respectively.

Studies of the electrochemistry of quinones can be placed in two groups: those using non-aqueous solvents and those using aqueous solvents.

3.5.1 Quinones in Non-aqueous Solvents

Cyclic voltammetry, one of the voltammetric (control potential) techniques, can be used to study the redox behavior of quinones. The cyclic voltammogram of quinones in aprotic solvents can be affected by any variation of the quinone concentration, the semiquinone concentration or the quinone dianion concentration in the diffusion layer at the surface of the electrode. The perturbations of those concentrations mostly come from the acid-base reactions, ion pairing and complex formation equilibria (*Chambers, 1974*).

In non-aqueous solvents, the presence of a proton donor such as phenol or benzoic acid in the electrochemical cell can shift the reduction and oxidation

potential or reduce the magnitude of the reduction and oxidation peak of the quinone-quinone dianion couple. Badoz-Lambling and Demange-Guerin stated that 1,4-benzoquinone is not protonated by perchloric acid in dimethylformamide based on spectroscopic data (*Badoz-Lambling, Demange-Guerin, 1968*). A shift in the reduction potential can occur by varying the type and concentration of the proton donor. The semiquinone ($Q^{\cdot-}$) and quinone dianion (Q^{\ominus}) in the electrode process are capable of accepting one or two protons from the proton donor.



A typical cyclic voltammogram (**figure 1**) of a quinone usually shows two reduction peaks (I and II) and two oxidation peaks (II and IV). The first reduction peak (I) represents the reduction of quinone to semiquinone, and the second reduction peak (II) represents the reduction of semiquinone to quinone dianion. The presence of a proton donor, such as water or phenol, shifts the second reduction peak to a less negative potential. This indicates that rapid protonation of the quinone dianion is taking place in the diffusion layer at the electrode surface (*Wawzonek, et al., 1956*). This shift agrees with the Nernst equation (3-15).

In the presence of a proton donor such as benzoic acid, protonation of the semiquinone anion also occurs. Under these conditions the height of the first

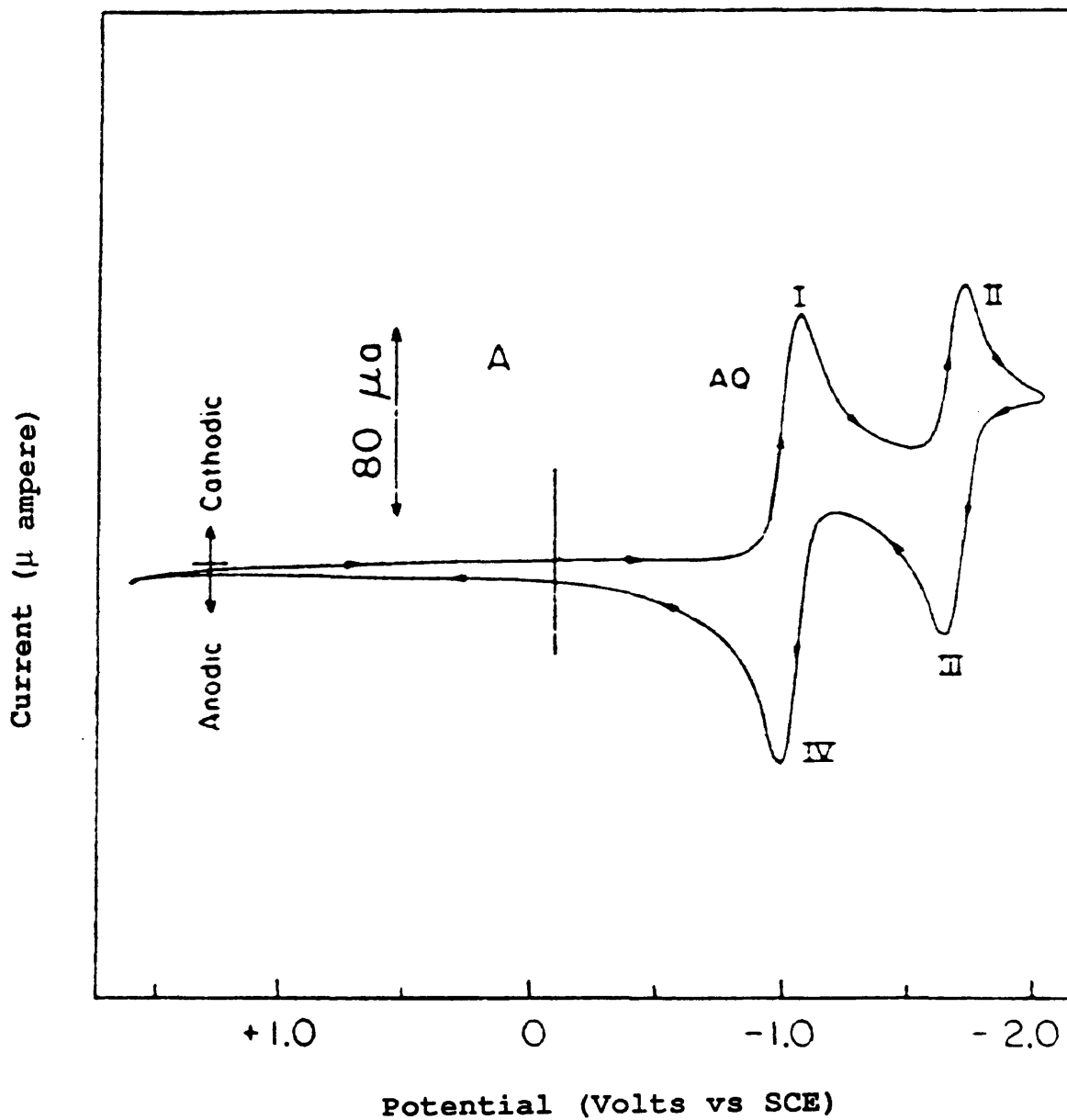
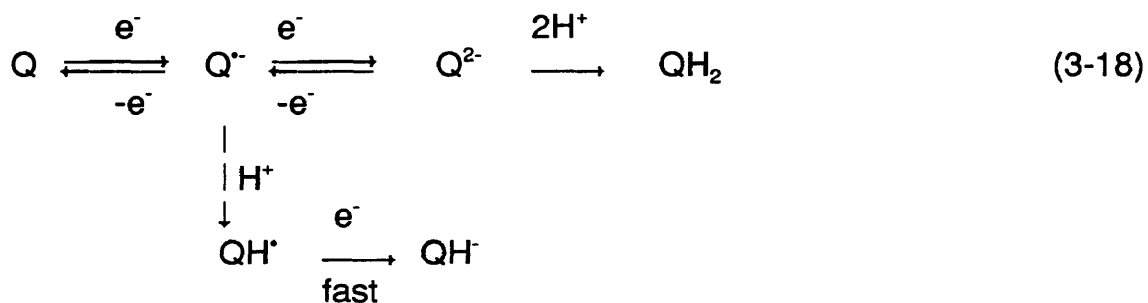


Figure 1. Cyclic voltammogram of 9,10-anthraquinone in 1,2-dimethoxyethane
From ref. : Koshy, V. J, et.al, 1980. J. Electrochem. Soc., 127:2761.

reduction peak is increased at the expense of the second reduction peak until a single peak is observed at a 5:1 mole ratio of acid to quinone (*Given and Peover, 1960*). Protonation of the semiquinone ($Q^{\cdot-}$) forms the hydroquinone radical (QH^{\cdot}), which is then rapidly reduced to form the anion of hydroquinone (QH^-). It was found that the electron affinity of the hydroquinone radical (QH^{\cdot}) is higher than that of the radical anion ($Q^{\cdot-}$). Under these acid conditions the fast reduction of the hydroquinone radical (QH^{\cdot}) occurs at the same potential as the reduction of quinone (*Chambers, 1967*).



Chambers (*Chambers, 1974*) found, contrary to the results of Badoz-Lambling and Demange-Guerin, that if the proton donor is a strong Bronsted acid, then preprotonation (prior protonation) of the quinone can take place. It was found that the new peak occurs at a potential as much as 0.6 V more positive than the first reduction peak potential of the corresponding quinone (*Chambers, 1967*). The proposed mechanism involves the reduction of the protonated quinone to form first

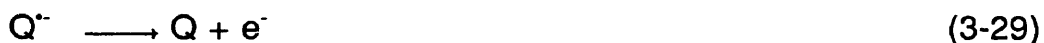
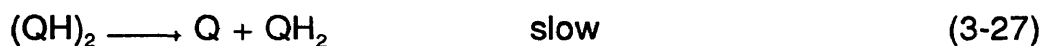
the hydroquinone radical (QH^\cdot) and then the hydroquinone anion (QH^-), which is rapidly protonated to form hydroquinone (equations 3-19 to 3-22).



It was reported (*Chambers et al., 1974*) that oxidation of the hydroquinone can occur via an irreversible two-electron process.



The oxidation of the hydroquinone can also occur with the protonated semiquinone (QH^\cdot) as intermediate.



The formation of an intermediate dimer $(QH)_2$ of the protonated semiquinones (QH^+) was suggested because the oxidation peak of the hydroquinone (QH_2) disappeared at fast scan rates (*Eggins and Chambers, 1970*).

3.5.2 Quinones in Aqueous Solvents

The rate of electron transfer to organic compounds in aqueous solutions is a slow process (*Peover, 1967*). *Vetter (Vetter, K.J, 1967)* suggested that the mechanism of quinone reduction in aqueous solutions can be expressed as an *HeHe* mechanism at $pH < 5$ and as an *eHeH* at $pH > 6$.



Hydrogen bonding of water molecules to the anions causes quinones in water to have larger reduction potential than in non-aqueous solvents (*Peover, 1967*).

3.6 Sulfanes

The chemistry of sulfanes or hydrogen polysulfides will be described in this section because these intermediates are the likely precursors of sulfur in the HYSULFSM process. It has been reported that the decomposition of long chain sulfanes can result in sulfur (S_8) formation (*Burton and Machmer, 1968*).

A sulfane with various sulfur chain lengths can be represented as H_2S_n , an alkali sulfane as M_2S_n , a halosulfane as X_2S_n , and the dialkyl or diaryl sulfane as R_2S_n , where M, X, and R represent a metal cation, a halogen anion and an alkyl or aryl group, respectively (*Brasted, 1961*).

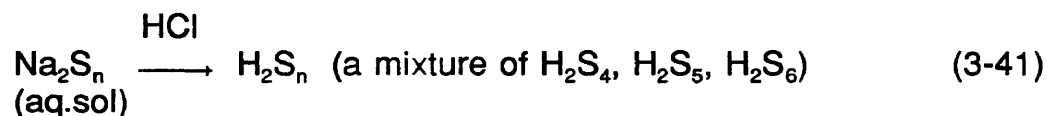
Polysulfanes have been known since the eighteenth century, but they are difficult to handle and to purify. Bloch and Huhn (*Bloch, 1908*) suggested that sulfur compounds in crude oil are a mixture of polysulfanes, and were able to isolate the di- and trisulfanes. In 1941 Feher determined the Raman spectrum of disulfane and found that crude oil does not contain H_2S_2 and H_2S_3 , but only H_2S_5 , H_2S_6 , and higher sulfanes. He suggested that the di- and tri-sulfanes produced by the Bloch-Huhn vacuum distillation process were formed by cracking the longer chain sulfanes (*Burton and Machmer 1968*).

3.6.1 Sulfanes Preparation from Aqueous Polysulfide Solutions

An alkali polysulfide solution is prepared by heating a mixture of sodium sulfide with sulfur.



By increasing the sulfur content in the sodium polysulfide, the average chain length of the sulfane mixture can be increased. A sulfane mixture is formed by acidification of this aqueous solution of higher alkali or alkali earth polysulfides. This sulfane mixture contains mainly tetra-, penta- and higher sulfanes.



It was found that a temperature range of -10°C (263.1 K) to -15°C (258.1 K) was the most suitable condition for polysulfide-acid reaction (*Burton and Machmer, 1968*). The concentration of the polysulfides has no effect on the average chain length of sulfane, but the type of acid does have some influence on the yield and type of the sulfane mixture. The presence of alkali will catalyze the decomposition of the sulfane mixture to H_2S and sulfur, therefore, an excess of acid must be added.

An X-ray crystallographic study of anhydrous sodium polysulfide indicates that the sulfur chains are already present in the solid alkali polysulfide and are not produced during the acidification step (*Burton, Machmer, 1968*).

Polysulfane formation occurs first by acidification of the polysulfide dianion

(S_n²⁻) (equation 3-41) followed by decomposition and disproportionation reactions.



The di- and trisulfanes, which are primarily formed, are very reactive, and are not stable under the preparation conditions in an aqueous medium. Therefore, sulfane with lower average sulfur chain length than H₂S₄ cannot be obtained by this method.

3.6.2 Polysulfane Preparation from Anhydrous Polysulfides

Acidification of the alkali polysulfide in an anhydrous solvent system can eliminate the decomposition reactions. Investigation by Feher and Berthold (*Feher and Berthold, 1957*) has shown that reaction of the tetra- or pentasulfides of sodium or potassium with anhydrous formic acid produced very pure sulfanes. Disproportionation reactions can form long-chain sulfanes as the main products



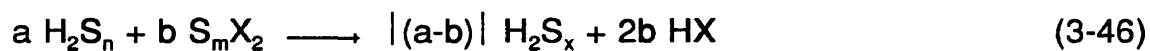
$$(n = 2,3,4,5)$$

3.6.3 Polysulfane Preparation by Cathodic Reduction of SO₂

The electrolytic reduction of a saturated aqueous sulfur dioxide solution, which contains hydrochloric acid or sulfuric acid, forms a thin film of crude polysulfanes on the cathode. The mixtures contain an average chain length H₂S₇-H₂S₁₂ and a small amount of dissolved S₈ sulfur. Study of the electrode processes has shown that the initial reaction product on the cathode is dithionous acid, H₂S₂O₄, which decomposes in strong acid solution to form sulfurous acid, H₂SO₃ and sulfanes (*Burton and Machmer, 1968*).

3.6.4 Polysulfane Preparation via Condensation Reactions

Condensation reactions are used for preparation of polysulfanes of chain length ≥ 7 . The condensation reaction between sulfanes and halosulfanes is described by this equation :



$$\text{where } x = (na+mb)/|(a-b)|$$

$$n = 1,2,3,.. \quad m = 0,1,2,3,....$$

$$\text{X} = \text{Cl or Br}$$

When $b > a$, this method can be used for preparation of halosulfanes.

The synthesis of sulfanes from the reaction of excess disulfane with sulfur monochloride forms a mixture of the sulfane homologues H₂S₆, H₂S₁₀, H₂S₁₄,.... and

the general formula of the sulfane molecules is H_2S_{4k+2} .

The primary reaction is:

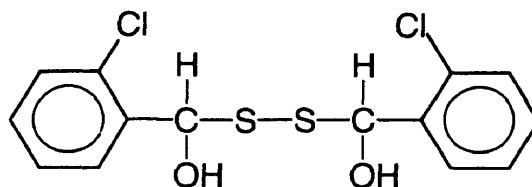


followed by the disproportionation reaction.

The lower sulfanes used as reactants in this method are the volatile sulfanes such as H_2S and H_2S_2 . When using H_2S the tri- to pentasulfane can be produced, while the penta- to octasulfane can be obtained from H_2S_2 . H_2S in general reacts slower than disulfane and the reaction is catalyzed by dissolved hydrogen chloride. To obtain high purity sulfanes from this condensation method it is necessary to maintain anhydrous conditions at a temperature of $50^\circ C$ ($323.1 K$) since at higher temperatures side reactions can occur.

3.6.5 Chemistry of Sulfanes

The reaction of sulfane with ketones and aliphatic aldehydes was unsuccessful because of sulfane decomposition (*Bloch et al., 1910*), but sulfane can react with aromatic aldehydes and ortho- or para-chlorobenzaldehyde to form disubstituted adducts of the general formula RS_xR . An example of the para-chlorobenzaldehyde adduct is shown below (*Feher and Winkhaus, 1956*).



H_2S can react with perchloromethyl mercaptan to form higher sulfides of the type $\text{Cl}_3\text{C-S}_x\text{-CCl}_3$, by elimination of hydrogen chloride (*Feher and Berthold, 1955*).



The reaction occurs at a higher temperature of about 85°C (358.1 K).

The reaction of excess thiol with a chlorosulfane will produce symmetrical derivatives:



In the presence of excess chlorosulfane, the reaction produces asymmetrical chloro-derivatives :



These derivatives are liquid at room temperature and have a deep yellow or

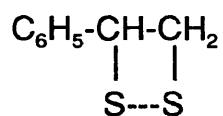
orange color.

The sulfanes are considerably stronger acids (pK_a values range from 3.5 to 5.0) than H_2S (pK_a 6.8). In water, or in alcohol, decomposition of the sulfanes occurs to produce sulfur and H_2S . In dilute hydrochloric acid the sulfanes are insoluble, but in dry ether or dioxane, di- and trisulfane are soluble without decomposition.

The sulfanes are stable in alkali media as the S_n^{2-} species and in strongly acidic media as the H_2S_n species. In neutral solutions there are S_n^{2-} species in equilibrium with H_2S_n species .



Sulfanes undergo an addition reaction with carbon-carbon double bonds (*Brasted, 1961*); for example the reaction of a sulfane mixture with styrene in liquid H_2S produces



It was found that in a non-aqueous medium, the hydrogen atoms of trisulfane (H_2S_3) are involved in intermolecular and intramolecular hydrogen

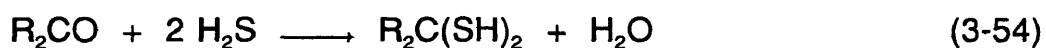
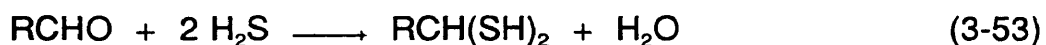
bonding. In CS₂ solvent the intramolecular hydrogen bonding decreases because of the interaction of CS₂ with trisulfane. Infrared analysis suggests that the intermolecular sulfane-solvent interaction is stronger in CS₂ solvent than in CCl₄ solvent (*Muller and Hyne 1968*).

3.6.6 Hydrogen Sulfide

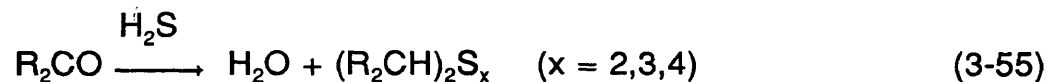
Hydrogen sulfide (H₂S) is the most common of the sulfanes. It occurs naturally in small concentrations in petroleum and natural gas. The usual method of preparation is by the hydrolysis of sulfides such as alkali and alkaline earth metal sulfides. A high purity product may be produced by direct reaction of sulfur vapor and hydrogen over a pumice stone catalyst at 600 °C (*Burton and Machmer, 1968*).

H₂S is a weak acid with pK_{A1} of 6.8 and pK_{A2} about 14, and it is also a reducing agent. Oxidation of H₂S may form sulfur or sulfur dioxide. The pyrolysis of H₂S leads to decomposition to the elements.

Reaction of aldehydes or ketones with H₂S at pressures between 35 and 8500 atmospheres forms gem-dithiols having the general formula R₂C(SH)₂ (*Cairns et al., 1952*):



Low yields can be caused by a competing reaction for the formation of polysulfides.



Ketones are less reactive to H_2S than are aldehydes. The gem-dithiols formation reactions are favored when the ratio of H_2S to carbonyl compounds is high.

It also has been reported by Wiewiorowski and Touro (*Wiewiorowski et al., 1968*), that H_2S reacts with molten sulfur to form hydrogen polysulfides (polysulfanes).

Chapter 4

EXPERIMENTAL

The reduction of TBAQ by H₂S was conducted in glass stirred-tank batch reactors. Kinetics were determined through NMR analysis of the reaction products. Mechanistic details of the reaction were obtained using cyclic voltammetric, NMR, and UV-visible techniques.

4.1 Solvents

The solvents used in this study were selected according to their boiling points, dipole moments, quinone solubility and molecular structure. The solvent name, name abbreviation, boiling point, dipole moment, purity, and source are listed in **table 1**. The solvents were used as received.

4.2 Solubility of TBAQ

The solubility limit of TBAQ in each solvent was determined by preparing a saturated solution, filtering away the excess solid, and analyzing the filtrate by NMR. Peak areas were selected from regions in the spectrum where no overlap in signal was observed. The concentration of TBAQ in the solvent (**table 2, appendix B**) was determined by comparing the integrated area for the selected

Table 1. Solvent Properties, Purity and Source.

Solvent Name	Name Abbreviation	Boiling Point (°C)	Dipole Moment (Debye)	Purity (Mole %)	Source
N-methylpyrrolidinone	NMP	202	4.09	99	Aldrich
N,N-dimethylacetamide	DMAC	166	3.71	99	Aldrich
γ -butyrolactone	GBL	204	4.12	99	Baker
2-pyrrolidinone	PN	245	3.55	99	Aldrich
N-methylacetamide	MAC	206	4.27	99+	Aldrich
N,N-dimethylformamide	DMF	153	3.24	99+	Aldrich
ethylenediamine	EDM	117	1.90	99	Aldrich
pyridine	PY	115	2.37	99	EMS ¹
acetonitrile	AN	82	3.53	99.9	Baker
2-nitropropane	2NP	120	3.73	99	Aldrich
ethyl acetate	EA	77	1.82	99	Aldrich
tetrahydrofuran	THF	66	1.75	99+	Aldrich
3-pentanone	3PO	102	2.82	99	Aldrich
N-methylpyrrolidine	MPD	80-81	\approx 2.0	97	Aldrich
4-hydroxy-4-methyl-2-pentanone	HMP	168	3.24	99	Aldrich
4-methyl-2-pentanol	MPL	132	1.70	99	Aldrich
p-xylene	PX	138	0.01	99	Phillips
1,4-dioxane	DX	101	0.45	99+	Aldrich
propylene carbononate	PC	242	4.94	99	Aldrich

¹ EMS = EM Scientific

TBAQ peaks to that for the solvent. The number of hydrogens responsible for each set of peaks was factored into the calculation.

4.3 Reaction Mixture Preparation

The reaction mixture consists of a polar solvent, TBAQ and H₂S. Only those solvents demonstrating a solubility equal to or greater than 15 weight percent were used for study in the stirred tank reactors. The TBAQ was selected as the H₂S oxidizing agent since it has higher solubility in polar organic solvent than does anthraquinone.

For the microreactor and minireactor feedstock, a known weight of TBAQ was dissolved into the solvent so as to make a 15 weight percent solution. A solution volume of 30 mL and 60 mL was used in the micro- and minireactors, respectively. Detailed preparation procedure can be found in appendix A.

4.4 Sulfur Recovery Technique

Sulfur solid (S₈) can precipitate in the stirred tank reactors when the TBAQ conversion reached a certain minimum value. At the end of reaction, the H₂S pressure was gradually lowered and the water bath was replaced by an ice bath. The rate of sulfur precipitation increased when H₂S pressure and temperature were lowered.

The solid sulfur was filtered and washed several times with acetone. After

it was dried, the sulfur was weighed. Appendix A contains the detailed procedure for the sulfur recovery technique.

4.5 Mini and Microreactors

The rates of quinone reduction and sulfur formation were studied in the stirred tank reactors shown in **figures 2 and 3**. Both reactors use only a small volume of the feedstock, in order to minimize waste production. The small size of the reactor permits the placement of the entire system inside a laboratory hood for increased safety.

The glass microreactor, which was designed for experiments at atmospheric pressure, is shown in **figure 2**. A 60 mL serum bottle with a rubber septum is used as a reactor vessel. The feedstock (30 mL) and a small Teflon-coated magnetic stirbar are placed into the bottle prior to sealing with a rubber septum. The feedstock was purged with N_2 (60 cc/min) for 15 minutes to remove air prior to flowing H_2S (60 cc/min) through the liquid. Air removal is required to prevent H_2TBAQ oxidation. Stainless steel needles which penetrate the rubber septum at the top of the reactor serve as an inlet and outlet for the gases. The glass reactor was placed into a heated water bath. Thermocouples monitored the temperature of the water bath and the solution inside the reactor. The hot plate below the water bath is connected to the temperature controller in order to maintain the temperature of the water bath. A gas-tight syringe with needle is used to remove

1 mL samples from the reactor vessel for analysis by NMR. Unreacted H₂S gas is vented through a gas scrubber filled with 1.0 M sodium hydroxide.

The possible effect of hydrogen sulfide pressure on the reaction rate was studied in a second reactor shown in **figure 3**. This reactor system is basically a larger version of the reactor shown in **figure 2**. With exception of the glass reactor vessel the reactor components were made of stainless steel to prevent corrosion by H₂S. The feedstock (60 mL) and a magnetic stirbar were placed into the 100 mL glass reaction vessel prior to purging with N₂ gas. The reactant H₂S gas was introduced to initiate the reaction. A forward pressure regulator was used to control the H₂S pressure, which was monitored by a McDaniels pressure gauge. The inlet and outlet gas lines are 1/8" stainless steel tubing. A 1/16" siphon tube inserted into the reaction mixture was used to collect samples for analysis. Approximately 10 cc of the 60 cc reaction mixture was removed for analysis. The H₂S pressure remained constant during the reaction and the temperature of the reaction mixture was monitored by a thermocouple and digital readout. A more detailed description of this procedure is given in Appendix A.

4.6 NMR Tube Reactor

The NMR tube reactor was designed and built to investigate the intermediate species in the reaction. An NMR tube with a medium wall thickness (0.77 mm) was used as reactor vessel (**figure 4**). This reactor vessel was connected

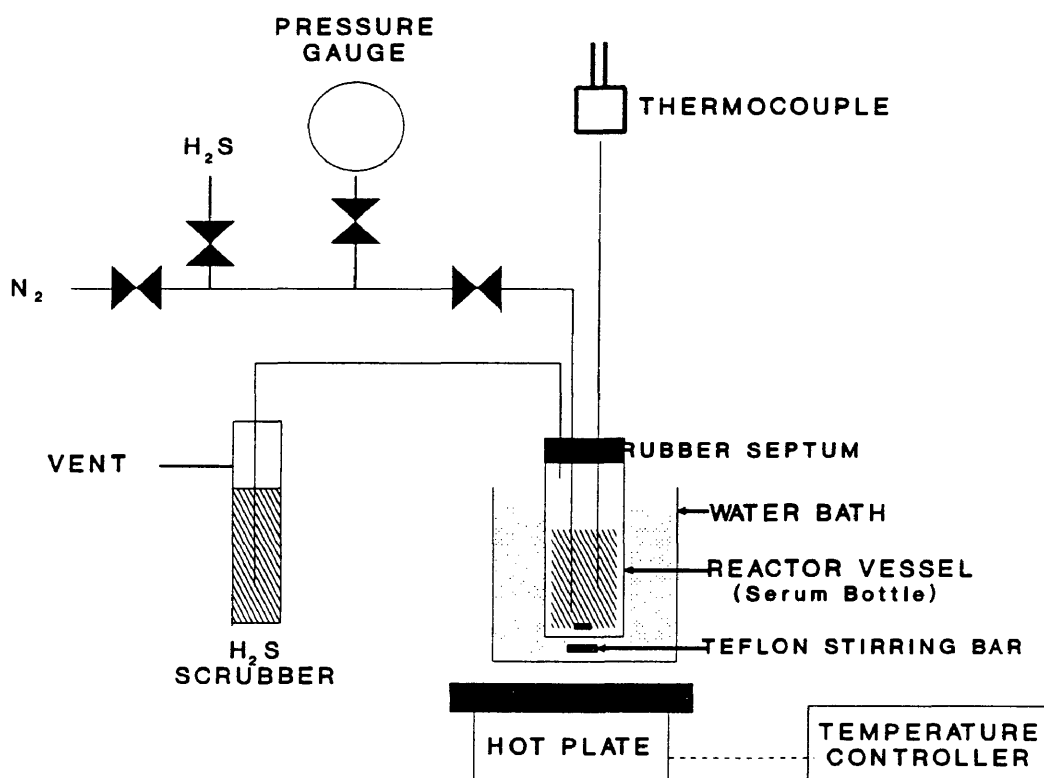


Figure 2. Low Pressure Glass Microreactor

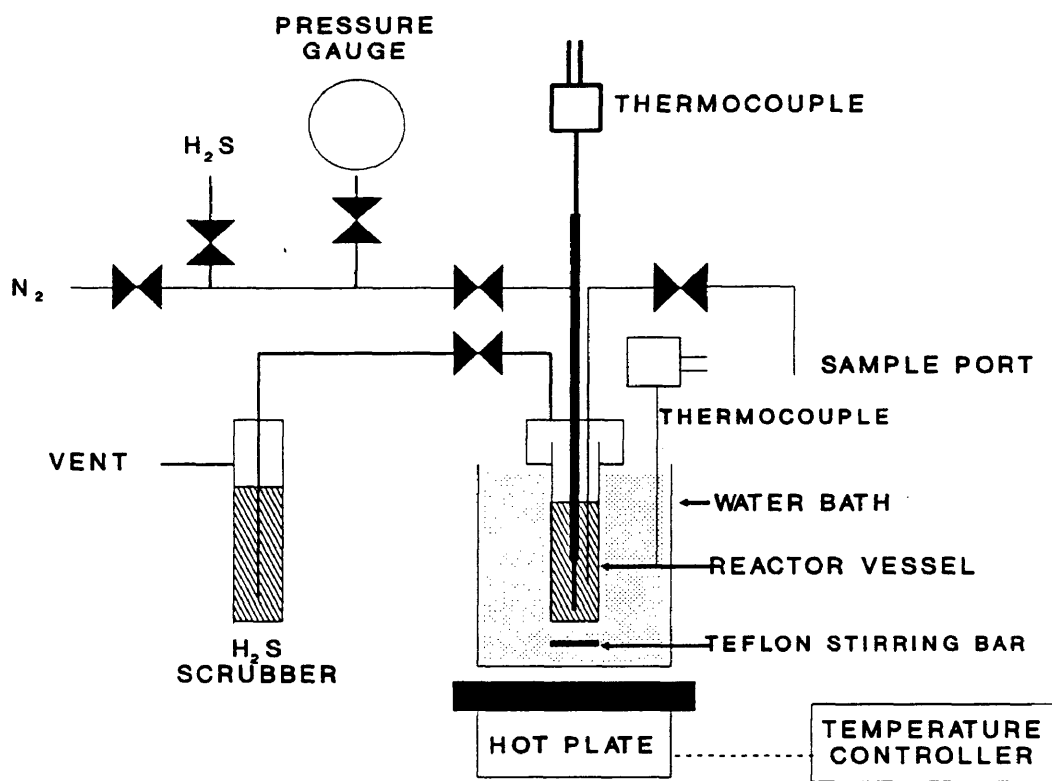


Figure 3. High Pressure Glass Minireactor

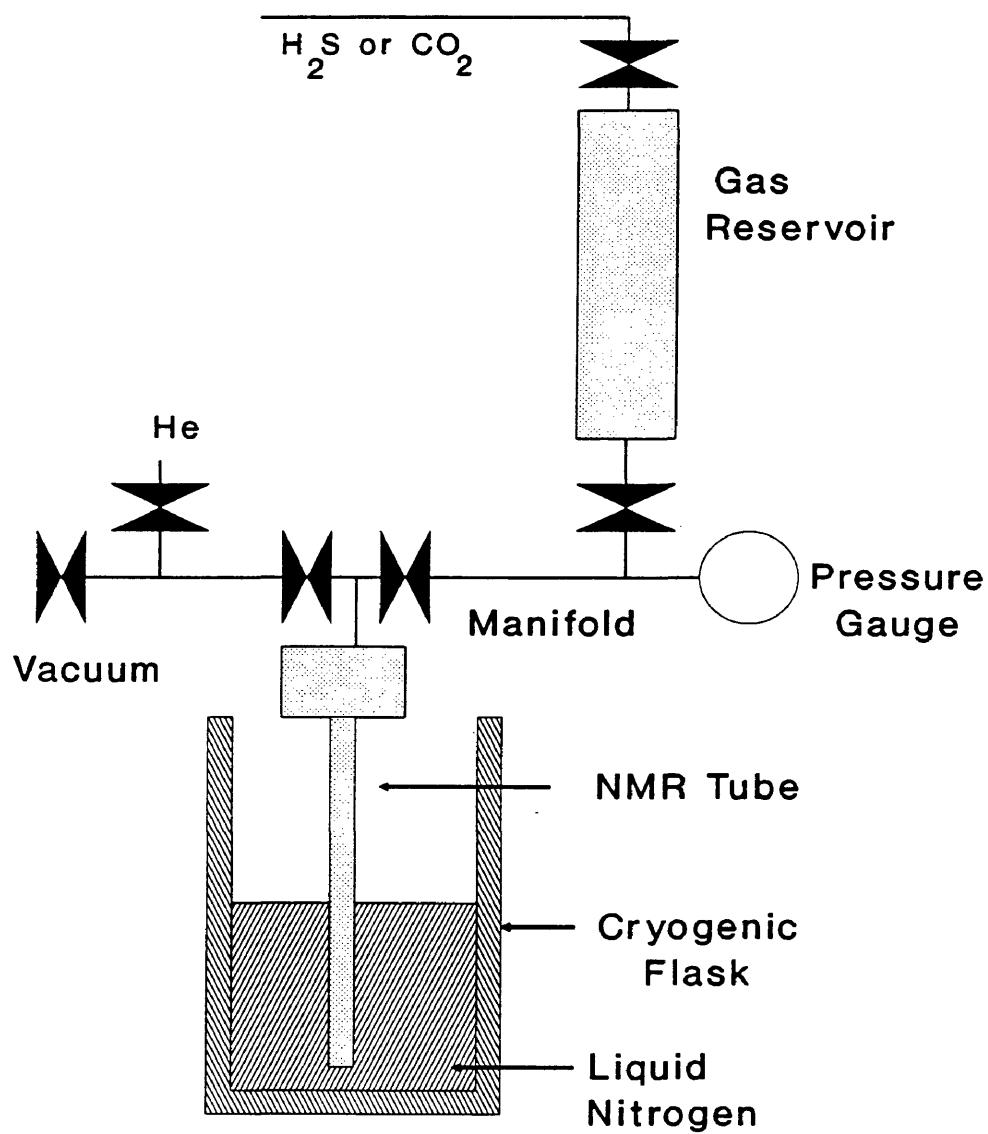


Figure 4. NMR Tube Reactor System

by a 1/4" stainless steel tube to a gas reservoir made from a 1/2" stainless steel tubing. A vacuum pump and pressure gauge are also connected to the reactor vessel. Unreacted H₂S was vented through a gas scrubber filled with 0.1 M sodium hydroxide.

The feedstock (0.4 mL) was placed into the NMR tube, evacuated to 10⁻² torr. The feedstock was frozen in liquid N₂ and sufficient H₂S was condensed into the tube to produce the desired final pressure. The amount of H₂S added was estimated by monitoring the pressure drop in the gas reservoir. The top of the tube was sealed with a torch. The NMR tube reactor can hold pressures up to 80 psig. The frozen tube was placed behind an explosion shield and removed from the liquid N₂ until the reaction mixture had completely thawed. The progress of the reaction was monitored by NMR. Further details of the NMR tube reactor procedure are presented in Appendix A.

4.7 Analytical Methods

The reaction systems and the product of the reaction between TBAQ and H₂S in the micro and minireactors and NMR reactor were analyzed by Nuclear Magnetic Resonance (NMR) and UV/visible spectroscopy. The NMR spectrum gave information on the role of solvent and kinetic data of the TBAQ conversion to H₂TBAQ. UV/vis spectroscopy was used to investigate the interaction between solvent and TBAQ.

Cyclic voltammetry was used in order to understand the reaction mechanisms of TBAQ reduction. Cyclic voltammetry provided the information on the role of solvent and the effect of protic agents in the solution.

4.7.1 Nuclear Magnetic Resonance

NMR studies were conducted using a Varian EM390 90 MHz machine. TBAQ solubility was determined by comparing the peak area of TBAQ with the peak area of the solvent.

The rate of TBAQ reduction by H_2S was also monitored by NMR. Approximately 1 mL of sample was removed from the reaction vessel and placed in an NMR tube. The conversion of TBAQ to H_2 TBAQ was determined by integrating the peak areas in the aromatic proton region of the NMR spectrum. When TBAQ is converted into H_2 TBAQ, the two sets of peaks belonging to H_2 TBAQ (centered at 7.5 ppm and at 8.6 ppm) increased while peaks belonging to TBAQ (8.0 - 8.4 ppm) decreased. The ratio of H_2 TBAQ peak areas to the total aromatic peak area was used to calculate the mole percent of converted TBAQ.

NMR can also be used to identify polysulfane intermediates (H_2S_x). However, the reduction in pressure as the sample was transferred from the reactor to the NMR tube resulted in the rapid decomposition of the polysulfanes. This caused NMR analysis of the sulfur intermediates to be impossible. Conducting the reaction at pressure inside a sealed NMR tube overcame this problem. The

polysulfanes can be detected by observing the chemical shifts of the polysulfane protons, located at 2.63 ppm for H_2S_2 , at 3.98 ppm for H_2S_3 , and at 4.03 to 4.27 ppm for H_2S_4 to H_2S_9 in CCl_4 (Muller and Hyne, 1968).

4.7.2 Ultraviolet-Visible Spectroscopy

The possibility of solvent- H_2S interaction was investigated by using a Cary 219 Ultraviolet-Visible spectrometer by Varian. When an amide solvent such as NMP is used, electron transfer between the solvent and hydrogen sulfide can be detected in the UV spectrum.

Quinones, which contain carbonyl groups, have two types of readily available electrons that can undergo transition in the UV: the π -electrons and the non-bonded unshared electrons or n -electrons. Since the non-bonded electrons are not stabilized directly by the π -bond, the n - π^* transitions are found at higher wavelengths or lower energies than the π - π^* transitions. Quinones with conjugated systems will show both n - π^* and π - π^* transitions.

Unsubstituted 1,4-benzoquinone has been reported to have absorptions at 476 $\text{m}\mu$ (n - π^* transition) and at 244 $\text{m}\mu$ (π - π^* transition) (Gleicher, 1974). Change in solvent polarity can affect the wavelength of the transition. More polar solvents shift the n - π^* transition toward a shorter wavelength and the π - π^* transition toward a longer wavelength. The amount of shift to a lower wavelength can be used as a measure of the strength of the hydrogen bonding between the solvent and the



quinone.

Possible charge-transfer complex formation between quinones and hydrogen sulfide would result in a change in the UV spectrum of quinone. A new band appears, in addition to the original $n-\pi^*$ transition and $\pi-\pi^*$ transition.

Structural variations of quinone and solvent will provide information about the nature of the charge-transfer complex. This information can be very useful to determine the reaction mechanisms of quinone reduction.

4.7.3 Cyclic Voltammetry

Details of the TBAQ to H_2 TBAQ reaction mechanisms were studied using cyclic voltammetry (CV) and an electrochemical cell as shown in **figure 5**. CV consists of cycling the potential of a working electrode, immersed in an unstirred solution, and measuring the resulting current through the cell. The potential of this working electrode was read relatively to a reference electrode. By applying a triangular voltage wave form to the electrode, the potential of the working electrode sweeps from the initial potential to the final potential.

A cyclic voltammogram is obtained by measuring the current at the working electrode during the scan of the potential. The voltammogram displays current (vertical axis) versus potential (horizontal axis). A typical cyclic voltammogram is shown in **figure 6**. The important parameters of a cyclic voltammogram are the magnitudes of the anodic peak current (i_{pa}), cathodic peak current (i_{pc}), anodic peak

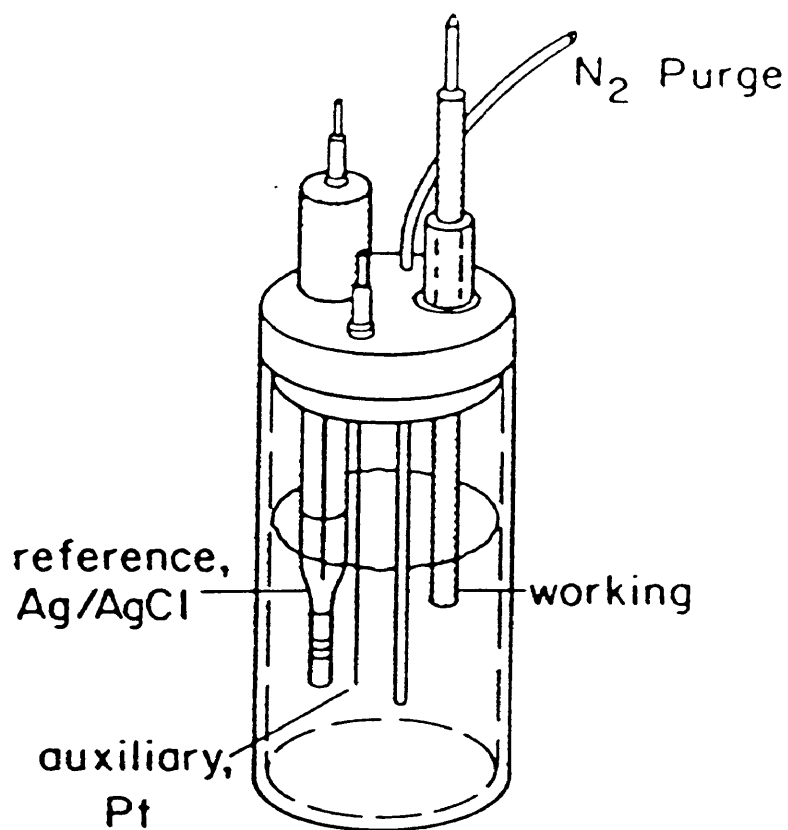


Figure 5. Electrochemical Cell
(From Bioanalytical Systems, Inc., ref.: Kissinger, P. T, 1983. J. Chem. Ed. 60:702.

potential (E_{pa}), and cathodic peak potential (E_{pc}).

Good solvents for the CV should not show redox potential in the region of interest; the redox of TBAQ in this study. Several solvents with different polarities and dipole moments were selected in order to investigate the effect of these on the reduction potential of TBAQ.

The effect of protic agents in the system were also investigated by addition of an organic acid into the cell. A mercaptan or a bisulfide salt was added into the electrolytic cell to replace hydrogen sulfide as a protic agent. Lastly, sodium hydrogen sulfide salt (NaHS) was added into TBAQ solution to investigate the effect of HS^- anion as an electron donor agent. Appendix A contains the step by step details of the procedures used in cyclic voltammetry.

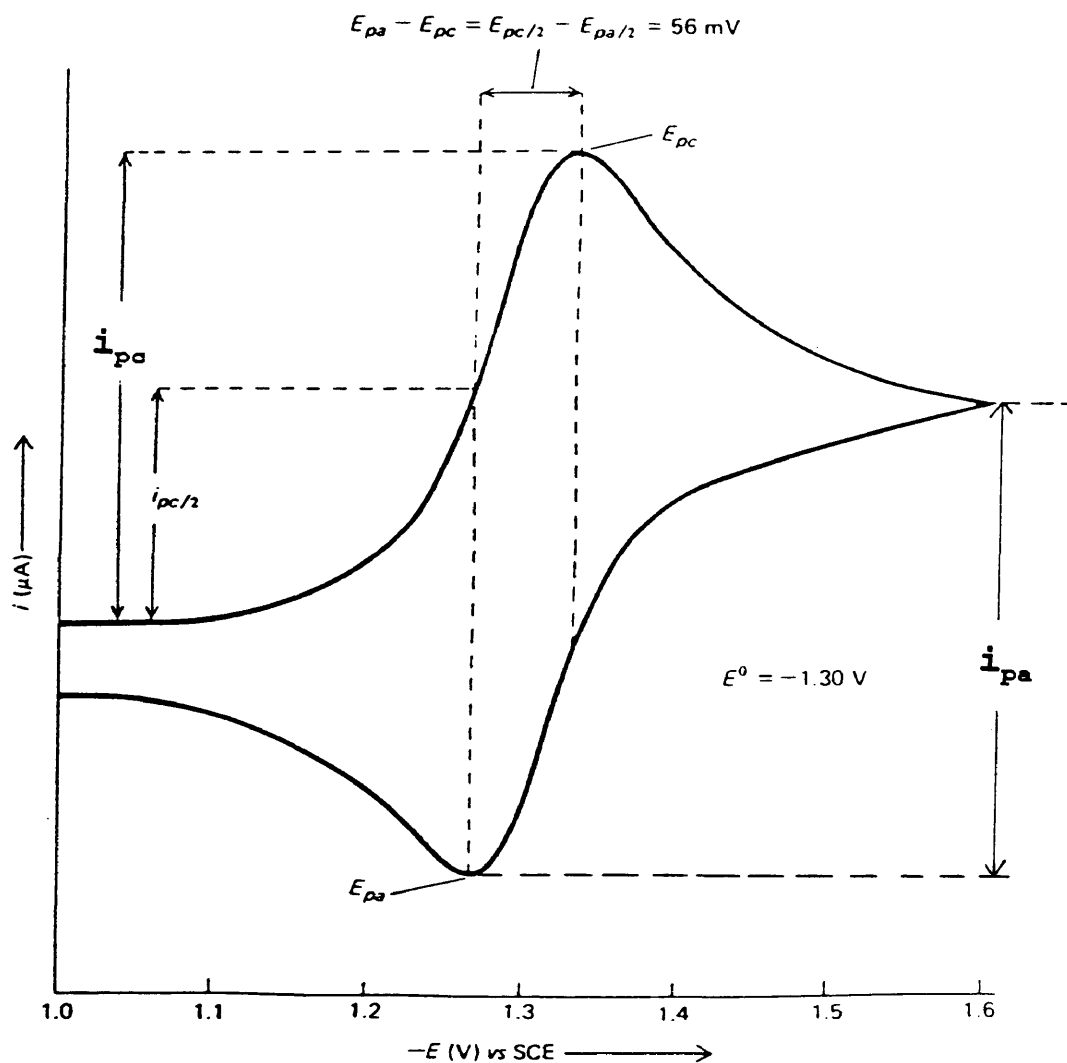


Figure 6. Typical Cyclic Voltammogram
(From ref.: Fry, A.J., 1989. Synthetic Organic Electrochemistry,
2nd.ed., John Wiley & Sons.

Chapter 5

RESULT AND DISCUSSION

5.1 NMR Analysis

Nuclear Magnetic Resonance (NMR) was used to analyze the effect of H₂S pressure, temperature, and solvent polarity on TBAQ reaction kinetics, and to identify reaction intermediates produced in a stirred tank reactor. **Figure 7** shows the NMR spectrum of TBAQ in N,N-dimethylacetamide (DMAC) solvent before and after reaction with H₂S. The degree of TBAQ conversion is calculated by comparing the peak areas of the TBAQ and H₂TBAQ aromatic protons. TBAQ has peaks centered at 8.2 ppm and H₂TBAQ has two groups of peaks centered at 7.5 ppm and at 8.6 ppm. The ratio of the H₂TBAQ aromatic proton area to the total aromatic proton area is equal to the mole percent of converted TBAQ.

5.1.1 The Effect of H₂S Pressure on TBAQ Conversion

Hydrogen sulfide concentration in solution, [H₂S], depends on the Henry's law constant, K_s, and the total pressure of H₂S:

$$K_s (T) = [H_2S] / P(H_2S) \quad (5-1)$$

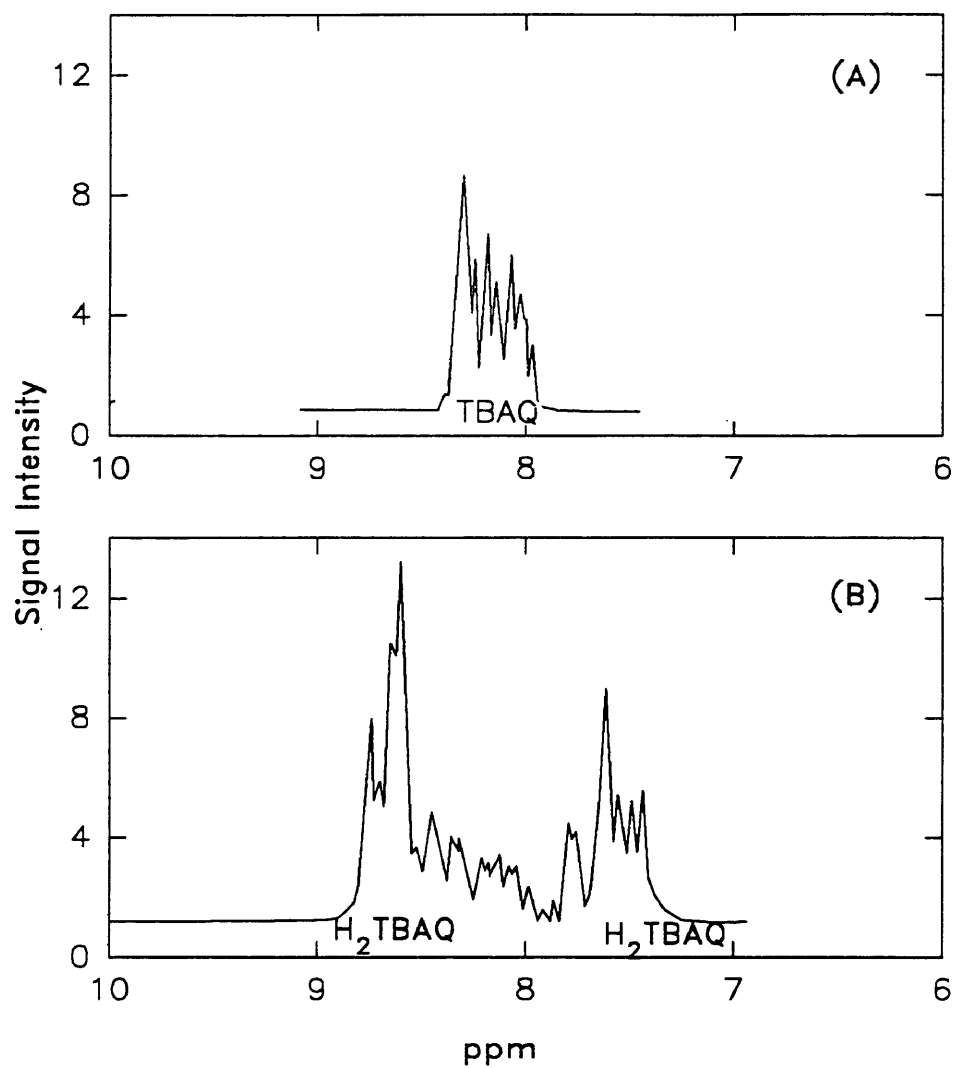


Figure 7. NMR spectra of A) unreacted TBAQ feedstock and B) H₂TBAQ product after reduction of TBAQ with H₂S.

At constant temperature, the concentration of H₂S in the solution increases when the total pressure of H₂S is increased.

In each set of experiments, the H₂S pressure was kept constant during the reaction, and the temperature was monitored. An increase of approximately 3°C was observed when H₂S was introduced into the reaction mixture containing TBAQ and the DMAC solvent. After 2-3 minutes the excess heat dissipated and the reaction mixture returned to the desired reaction temperature.

Before H₂S can react with TBAQ, it must diffuse from the bulk phase of the bubble to the surrounding liquid surface, dissolved into the liquid phase, and diffuse through the liquid bulk phase. The effect of the mass transfer in the liquid phase was reduced by stirring the liquid using a magnetic stirrer. The diffusion of H₂S in the bulk phase of the bubble to the liquid surface can also be minimized by using a sparger. However, our reactor was designed without a sparger. Therefore, it is noted that the measured rates include the effects of both the intrinsic reaction rate and the effect of H₂S diffusion.

Higher conversion of TBAQ results from higher H₂S pressure over a 32.2 to 92.2 psia range as shown in **figure 8**. Based on this result (see **table 3, appendix B**), it is suggested that the reaction mechanisms for the conversion of TBAQ to H₂TBAQ is initiated by:



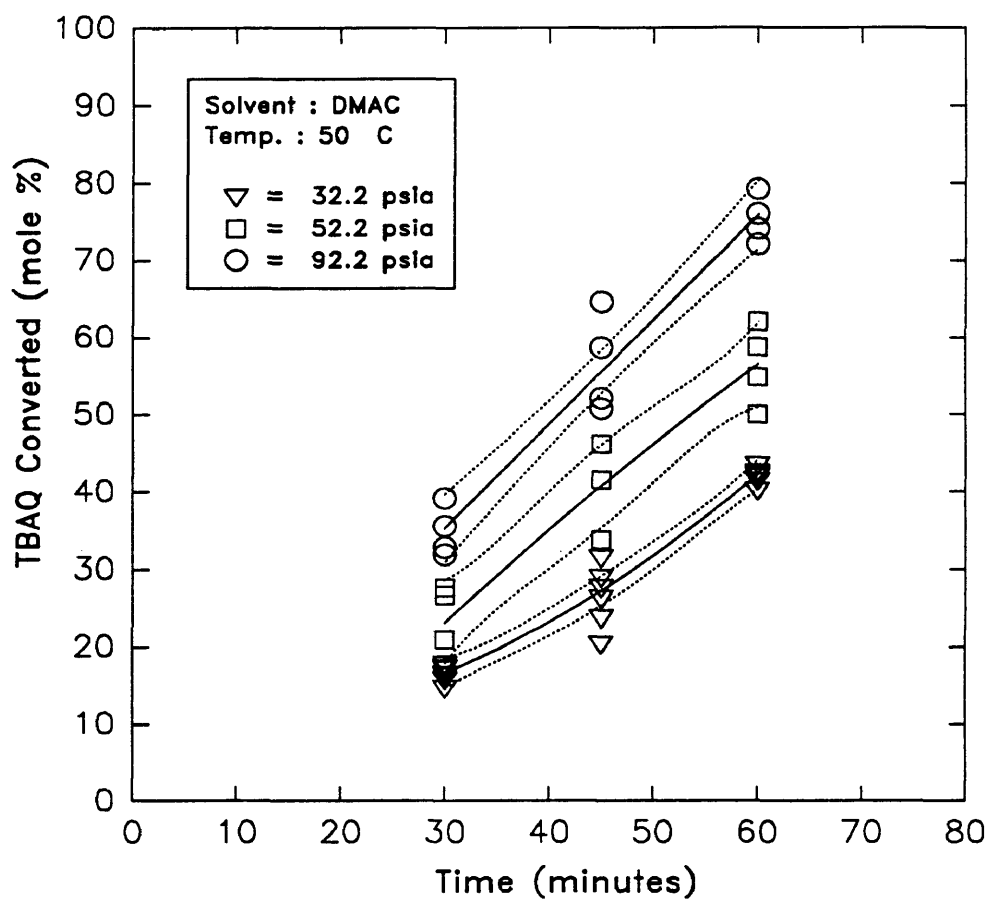


Figure 8. Effect of H₂S Pressure on TBAQ Conversion. The dotted lines represent the 95 % confidence range for each pressure studied.

where HS^- comes from the interaction between solvent and H_2S which forms a complex $[\text{solventH}^+ \text{HS}^-]$. If the step in equation 5-2 has the highest activation energy, then it will be rate limiting. Assuming that other steps are fast and irreversible, then the rate expression can be written as follows :

$$\text{rate} = k [\text{H}_2\text{S}] [\text{TSwQ}] \quad (5-3)$$

$$[\text{H}_2\text{S}] = K_s P(\text{H}_2\text{S}) \quad (5-1)$$

The reaction rate is first order in H_2S and TBAQ concentrations. Since the total H_2S pressure remains constant, the concentration of H_2S in the solution will be constant and the rate expression becomes pseudo first order:

$$\text{rate} = k' [\text{TBAQ}] = -d[\text{TBAQ}] / dt \quad (5-4)$$

$$\ln [\text{TBAQ}] = -k't$$

where $[\text{TBAQ}] = \text{mole \% of unconverted TBAQ}$

The rate constant k' is a function of H_2S pressure. For a constant H_2S pressure, the reaction rate is dependent on the TBAQ concentration only.

The obtained data (**table 3 in appendix B**) fits a $\ln[\text{TBAQ}]$ versus time (t) plot typical of a first order reaction (**figure 9**). Zero percent reaction did not occur at zero time but at 15 to 20 minutes indicating an induction period for the reaction.

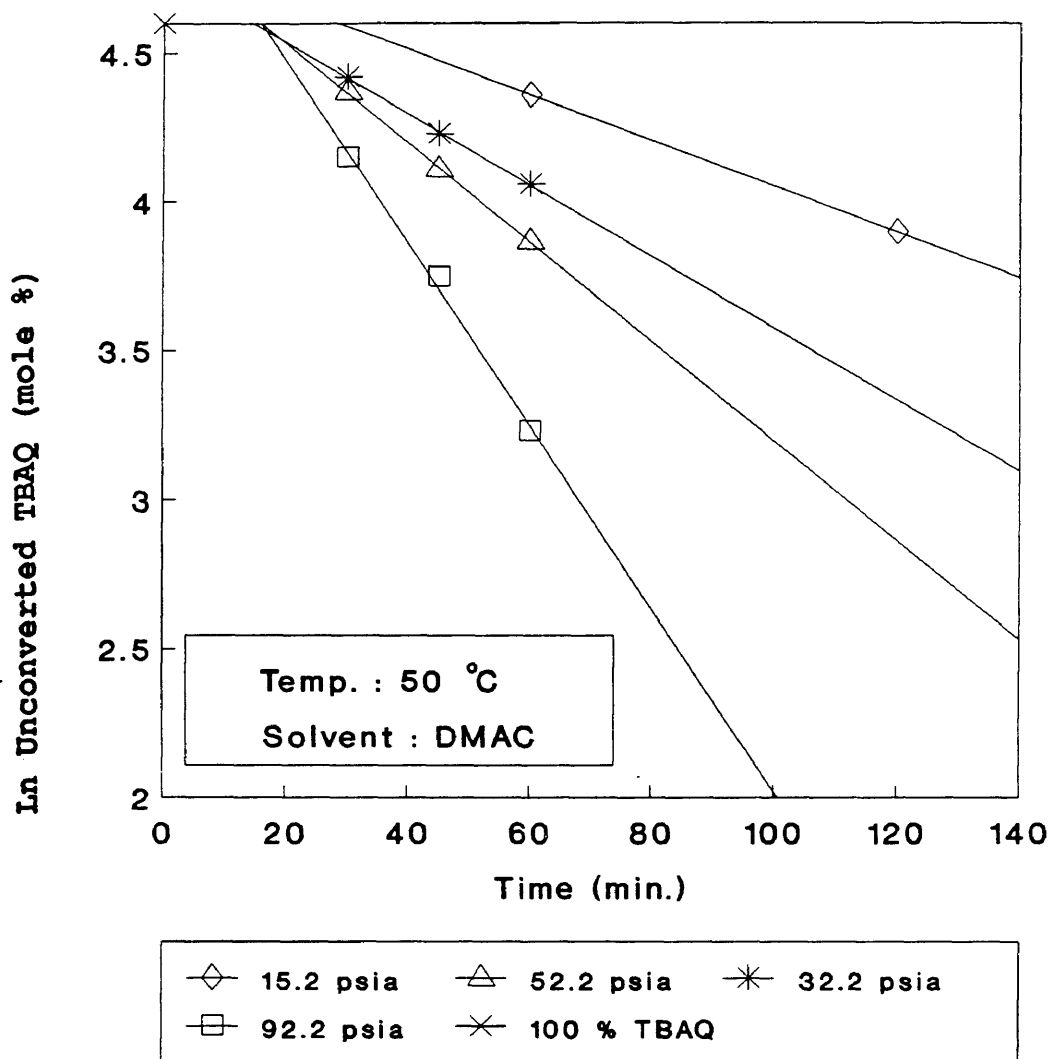


Figure 9. First Order Plot of TBAQ Conversion. Data for pressure at 92.2 psia, 52.2 psia, 32.2 psia, and 15.2 psia are from experiment # M8, # M15, # M16, # Mc7, respectively.

Analysis of NMR spectra indicated that there was some small amount of reaction at 15 minutes.

5.1.2 The Effect of H₂S Pressure on the TBAQ Reduction Rate Constant

The pseudo rate constant obtained from **figure 9** should increase linearly with an increase of H₂S pressure, if the reaction obeys the following equation:

$$k' = k [\text{H}_2\text{S}] = K_s k P(\text{H}_2\text{S}) = k'' P(\text{H}_2\text{S}) \quad (5-5)$$

Figure 10 shows that the measured reaction rate constant (*k'*) increased linearly as the pressure of H₂S increased for both DMAC and N-methyl-2-pyrrolidinone (NMP) solvents (data in **table 3, appendix B**). These results show that the reaction is first order with respect to H₂S pressure. The reaction rate constant of a system using DMAC as a solvent is higher than in NMP. It is reported that the H₂S solubilities in both solvents are not much different (*Murrieta-Guevara, Rodriguez, 1984; Hayduk, Pahlevanzadeh, 1987*). Hence, there is a possibility that molecular structure of the solvent has an important role in the interaction between solvent and H₂S (*Plummer, GRI 1990-5*).

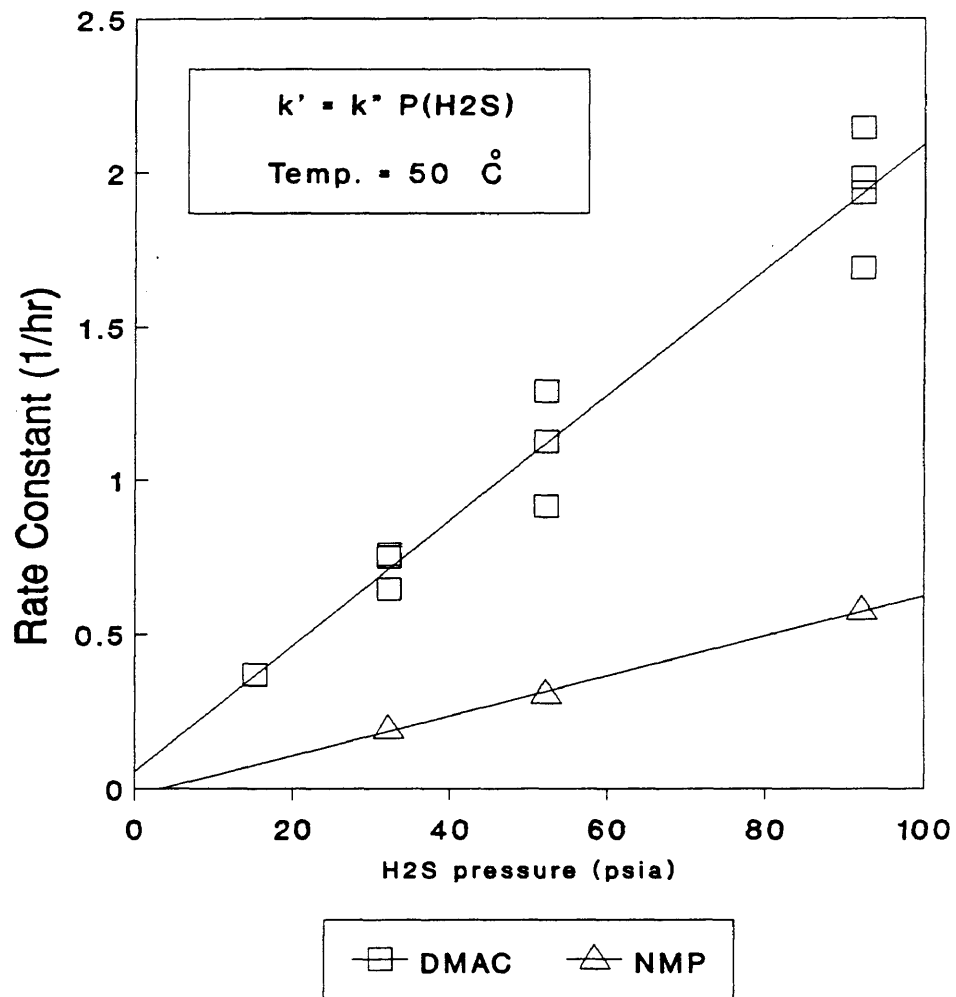


Figure 10. Rate Constant as a Function of H₂S Pressure

5.1.3 The Effect of Temperature on TBAQ Conversion

The effect of temperature on the TBAQ reaction rate was investigated using both the micro- and mini-glass reactors, see **table 4, appendix B**. DMAC was used as a solvent and the H₂S pressure was kept at 14.2 psia in the micro-reactor and about 52.2 psia in the mini-reactor. Increasing the temperature from 40 °C (313.1 K) to 60 °C (333.1 K) gave a significant increase in the conversion rate; see **figure 11**. A further increase of temperature to 70 °C (343.1 K) decreased the conversion rate significantly. It seems that the TBAQ conversion reached a maximum value at a temperature of about 60 °C (333.1 K). Reaction temperature affects both the reaction rate constant and the H₂S solubility. As the temperature increased, the H₂S solubility in DMAC decreased. Probably at temperatures above 60°C the decreased H₂S solubility decreased the reaction rate.

5.1.4 The Effect of Temperature on the TBAQ Reduction Rate Constant

More studies were made at various temperatures in order to investigate the effect of reaction temperature on the reaction constant. Based on the assumption of a pseudo first order reaction, the TBAQ conversion rate constant can be correlated to reaction temperature by the Arrhenius equation.

$$\ln k' = - Ea/(RT) + \ln A \quad (5-6)$$

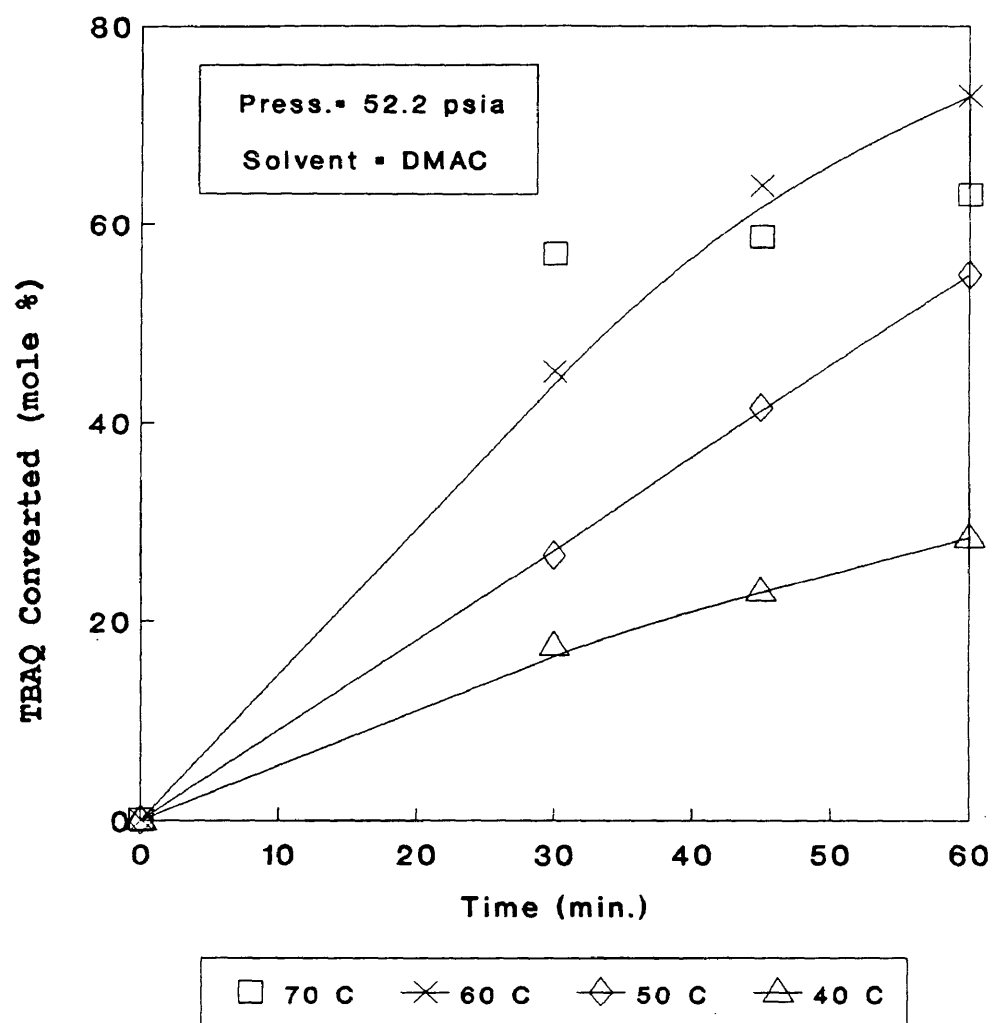


Figure 11. Effect of Temperature on TBAQ Conversion

where T = absolute temperature

R = Gas Constant

E_a = Activation energy

A = Pre-exponential factor

The plot of $\ln k'$ versus $1/T$ data obtained (table 3 appendix B) using a H_2S pressure of 52.2 psia in DMAC is shown in **figure 12**. With the H_2S pressure at 92.2 psia, the rate constant was larger than at 52.2 psia for the same temperature, but the slopes of the two Arrhenius plots were identical. This shows that the activation energy of the TBAQ conversion in DMAC (22.3 kcal/g-mole) does not depend on the H_2S pressure.

The activation energy of the TBAQ conversion in NMP (*Plummer, 1987*) is about 1/4 that found in this work for DMAC. This lower activation energy in NMP may be due to the higher polarity of NMP as suggested by Plummer. *Plummer (1987)* showed that TBAQ conversion increased with increasing solvent polarity.

5.1.5 Reaction Mechanisms

Based on the NMR, cyclic voltammetry and UV/visible data, the mechanisms of TBAQ reduction and formation of sulfur in amide solvents are presented here to make the discussion of the data more clear:

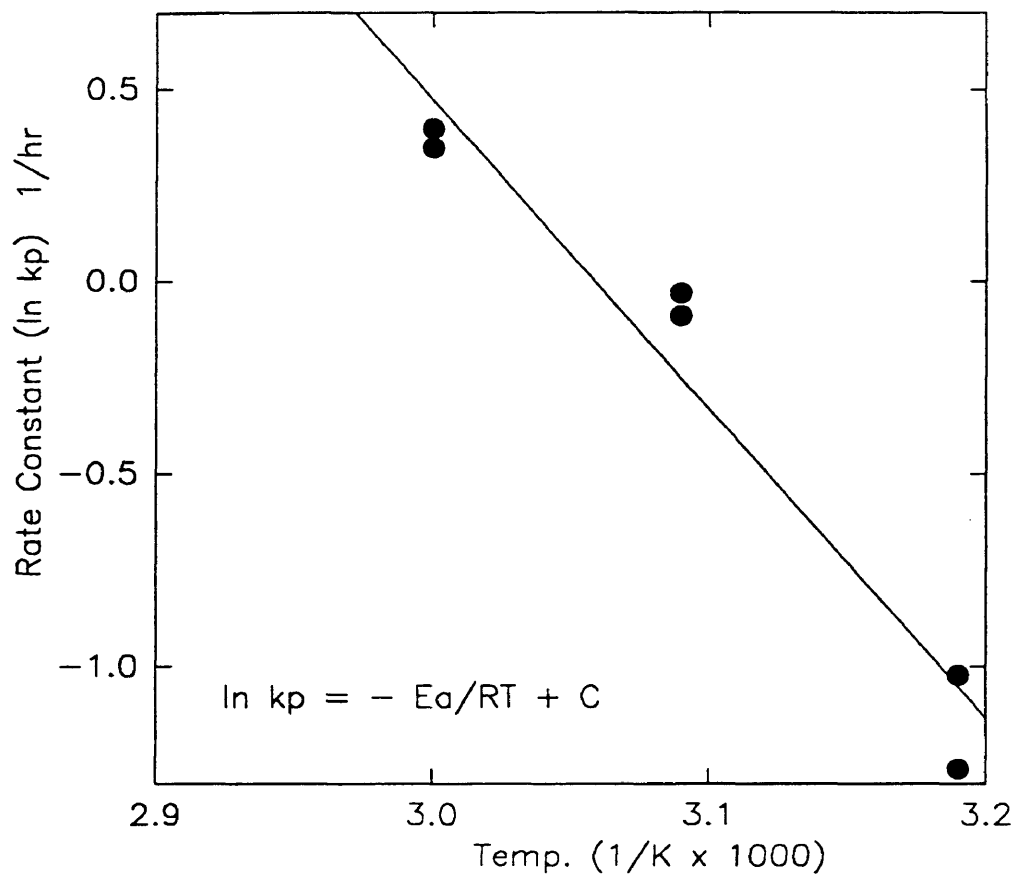


Figure 12. TBAQ reduction rate constant versus temperature (1/K); H₂S pressure = 52.2 psia; concentration of TBAQ = 15 wt.%; solvent = DMAC.



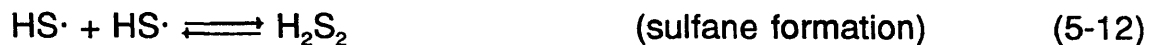
where A is an amide solvent such as NMP and DMAC. When H₂S is added to NMP solvent there is a strong interaction between H₂S and NMP, which can further undergo partial dissociation of H₂S into HS⁻.

A small amount of HS⁻ is required for the electron transfer step in equation 5-8. The equilibrium concentration of HS⁻ is small, but it is regenerated in further step 5-9 and its concentration remains constant.



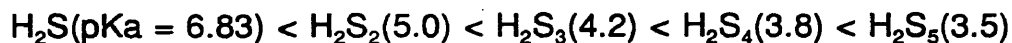
The electron and proton transfer reactions in equations 5-8 to 5-11 will be verified by cyclic voltammetry.

The sulfane formation during TBAQ reduction may be expressed as



Due to higher acidity, further TBAQ reduction will employ sulfane instead of H₂S.

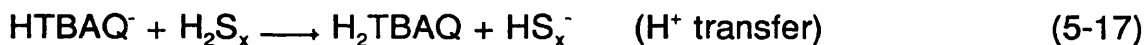
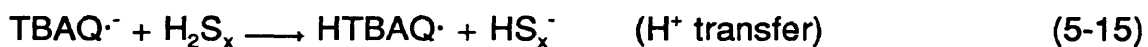
The acidity of sulfanes increases with increasing sulfur chain length and the order of acidity is given below (*Burton, Machmer, 1968*).



Therefore, longer chain sulfanes are likely to form complexes with an amide solvent more readily than does H_2S .



HS_x^- will reduce TBAQ more readily than HS^- or H_2S since it is a stronger electron donor agent. The TBAQ reduction with sulfane anions can be expressed as



This sequence of reactions could occur more rapidly than reactions 5-8 through 5-11. This is due to higher acidity of sulfanes than H_2S (*Burton and Machmer, 1968*). Since sulfanes have higher acidity than H_2S , reaction 5-13 is more favor-

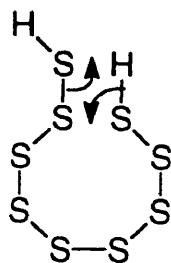
able than reaction 5-7. As a result, the chain growth is preferred because concentration of HS_x^- is greater than HS^- .

The chain growth probably occurs when sulfane radicals are consumed by a free radical termination process such as in equation 5-18.



Sulfur precipitation will occur when the sulfur atoms in the sulfanes grow to S_9 or higher. The mechanisms of sulfur precipitation can be expressed as:

when $x+y = 9$



(ring formation)

when $x+y > 9$



when $x+y < 9$



The possibility that polysulfane growth proceeds via a free radical mechanism has been reported in the literature (*Pryor W. A., 1962; Grant D., 1964; Burton K. W. C., Machmer P., 1968; Wallace T. J., 1963*). The presence of radicals has been confirmed indirectly by the development of blue or green color in polysulfanes solutions (*Pryor W. A., 1962*). A similar coloration occurred in this study. Anionic mechanisms for the sulfane formation have also been proposed (*Pappas J. A., 1977; Hyne J. B. and Derald. D., 1980; Burton K. W. C., and Machmer P., 1968*). However, the chain growth of polysulfane via an anionic mechanism seems unlikely in this process. There is no evidence for polysulfanes formation from HS_x^- species and H_2S , nor from the condensation of HS_x^- species. With H_2S as a source of sulfur atoms, it is most likely that polysulfane chain growth proceeds via a free radical termination process (equation 5-18).

5.1.6 The Effect of Temperature on Sulfur Formation

The percentage of sulfur recovered is calculated from the solid sulfur obtained and the amount of converted TBAQ. Since conversion of one mole of TBAQ to H_2TBAQ requires one mole of H_2S , then one mole of converted TBAQ yields one mole of S atoms in solution. However, sulfur (S_8) recovered is less than the amount of S atoms in solution, due to several steps involved in the sulfur formation, i.e. equations (5-7) through (5-19).

There was only a small increase in the percent of sulfur recovered as the

temperature increased, see **table 5, appendix B**. The sulfur formation data were poorer in reproducibility than the TBAQ conversion data. In some cases, there was a small amount of additional solid sulfur formed after the filtrate had been stored for 24 to 48 hours at room temperature.

If the sulfur formation process can be represented as first order with respect to the concentration of S atoms in solution, then the rate of sulfur formation can be expressed:

$$\text{rate} = -d[S]/dt = k_s [S] \quad (5-23)$$

where k_s = the first order rate constant

[S] = sulfur in solution

An approximate rate constant k_s can be calculated from the data. Using the plot of k_s as a function of temperature (see **figure 13**), the activation energy of sulfur formation can be obtained. The calculated activation energy of 2.58 kcal/g-mole seems very low, and it is much lower than the activation energy for the TBAQ conversion of 22.3 kcal/g-mole. It is suggested that the chain growth of polysulfanes occurs via the termination of an $HS_x\cdot$ and $HS_y\cdot$, two $HS_x\cdot$, or two $HS_y\cdot$ radicals, where x and y are even and odd integers respectively. Also, it is known that free radical termination reactions have low E_a values (*Lowry and Richardson, 1987*), which is consistent with the calculated value obtained from figure 13. This

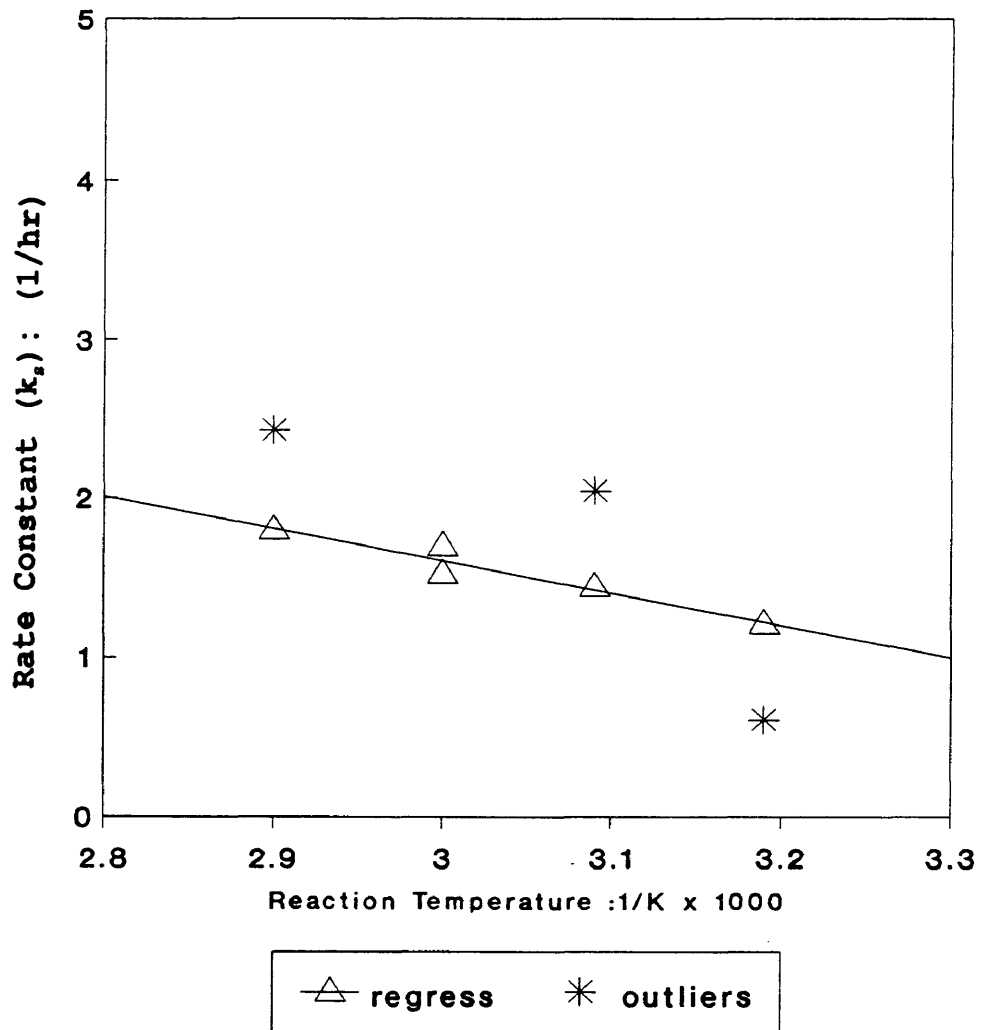


Figure 13. Arrhenius Plot of Sulfur Formation
(Solvent: DMAC; H_2S Pressure : 52.2 psia)

result supports the reactions in equations 5-12 and 5-18.

5.1.7 The Effect of H₂S Pressure on Sulfur Formation

The effect of H₂S pressure on sulfur formation was studied using DMAC as solvent at a reaction temperature of 50 °C and at a pressure of 15.2 to 92.2 psia. **Figure 14** shows the data of mole percent of sulfur recovered versus the H₂S pressure from **table 6, appendix B**. This figure shows that sulfur recovery data are scattered. It is difficult to draw a conclusion about the effect of H₂S pressure on sulfur recovery from these data. It seems that H₂S pressure is not the only factor controlling the sulfur recovery. Sulfur polymerization chemistry is known to be complex and large variations in results have been reported (*Burton and Machmer, 1987*).

5.1.8 The Role of Solvent on TBAQ Conversion

Several solvents for use in the microreactor were initially screened in order to investigate the role of polarity and molecular structure on TBAQ reduction. Some solvents had aromatic protons or amide protons with chemical shifts which overlapped the NMR aromatic region for TBAQ and thus were not selected for this study, even though they exhibited very high TBAQ solubility. Solvents tested in the microreactor system have the structures as shown in **figure 15**.

A previous NMR study (*Plummer, GRI 1991-9*) showed a large variation in

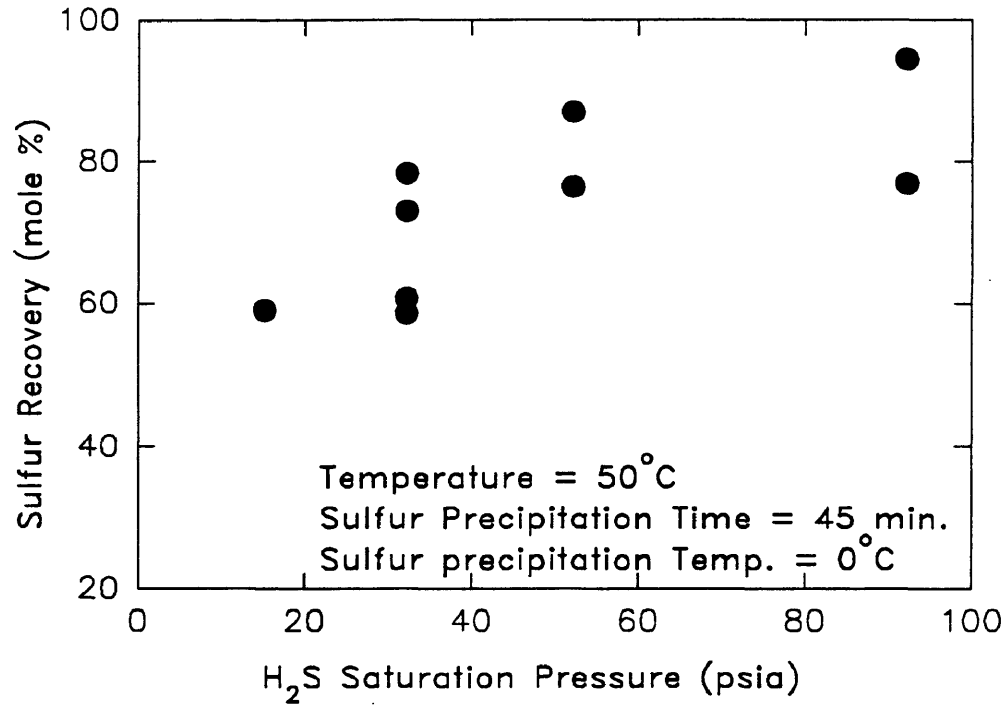
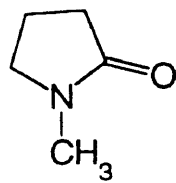
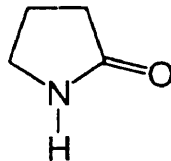


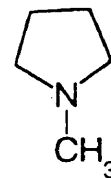
Figure 14. Sulfur Recovery as a Function of H₂S Pressure



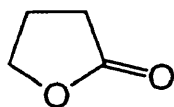
NMP



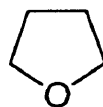
PN



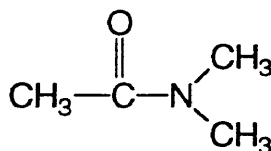
NMPY



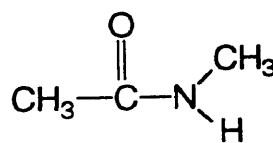
GBL



THF



DMAC



MAC

Figure 15. The Molecular Structure of Selected Solvents

the chemical shifts for the aromatic protons of TBAQ with solvents of different polarities and structure. In this Plummer study, these critical solvent polarity and structure differences were correlated to TBAQ conversion rate and extent. In this study, in THF, a low polarity solvent, the aromatic protons of TBAQ were found to be more widely separated (**figure 16**) than in NMP, a high polarity solvent. This result is in agreement with those of Plummer (*Plummer, GRI 1991-9*). The chemical shifts of some aromatic protons of TBAQ may be perturbed to a greater extent in NMP than in THF because of a stronger interaction between TBAQ and NMP. This interaction produces an external field effect that changes the ring current in TBAQ (*Foster, 1969*). Because the interaction between TBAQ and THF is much less, there is a smaller external field effect that can change the ring current in TBAQ. The ring-current effects on aromatic protons have been reported by Foster (*Foster, 1969*). Strong solute-solvent interaction may well lower the energy of the Lowest Unoccupied Molecular Orbital (LUMO) of TBAQ by stabilizing the excited state.

Addition of H₂S to NMP changes the solvent from colorless to transparent blue then to green. The blue color disappeared within one minute and the solution remained a green color. The solution then stayed green unless purged with N₂, then it turned yellow. The reason for the change in color from blue to green is not clear at this time. It may be due to a small amount of oxygen impurity in the solvent which oxidizes the blue species, probably a solvent-H₂S complex, into

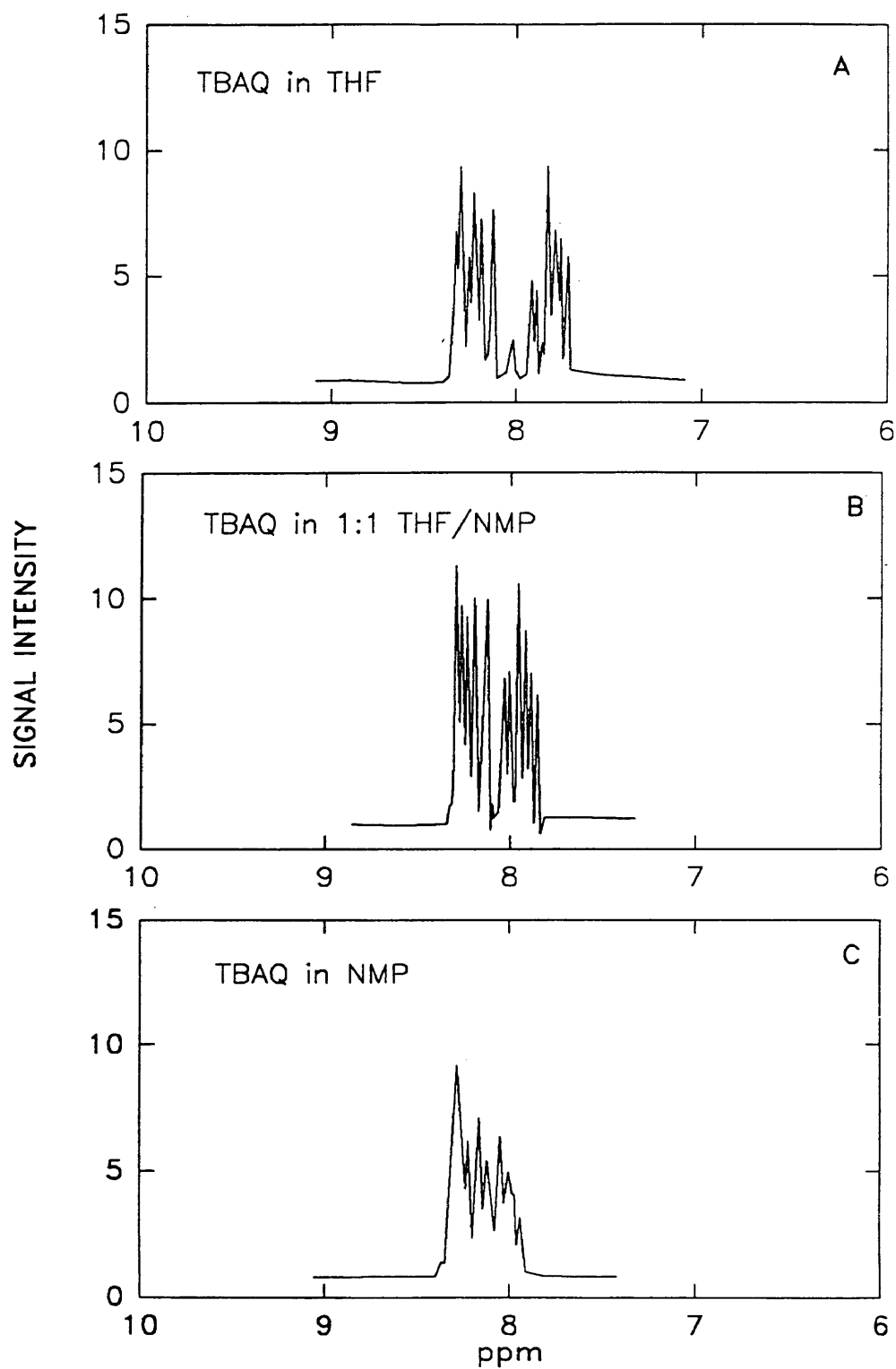


Figure 16. Effect of solvent polarity on the chemical shift of aromatic protons. The chemical shift is caused by a change in the aromatic electron density of the ring due to an interaction between the solvent and TBAQ.

another unknown species which is yellow. The combined blue and yellow species would produce the observed green color. Purging the green mixture with N_2 containing a trace of oxygen then resulted in a yellow solution. A blue solution is also obtained when NaHS is added to NMP. These color changes suggest the formation of a charge-transfer complex between H_2S or NaHS and NMP solvent.

NMP is known to have three resonance structures. The resonance structures of NMP are shown in **figure 17**. Of the three resonance structure, resonance form III is likely to have an important role in the formation of a complex with H_2S or NaHS. The resonance III of NMP can form polarized or ionized complexes (IV, V and VI) as shown in the **figure 17**. Even though these complexes have blue color, the exact nature of these complexes is unclear at this time. However, the UV/VIS spectra also provided evidence for this charge-transfer complex; these data are presented in a separate section.

The reduction of TBAQ by H_2S probably is initiated by a complexation step between solvent and H_2S forming HS^- ions. This complexation is followed by an electron transfer from HS^- to TBAQ. The electron is transferred from the Highest Occupied Molecular Orbital (HOMO) level of the solvent-complexed H_2S or HS^- species to the LUMO level of the solvent-complexed TBAQ molecule, see equations 5-7 and 5-8. The electron transfer step is followed by a proton transfer. Either H_2S or an intermediate sulfane (H_2S_x) can act as a proton donor (see equation 5-9). The possibility of the sulfane being an intermediate was discussed

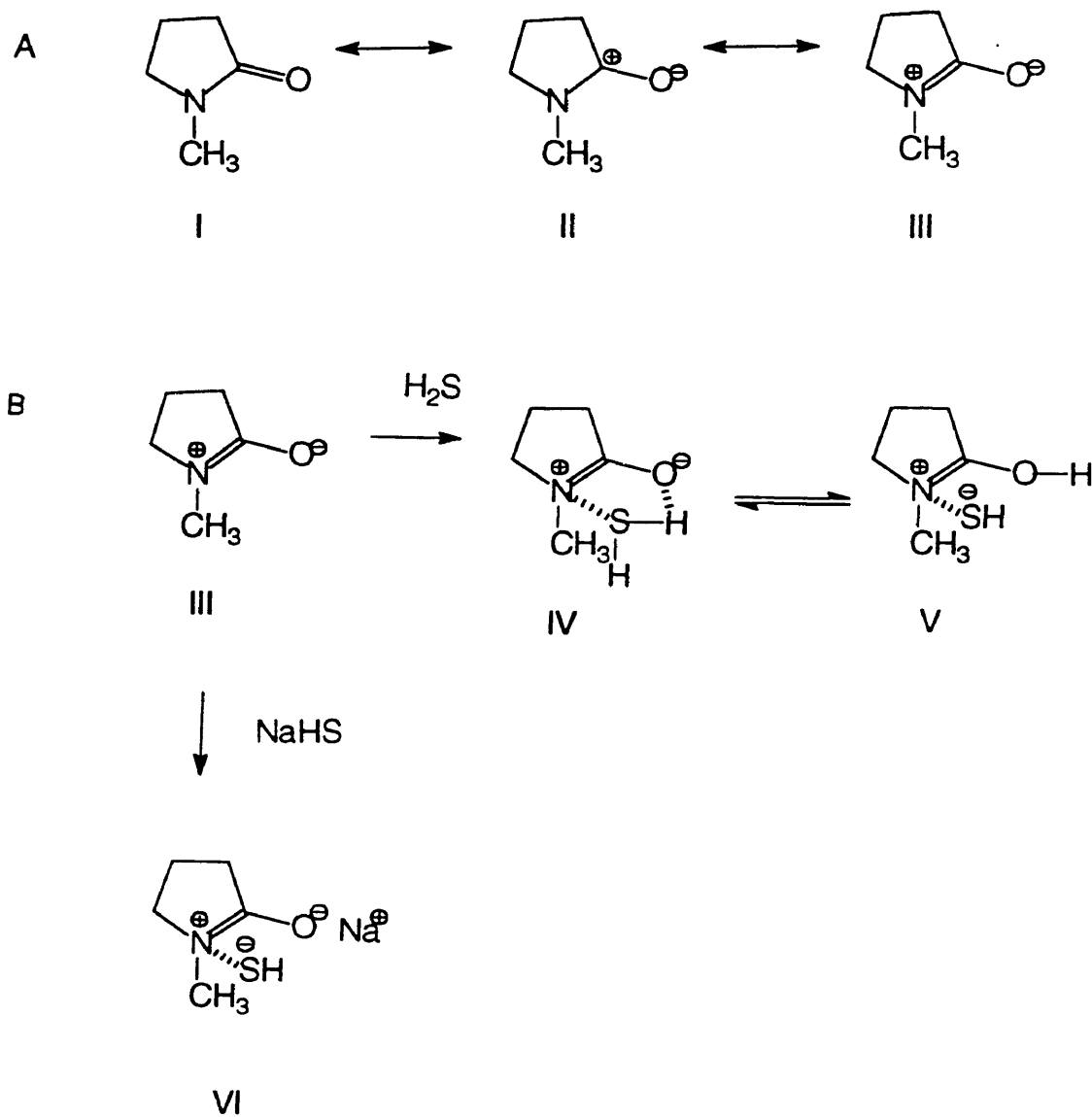
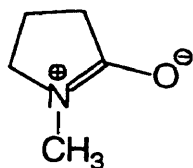


Figure 17. (A) Resonance structures of NMP; (B) NMP-H₂S and NMP-NaHS complexes.

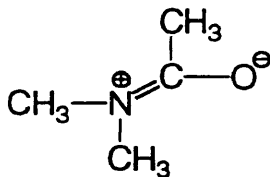
in the section on sulfur polymerization.

When H_2S was added into NMP-TBAQ solution, the transparent yellow solution turned green, then gold yellow, then an opaque dark brown within 15 minutes, and sulfur appeared as a yellow precipitate at the end of reaction (data in **table 3, appendix B**). The presence of the blue complex between H_2S and NMP in the yellow solution may be the cause of the green color in this mixture. This blue color is also present in other amide solvents such as DMAC, but not in non-amide solvents. This suggests that a complex between HS^- and the amide solvent is formed, which supports the reaction mechanisms in equation 5-7.

The reaction rate in DMAC, with a slightly smaller dipole moment (3.71 Debye) than that of NMP, is slightly faster than the reaction rate in NMP. The molecular structure of the solvent may affect the interaction with H_2S and quinones (*Plummer, GRI 1990-5*), as shown by the higher conversion rate in DMAC than in NMP. The resonance structures of NMP and DMAC are shown as



NMP



DMAC

The restricted rotation of the five-membered ring in NMP hinders proper orbital orientation for the formation of this resonance species. Therefore, this restricted rotation limits formation of this resonance form of NMP. Compared to the resonance structure of NMP, the resonance form of DMAC is more easily formed. Based on this structure hindrance, the population of H₂S-NMP complex will be lower than H₂S-DMAC complex. The polarity of the solvent appears not to be the only dominant factor in the TBAQ conversion.

Using γ -butyrolactone (GBL) as a solvent, no reaction was observed between H₂S and TBAQ and NMR analysis showed that no TBAQ was converted (**table 7, appendix B**). Solvent polarity can not be the sole influence, since GBL has the highest dipole moment (4.12 Debye) of all the solvents investigated. The molecular structure of GBL is similar to that of NMP (see **figure 15**), except oxygen in GBL replaces nitrogen in NMP. The solubility of H₂S in GBL was not found in the literature. Since H₂S has a significant solubility in other oxygenated compounds such as methanol, tetrahydrofuran and propylene carbonate, it is reasonable to assume there is also sufficient H₂S solubility in GBL for the reaction to proceed. The lack of any reaction suggests that more is involved than solvent polarity.

GBL has three resonance structure such as NMP. These resonance structures are shown below.

one of the methyl groups of DMAC replaced by a hydrogen atom in MAC (see **figure 15**). MAC has a higher dipole moment (4.27 Debye) than DMAC (3.71 Debye). It was expected that if the reaction rate depends only on the polarity of the solvent the reaction would go faster using MAC. But the result showed that the conversion of TBAQ was slower when using MAC (see **table 7, appendix B**).

In order to investigate the role of the carbonyl group, N-methylpyrrolidine (NMPY) was chosen as the solvent. NMPY is similar in structure to NMP solvent, but without a carbonyl group and has a low dipole moment of 2.0 Debye (see **figure 15**). The reaction using NMPY as the solvent was unusual compared to the reaction using other solvents. After 5 minutes of reaction, the solution turned an opaque orange and then an opaque dark brown after about 30 minutes. After 3 hours, the solution became opaque reddish black. An orange emulsion separated at the top of the system and after 22 minutes a yellow solid formed on the wall of the glass reactor. This yellow solid was removed, washed, and dissolved in acetone. NMR analysis showed it to be TBAQ. The remaining solution was also analyzed using NMR, but the NMR spectrum was completely different from that in other solvents and exhibited no peak of H_2TBAQ . It appears that if any reaction of TBAQ and H_2S occurs in NMPY, it is more complicated than the reaction in amide solvents and H_2TBAQ is not a product.

Reaction of TBAQ and H_2S in polar solvents such as NMP and DMAC showed that TBAQ conversion was higher, than in less polar solvents (*Plum-*

mer, 1987). In a mixture of methanol (2.87 Debye) and tetrahydrofuran (1.75 Debye), which has a much lower dipole moment than that of NMP (4.09 Debye), there was no reaction between TBAQ and H₂S; see **table 7, appendix B**. Also, in GBL (4.12 Debye), a more polar solvent than NMP, the TBAQ conversion was not observed. In MAC (4.27 Debye), a more polar solvent than NMP, the TBAQ conversion was smaller than in NMP. These results show that solvent polarity is not the only factor that affects the TBAQ conversion. The ability of the solvent to complex with H₂S may be a requirement. Tertiary amides, such as NMP and DMAC, appear to be better solvents for TBAQ reduction than secondary amides, cyclic ethers, alcohols, or lactones.

5.1.9 The Formation of Sulfanes as Intermediate Species in TBAQ Reduction and Sulfur Polymerization

To study sulfane formation, the experiments were conducted in a sealed NMR tube reactor since it was suggested that sulfanes H₂S_x are unstable and decomposed rapidly to form H₂S and sulfur. In the NMR tube reactor, the initial H₂S pressure was set at 52.2 psia to prevent the decomposition of sulfanes.

When H₂S was added to a solution of TBAQ in DMAC, the solution was yellow at room temperature. The initial H₂S pressure inside the NMR tube was 52.2 psia. The NMR spectrum showed that at 15 minutes no new peak appeared; see **figure 18**. After 1 week, the new peak appeared at 3.85 ppm and there was

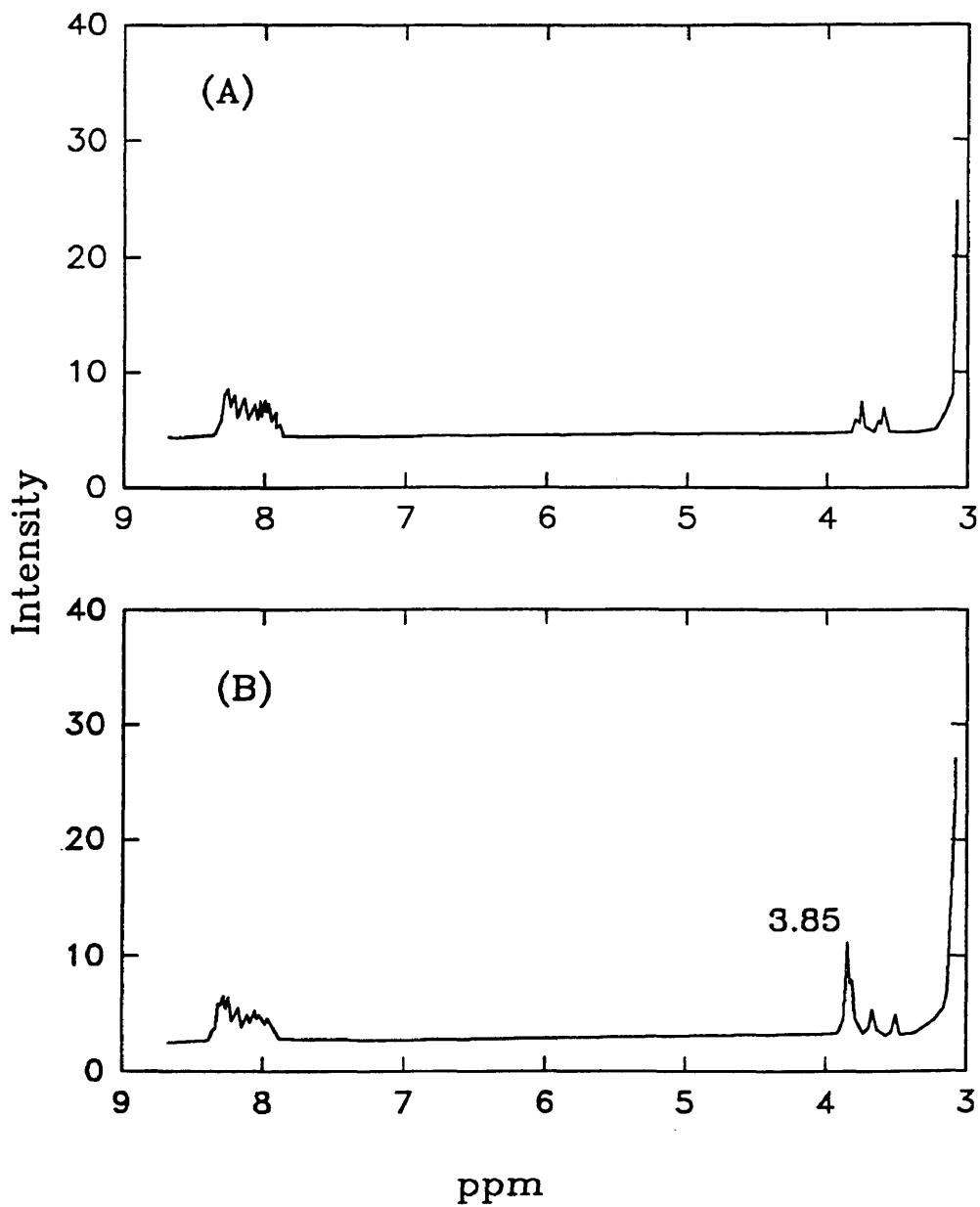


Figure 18. NMR spectra of TBAQ-H₂S in DMAC at initial pressure of 52.2 psia and at room temperature. (A) after 15 minutes of reaction, and (B) after 7 days. Sulfane peak appears at 3.85 ppm (TMS external is at 0 ppm)

a yellow solid at the bottom of the tube.

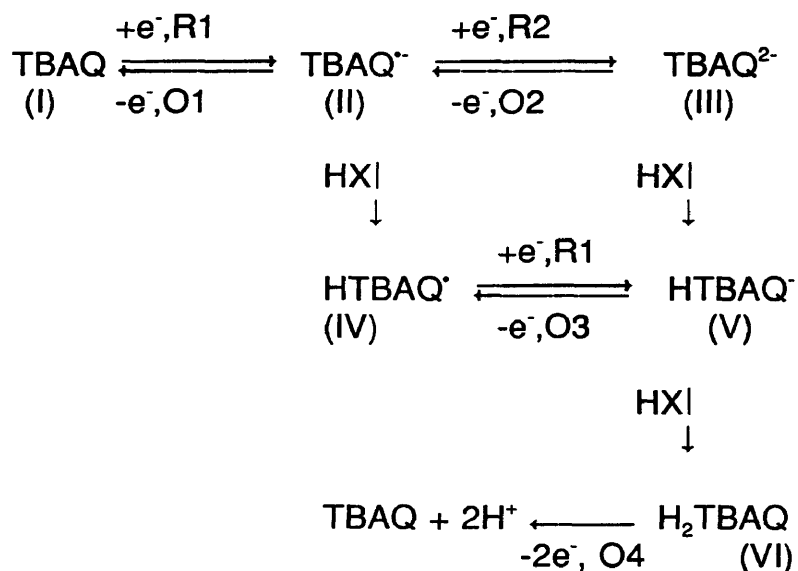
The appearance of a peak at about 3.85 ppm may result from the formation of sulfanes H_2S_x with $x \geq 3$ in DMAC solvent. Muller and Hyne reported that the chemical shifts in CCl_4 for the sulfanes H_2S_x with $3 \leq x \leq 9$ are between 3.98 ppm and 4.27 ppm (*Muller and Hyne, 1968*). The NMR signal for a shorter sulfane (H_2S_2) is shifted to much lower ppm values and may be obscured by the large solvent peak. The precipitation of sulfur indicated that polysulfanes are unstable. The long polysulfanes decomposed to form S_8 and H_2S or H_2S_x . The presence of sulfanes support the equations 5-18 to 5-20 in the proposed mechanisms of TBAQ reduction and sulfur formation.

5.2 Cyclic Voltammetry

Cyclic voltammetry has been used to study the mechanism of TBAQ reduction in the reaction system. The investigation focused on the role of the solvent and the effect of the proton donor agent in the solution. Also, the relationship between the measured reduction/oxidation potential and the Lowest Unoccupied Molecular Orbital (LUMO) and the Highest Occupied Molecular Orbital (HOMO) energy levels was studied.

5.2.1 Reaction Mechanisms in Cyclic Voltammetry

The proposed mechanisms for the electron and proton transfers in the cyclic voltammetry of TBAQ are represented below.



The structure of each molecule (I, II, etc) in the scheme of reaction is shown in **figure 19**, and the R1,R2, etc and the O1, O2, O3, O4 values are potentials of reduction and oxidation peaks.

The reduction peak of TBAQ (I) was represented by peak R1, and the oxidation peak of TBAQ \cdot^- (II) was represented by peak O1. Without any protic agent (HX) in the solution, TBAQ \cdot^- was reduced further to form TBAQ $^=$ which was represented by peak R2. Peak O2 represented the oxidation of TBAQ $^=$ back to TBAQ \cdot^- .

The presence of protic agent in the solution will protonate TBAQ \cdot^- to form HTBAQ \cdot^- (IV). Species IV is reduced rapidly to HTBAQ \cdot^- . The increasing height of the reduction peak R1 may be because the reduction of HTBAQ \cdot^- is taking place at the same potential as the reduction of TBAQ (peak R1) (*Chambers, 1967*). HTBAQ \cdot^- can also be formed from the protonation of TBAQ $^=$. Detailed discussion of the protic agent effect will be found in the next sections. It was suggested that HTBAQ \cdot^- could be a stable intermediate in the sequence of reactions. This suggestion is supported by the results from Koshy (*Koshy et al., 1980*) who reported that the hydroquinone anion is a stable species. Since HTBAQ \cdot^- can be an intermediate then the oxidation peak O3 may represent the oxidation peak of HTBAQ \cdot^- .

Protonation of HTBAQ \cdot^- could form H $_2$ TBAQ. The presence of H $_2$ TBAQ in the solution can be detected by the appearance of oxidation peak of H $_2$ TBAQ. Peak O4 may represent the oxidation of H $_2$ TBAQ. The presence of H $_2$ TBAQ and the

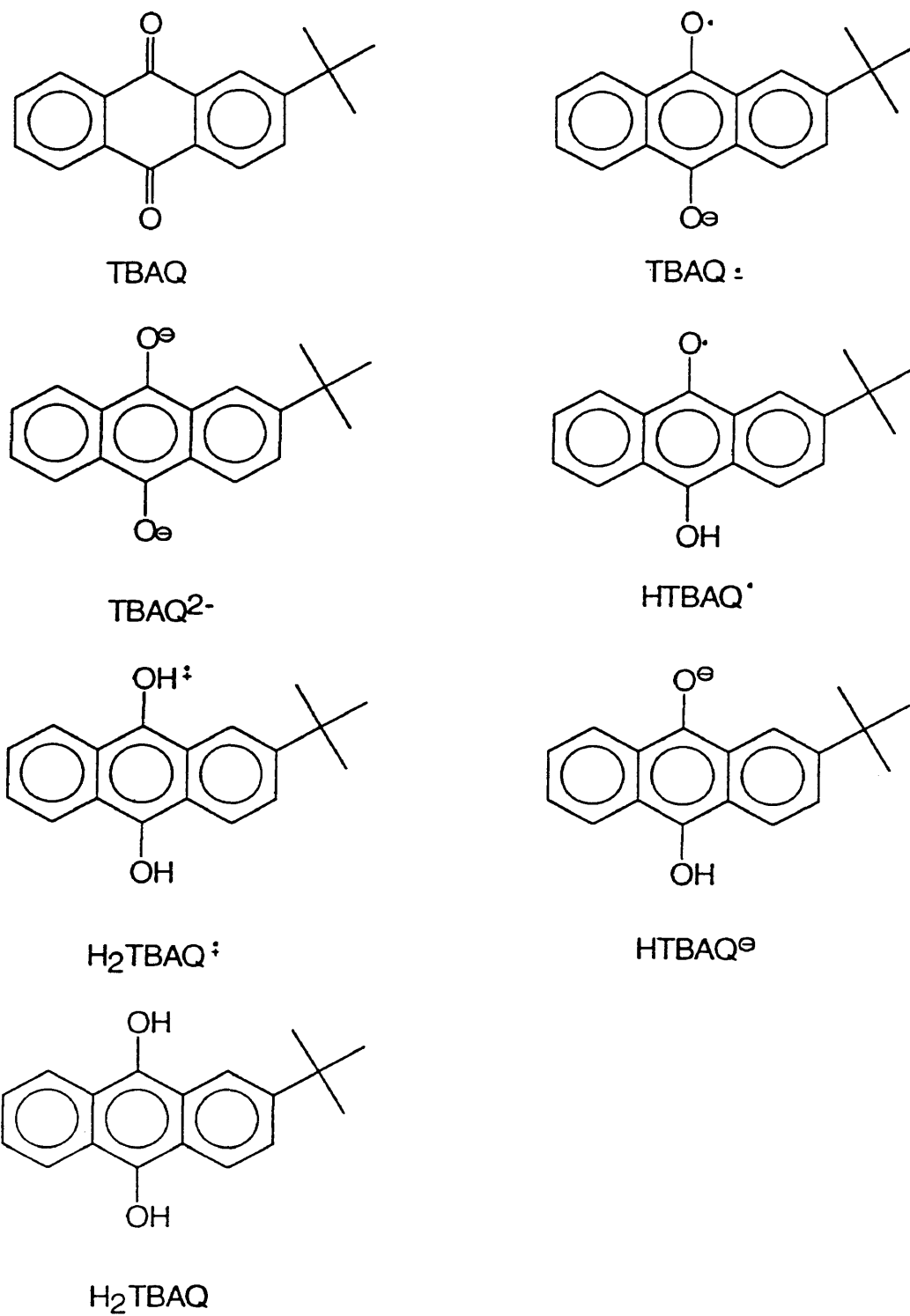


Figure 19. Structure of quinones in the scheme of reaction.

appearance of its oxidation peak (O4) will be discussed more detailed in the next sections

5.2.2 Aprotic Solvent Effect

The effect of solvent polarity on TBAQ reduction and sulfur formation has been studied in the previous section. By using cyclic voltammetry, the effect of solvent can also be investigated. TBAQ showed reversible two reduction peaks and two oxidation peaks in cyclic voltammogram. Reversible reduction and oxidation in cyclic voltammetry is known by a small potential gap between reduction and oxidation peaks, and also by the same peak height (current) of reduction and oxidation couple (*Fry, 1989*)

The effect of the solvent can be observed from the potential of the reduction and oxidation peaks of TBAQ in the cyclic voltammogram. A polar solvent is needed in cyclic voltammetry to maintain high ionic mobility and conductance. Several solvent and electrolyte combinations were studied to select an electrochemical system which gave a low background signal in the potential region where TBAQ reduction/oxidation (redox) occurs. The complete results of these studies are presented in **table 8, appendix C**.

As seen in **table 8, appendix C**, some solvents have a large potential window in certain electrolytes. Using sodium perchlorate as the electrolyte, NMP, DMAC, N,N-dimethylformamide (DMF), acetonitrile (AN), 4-hydroxy-4-methyl-2-

pentanone (HMP), and ethylacetate (EA) showed a clean background window from 1.3 Volts to - 2.5 Volts. Other solvents were rejected because they had a smaller window or did not dissolve sodium perchlorate. Solvents such as NMP, DMF, DMAC and pyridine (PY) gave an acceptable window using tetrabutylammonium perchlorate (TBAP) as the electrolyte.

In order to obtain information about the correlation between polarity of the solvent and the reduction/oxidation potentials of TBAQ, solvents with varying dipole moments were selected. The solvents selected are shown in **table 9, appendix C**. This table displays the reduction peaks (R1 and R2) and oxidation peaks (O1 and O2) potentials for TBAQ in selected solvents using a silver/silver nitrate reference electrode. This reference electrode has a potential difference of +0.426 Volts versus the saturated calomel electrode (SCE).

Compounds representing solvents with small dipole moments are p-xylene (0.01 Debye), dioxane (0.45 Debye) and tetrahydrofuran (THF) (1.75 Debye). p-Xylene was rejected because of its low solubility for the TBAP electrolyte. Dioxane appeared to dissolve the tetrabutylammonium perchlorate (TBAP), but TBAQ showed no redox signal in the cyclic voltammogram. The conductivity in this medium may have been insufficient to transfer an electron from the electrode to the electroactive TBAQ species. Hence, solvent polarities in the 0.01 to 0.45 Debye were not investigated.

In THF solvent, TBAQ has only a first reduction peak (R1) at potential of

-1.12 Volts (vs. SCE). The reduction potential for TBAQ was at -0.92 Volts in both a 50/50 molar mixture of THF and NMP and in pure NMP. NMP solvent with a higher dipole moment ($\mu = 4.09$ Debye) dominated the solvent effect in this mixture. The cyclic voltammogram of TBAQ in THF ($\mu = 1.75$ Debye) also showed an irreversible redox cycle and the first reduction peak was shifted to a more negative potential than the potential for the same peak in DMF or NMP. It is still unclear for the irreversible redox cycle in THF. The dielectric constant of THF ($\epsilon = 7.58$) is much less than NMP ($\epsilon = 32.2$). It was found that in the irreversible reduction of organic compounds, $E_{1/2}$ can be shifted to more negative values if the dielectric constant of the solution is decreased (*Tomilov, 1972*).

Solvents with higher polarity which stabilize the radical anion (TBAQ \cdot^- , structure II in **figure 19**) and dianion (TBAQ $^{2-}$, structure III in **figure 19**) were predicted to cause the potential of both reduction peaks of TBAQ to be more positive than in solvents with lower polarity. The experimental data are not consistent with these predictions. Pyridine (PY) (2.37 Debye) has a lower dipole moment than either DMF (3.24 Debye) or NMP (4.09 Debye). But the reduction potentials of TBAQ in pyridine are more positive than the potentials obtained in the other solvents, see **table 9 appendix C**. As mentioned above, the opposite was expected. The first TBAQ reduction peak (R1) in PY is shifted +0.02 Volts from the corresponding peaks in DMF and NMP, and the second TBAQ reduction peak (R2) is shifted +0.32 Volts, see **figure 20**. Hence, other factors in addition to polarity are needed to quantify solvent effects in order to explain the shifts of

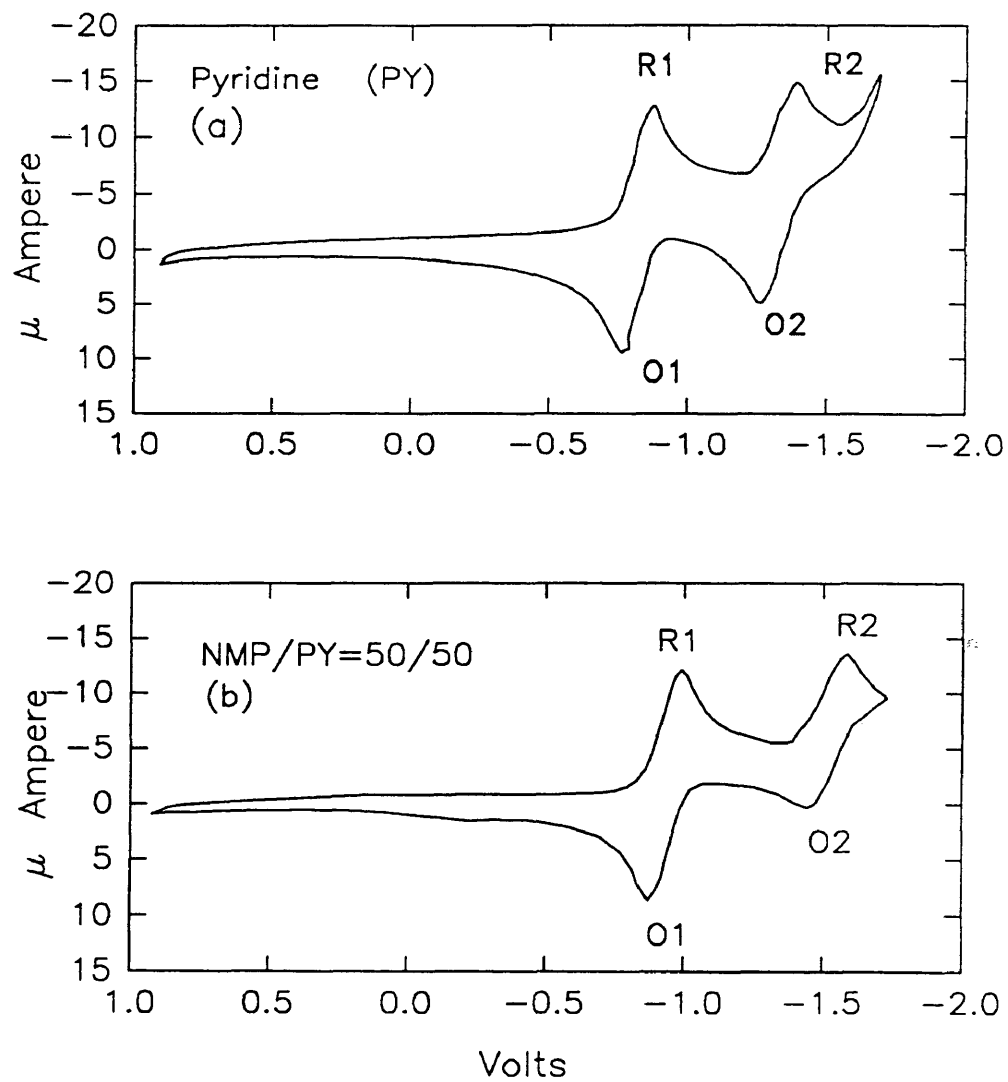


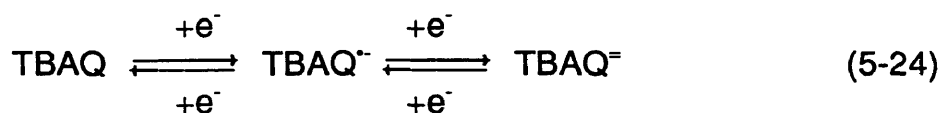
Figure 20. Cyclic voltammogram of TBAQ in pyridine (a); in mixture NMP/PY (b). The peaks are shifted to more positive potential in pyridine.

TBAQ reduction potentials. PY can act as electron donor in charge-transfer complexes (*Foster, 1967*). A complex may be formed between PY and radical anion TBAQ \cdot^- . This complex may stabilize the TBAQ \cdot^- . Therefore, it may cause the positive shifting of the second reduction potential of TBAQ in PY from the corresponding peak in NMP and DMF.

In a mixture of NMP and pyridine at 50/50 molar concentration, the first reduction peak of TBAQ is not significantly different from the value obtained in pure NMP. However, the second reduction peak is shifted + 0.32 V from the same peak in pure NMP solvent. These data support the previous explanation of a complex between PY and TBAQ \cdot^- .

In DMF ($\mu = 3.24$ Debye, $\epsilon = 36.71$) the TBAQ cyclic voltammogram showed two reduction peaks and two oxidation peaks. The shapes of these peaks establish that the TBAQ is a reversible redox couple involving two separate one-electron transfer steps. The voltammogram is presented in **figure 21 b**.

It is known from the study of the electrochemical behavior of anthraquinone and its derivatives, that these compounds have two reversible one-electron redox cycles. The two reduction steps are attributed to the formation of a stable semiquinone radical anion and a dianion (*Given and Peover, 1960*). The reaction sequence of TBAQ can be presented as follows:



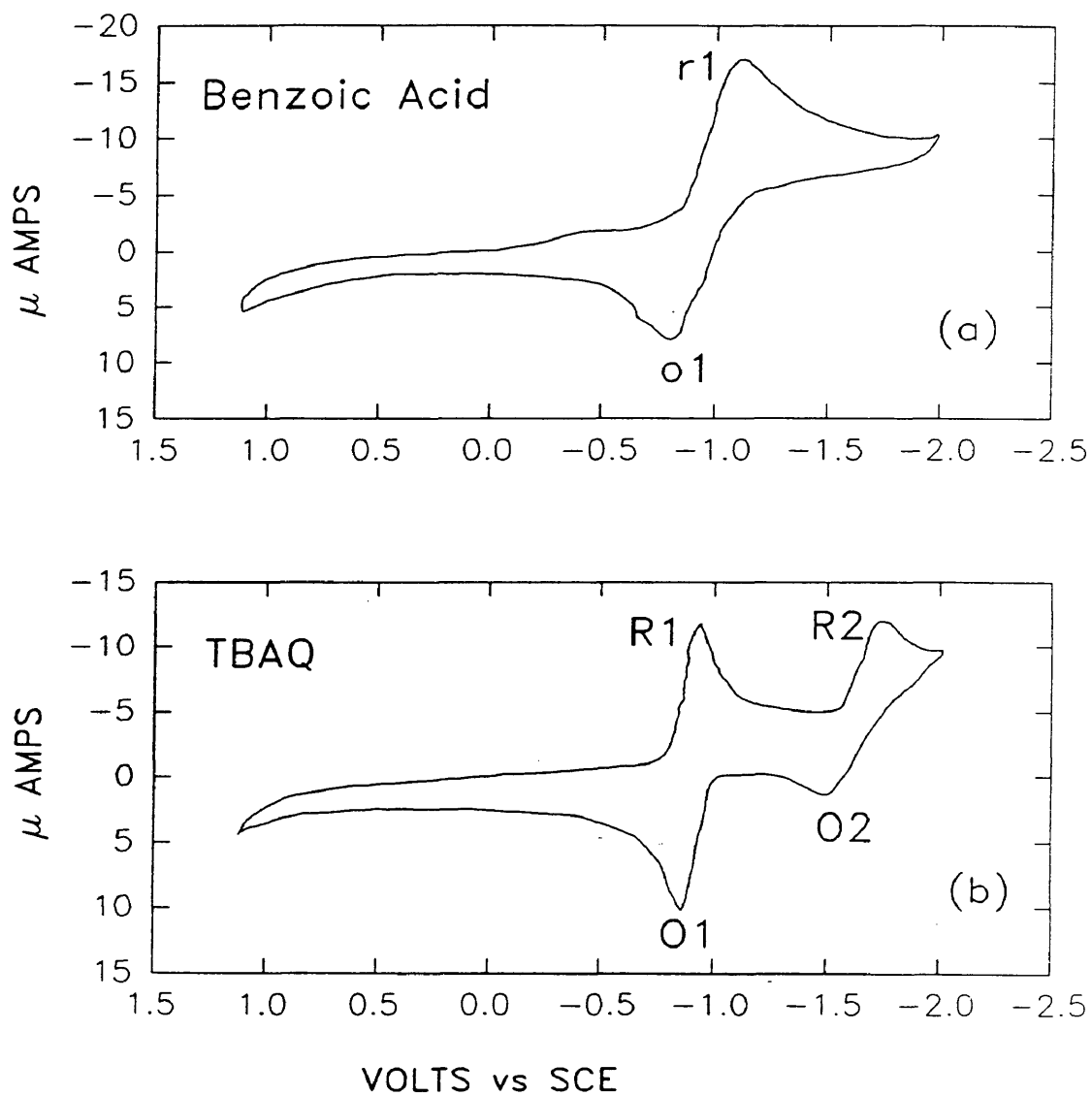


Figure 21. Standard cyclic voltammogram of (a) benzoic acid (4mM) and (b) TBAQ (2mM) in DMF solvent containing 0.1 M TBAP, Sweep rate is 0.1 V/s.

The first (O1) and second oxidation (O2) peaks in these solvents are attributed to the oxidation of the dianion (TBAQ^{2-}) followed by the oxidation of the radical anion of semiquinone ($\text{TBAQ}^{\cdot-}$).

In DMAC and NMP, the cyclic voltammograms showed two reduction peaks and only one oxidation peak (**figure 22**). The potential of the first reduction peak in both solvents is similar to that in DMF. In NMP and DMAC, the reduction mechanism is the same as in DMF, but the oxidation mechanism is different. The first oxidation peak in the voltammogram represents the oxidation of the radical anion $\text{TBAQ}^{\cdot-}$ to form TBAQ. The oxidation peak which should represent the oxidation of the dianion TBAQ^{2-} to form the radical anion $\text{TBAQ}^{\cdot-}$ does not appear.

The cause for the absence of the second oxidation peak of TBAQ in NMP and DMAC is still unknown. Probably the oxidation of TBAQ^{2-} to form semiquinone $\text{TBAQ}^{\cdot-}$ occurs rapidly in NMP and DMAC, and it is faster than the scan rates employed in the cyclic voltammetry.

However, in the experimental reaction in the reactor, reaction between TBAQ and H_2S , the TBAQ^{2-} dianion is never formed because the reaction proceeds via the intermediate $\text{HTBAQ}^{\cdot-}$ (see equation 5-9 and 5-10).

The first TBAQ reduction peak seems to be at more positive potential in the high polarity solvents (as shown in NMP, DMAC and DMF) than in the low polarity solvent (as shown in THF). However, the TBAQ reduction peaks are not very sensitive to the small difference in dipole moments of the solvents. In solvents

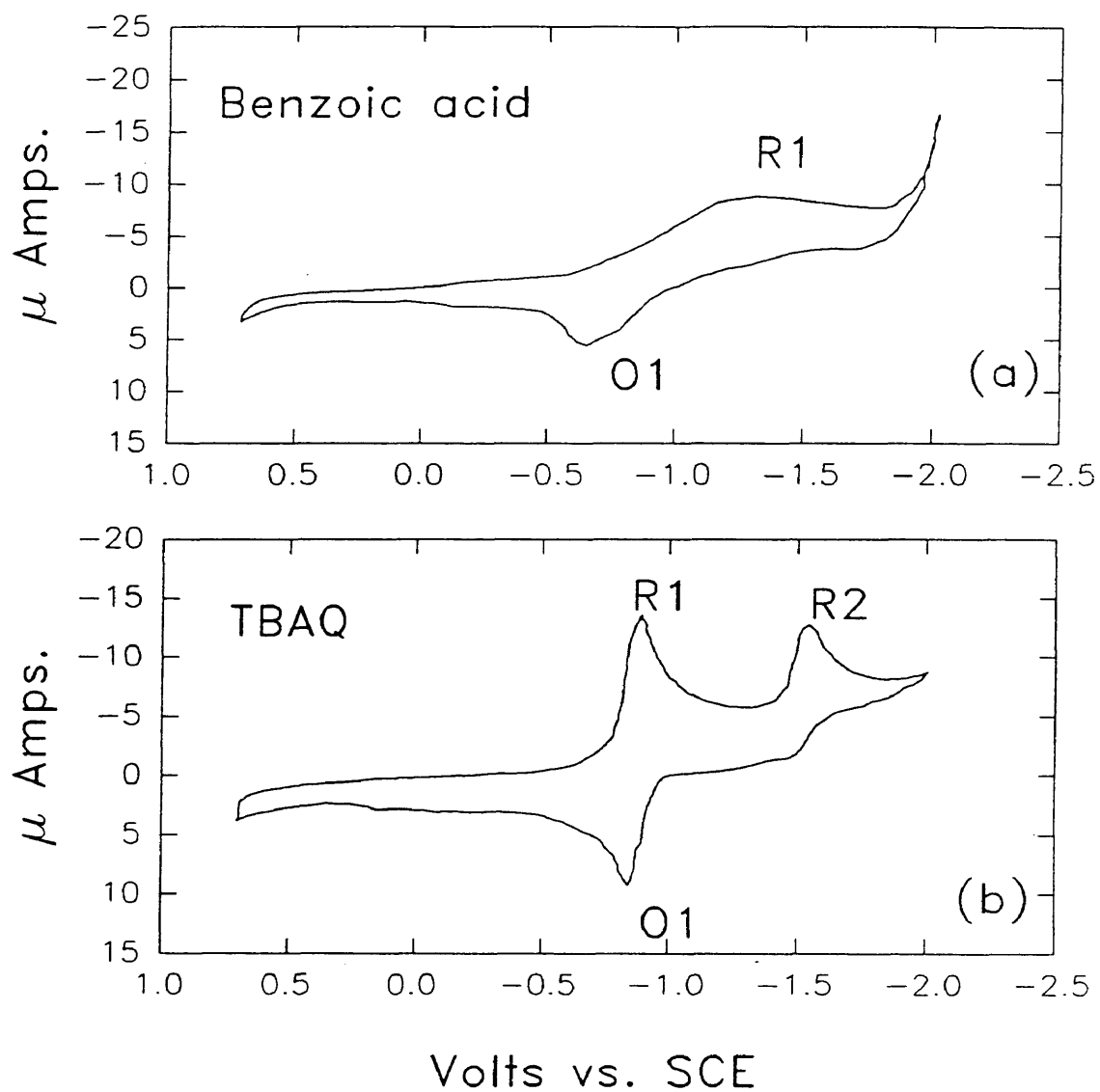


Figure 22. Standard cyclic voltammogram of (a) benzoic acid (4mM) and (b) TBAQ (2mM) in DMAC solvent containing 0.1 M TBAP. Sweep rate is 0.1 V/s

DMF, NMP and DMAC where dipole moment of these solvents are in 3.2 Debye to 4.09 Debye range, the first TBAQ reduction peaks are the same. It seems other factors can shift the TBAQ reduction and oxidation peaks. Charge transfer complex may be one of the factors that affect the peak potential for TBAQ reduction. This is observed when PY was used as solvent. Opposite to the prediction based on polarity, the first TBAQ reduction peak in PY had more negative potential.

5.2.3 The Effect of Protic Agents: Phenol and Butanol

In a previous discussion on the reaction mechanisms, it was suggested that there was a proton transfer from the H_2S or polysulfane to the radical anion $TBAQ^{\cdot-}$ (see equation 5-9). To duplicate this proton transfer, phenol and butanol as protic agents were added to the electrochemical cell containing TBAQ, solvent, and electrolyte in a steady state condition. The concentrations of the protic agents were approximately the same molar concentration as TBAQ. The pK_a values of some proton donors are listed in **table 10, appendix C**. If the proton transfer is rapid enough, these protic agents can change the voltammogram profile of TBAQ reduction and oxidation.

It has been found (*Given and Peover 1960*) that phenol did not change the first reduction potential of anthraquinone. But phenol did influence the second reduction potential, implying that the dianion undergoes protonation. The experi-

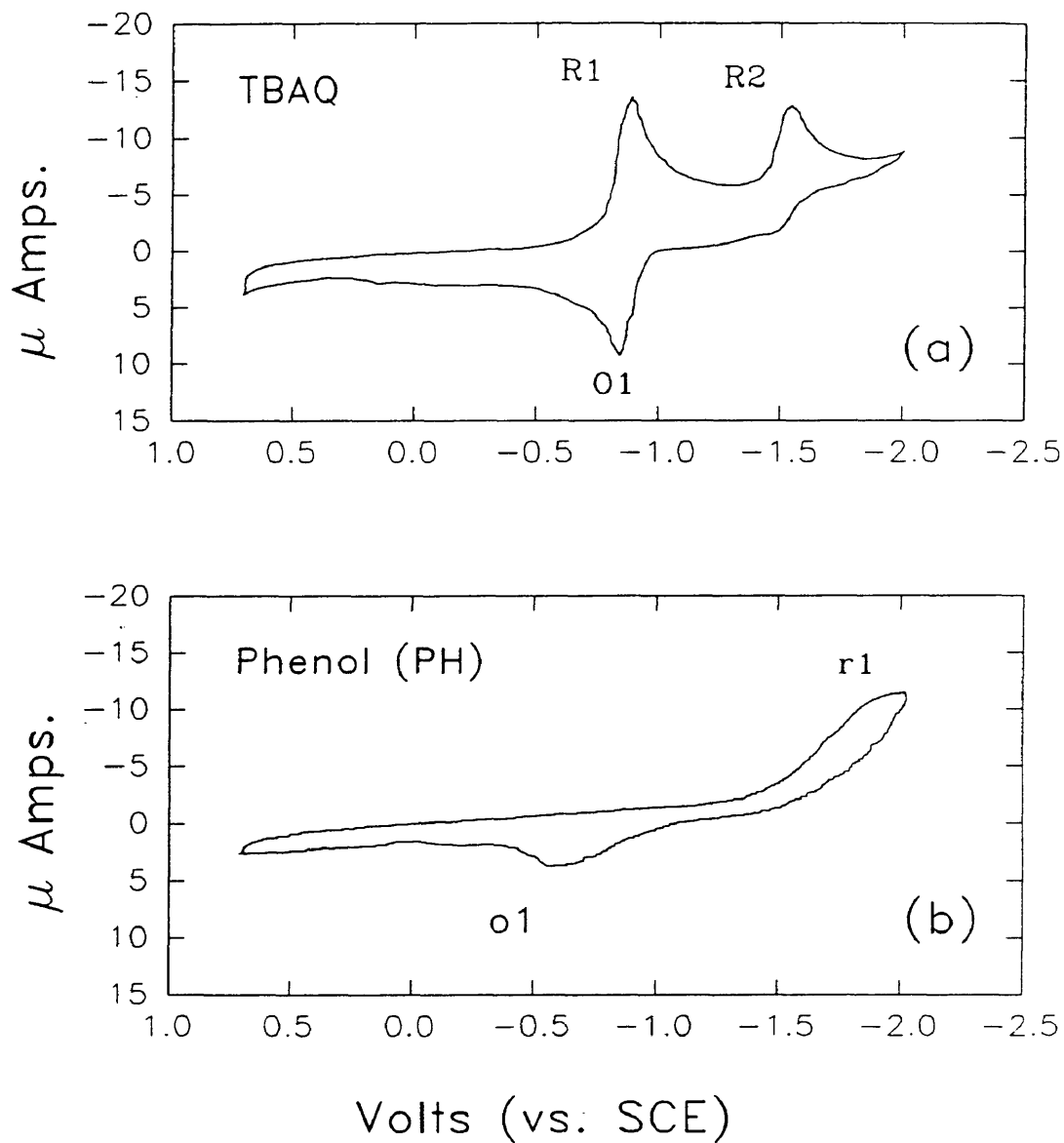


Figure 23. Cyclic voltammogram of (a) TBAQ (2mM) and (b) phenol (2mM) in DMAC solvent containing 0.1 M TBAP. Sweep rate is 0.1 V/s

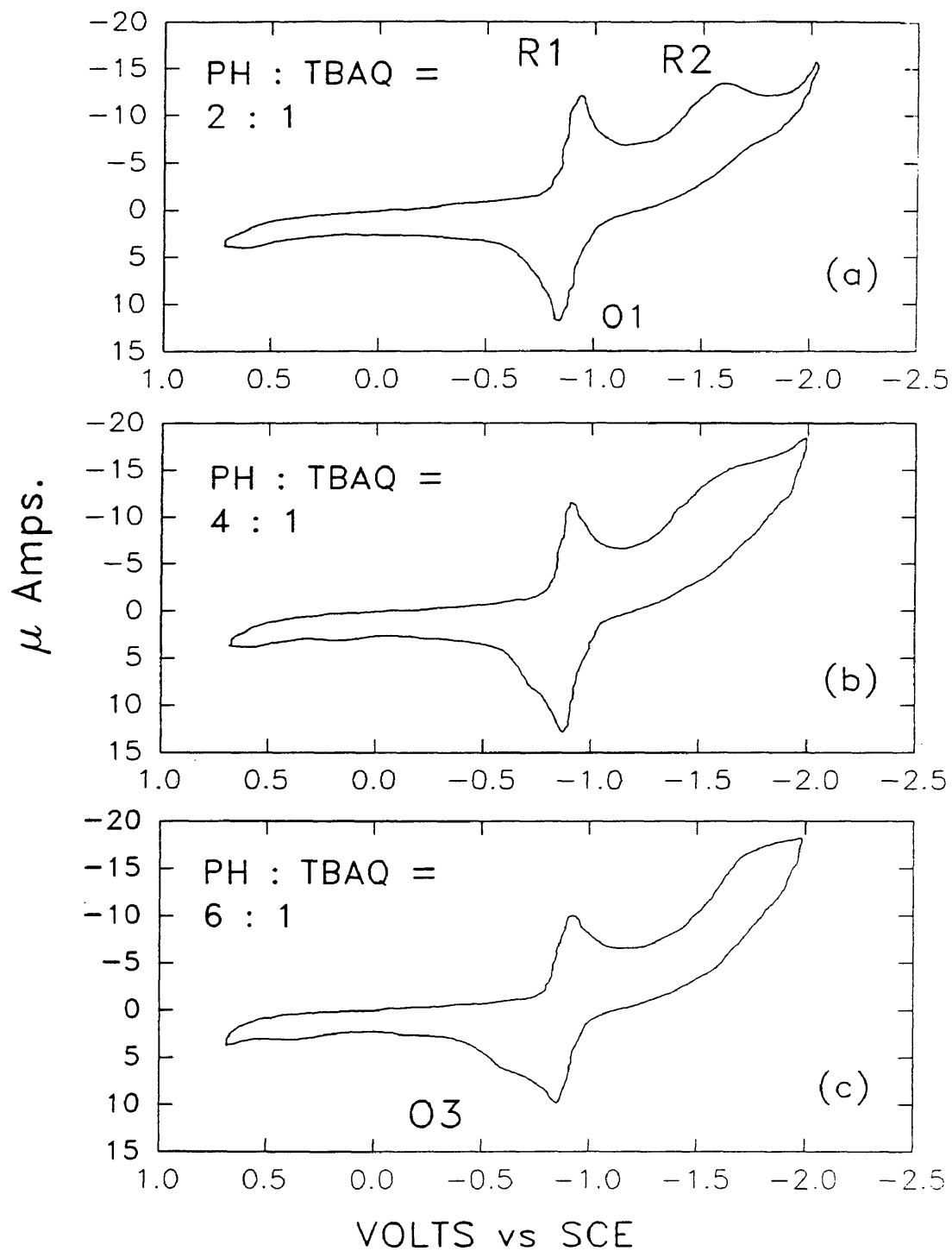


Figure 24. Cyclic voltammogram of TBAQ in DMAC in the presence of phenol: 2mM TBAQ, 0.1 M TBAP, 0.1 V/s.

mental data in **table 11 (appendix C)** and **figures 23 and 24** show that phenol in DMAC does not change the first reduction peak of TBAQ. However, the second reduction peak was shifted to a slightly more positive potential (from -1.62 Volts to -1.59 Volts). These results are consistent with the result of Given and Peover. As the phenol concentration increased, the phenol reduction peak became more significant and overlapped the second reduction peak of TBAQ.

Butanol behaves the same as phenol in TBAQ reduction. The shifting of the second reduction peak was due to protonation of the TBAQ⁻ dianion. With pyridine as solvent, the addition of butanol did not shift the first reduction peak but shifted the second reduction slightly. Addition of butanol in NMP or DMAC gave a similar result as in pyridine.

Phenol and butanol as acids are not strong enough to undergo a proton transfer to radical anion TBAQ^{•-}. However, addition of butanol or phenol as protic agent causes proton transfer to TBAQ⁻. This is shown by the shifting of the second TBAQ reduction to more positive potential after addition of phenol or butanol. Thus, to have proton transfer to the radical anion TBAQ^{•-}, a stronger acid than phenol or butanol is required.

5.2.4 The Effect of Protic Agent: Benzoic Acid

Since addition of phenol or butanol did not show a proton transfer to radical anion TBAQ^{•-}, benzoic acid (BA) ($pK_a = 4.2$) as a stronger acid than phenol or

butanol was added as protic agent. It was predicted that benzoic acid will be a better proton donor. Hence, addition of benzoic acid should produce a drastic change in the cyclic voltammogram of TBAQ.

In pyridine, the first TBAQ reduction peak was not shifted with benzoic acid addition but the second reduction peak was slightly shifted and became smaller and wider; see **table 11, appendix C**. It appears that there was a proton transfer to TBAQ^{\ominus} which took place at the second reduction potential.

A new oxidation peak (O3) appeared at -0.27 Volts (vs. SCE) in pyridine, which was a more positive potential than the first oxidation peak (O1) potential of TBAQ at -0.79 Volts (vs. SCE). Increasing the benzoic acid concentration eliminated both the second and the first oxidation peaks, but did not change the new oxidation peak O3. It appears that O3 was the oxidation peak of a stable intermediate.

In NMP, addition of benzoic acid did not shift the first reduction and oxidation peaks but shifted the second reduction peak to a more positive potential and made it wider. There was a small wide new oxidation peak (O3) at -0.27 Volts (vs. SCE), same as in pyridine, when the benzoic acid concentration was at a 2/1 molar ratio. This new oxidation peak (O3) can be due to the oxidation of a stable intermediate.

In DMAC, benzoic acid eliminated the second reduction peak (R2) and the first oxidation peak (O1). Benzoic acid also produced a new oxidation peak (O3)

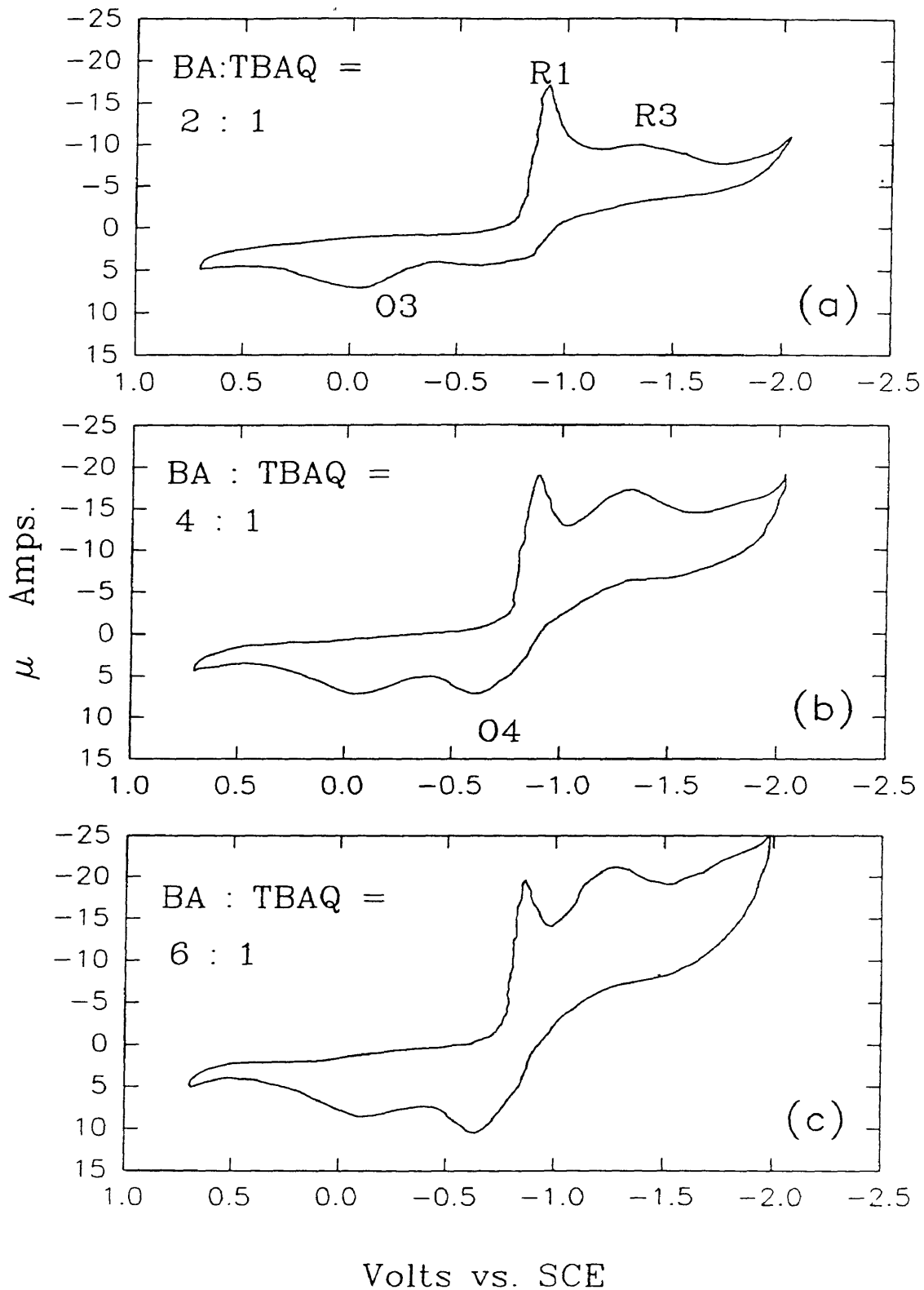


Figure 25. Cyclic voltammogram of TBAQ in DMAC in the presence of benzoic acid (BA): 2mM TBAQ, 0.1 M TBAP, 0.1 V/s.

at a potential more positive than the first oxidation peak (O1). Lastly, benzoic acid produced new reduction peak (R3) at a less negative potential than the second reduction peak (R2). The experimental results are presented in **figure 22 and 25** and **table 12, appendix C**. The new reduction peak (R3) had a potential similar to the potential for the reduction of benzoic acid in DMAC.

When the concentration of benzoic acid was increased to a 4/1 molar ratio, there was a small and wide oxidation peak (O4) at a potential less negative than the first oxidation peak (O1). This oxidation peak has a potential similar to the oxidation potential of the benzoate anion; therefore, it probably is due to the oxidation of benzoic acid in DMAC.

In DMF, the first reduction peak (R1) potential was shifted slightly to a more positive potential. The height of the first reduction peak (R1) increased with increasing concentration of benzoic acid until it formed a single two-electron peak with the disappearance of the second reduction peak (R2). **Figures 21 and 26** show the voltammogram of TBAQ in DMF with increasing concentrations of benzoic acid; **table 13, appendix C** shows the experimental data. With benzoic acid at a molar ratio of 1:1 to TBAQ, a new oxidation peak (O3) appeared at about - 0.19 Volts (vs. SCE), which increased and shifted negatively as the concentration of benzoic acid increased. This oxidation peak (O3) may be due to the oxidation of an intermediate. When benzoic acid was above a 1:1 molar ratio to TBAQ, the second reduction peak R2 and the second oxidation peak O2 began to disappear.

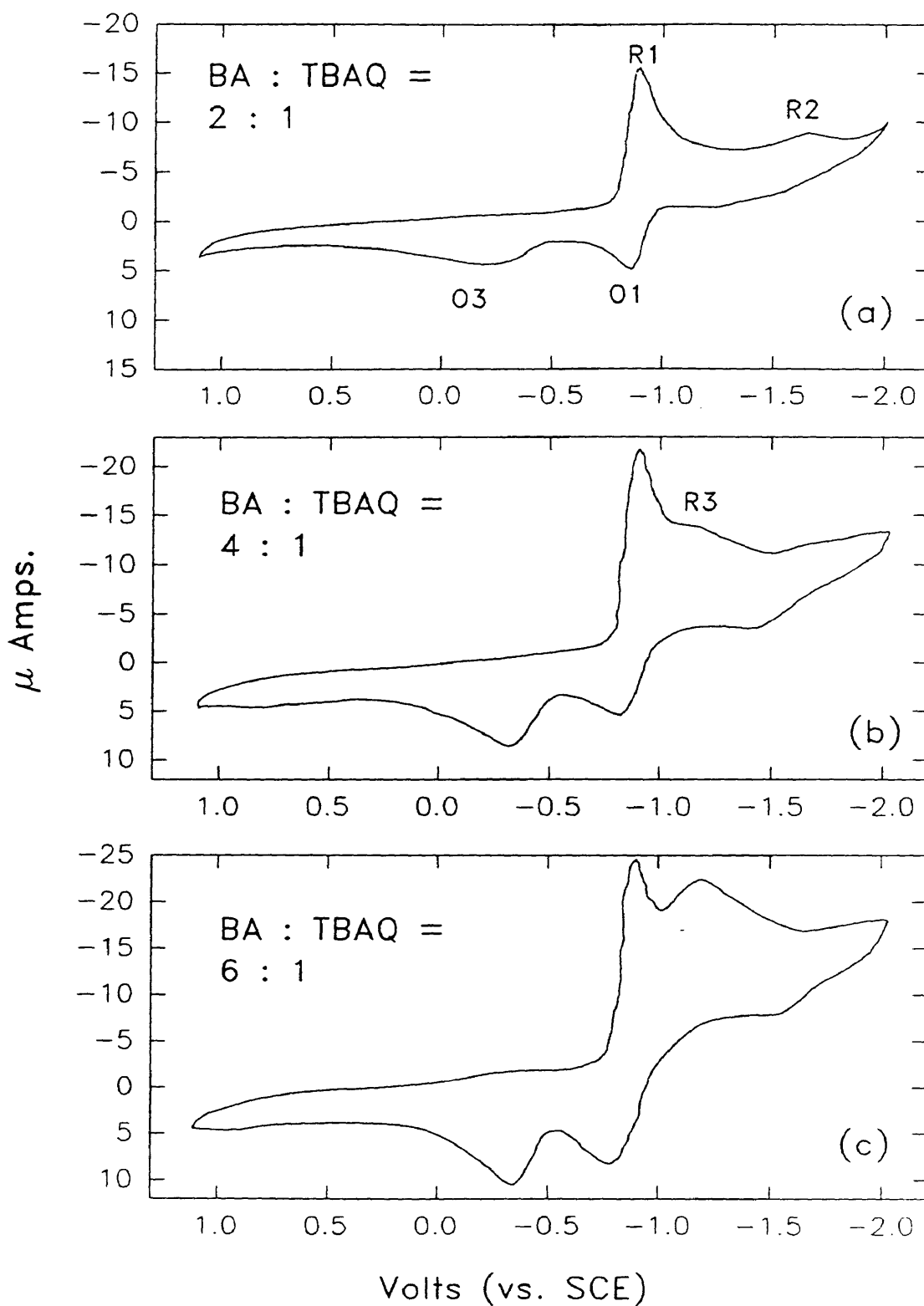


Figure 26. Cyclic voltammogram of TBAQ in DMF in the presence of benzoic acid (BA): 2mM TBAQ, 0.1 M TBAP, 0.1 V/s.

At a benzoic acid to TBAQ molar ratio of 2:1, the second reduction peak (R2) disappeared and a new reduction peak (R3) appeared as a shoulder. At higher concentrations of benzoic acid, this peak appeared at -1.18 Volts (vs. SCE). The height (current) of this reduction peak increased as the concentration of benzoic acid increased. This R3 peak has a similar potential to the reduction peak of benzoic acid in DMF; therefore, this peak is assigned to the reduction of benzoic acid in DMF.

The first oxidation peak (O1) was also positively shifted and increased when the benzoic acid molar ratio to TBAQ was greater than 2:1. At a benzoic acid to TBAQ molar ratio of 4:1, the first oxidation peak was at -0.79 V vs. SCE. This potential is close to the oxidation potential of benzoic acid in DMF (-0.80 V vs. SCE). Therefore, the potential shift and the increasing height (current) of the O1 peak may be due to the decreasing TBAQ^{•-} oxidation and the increasing benzoic acid oxidation.

In DMF, the current of the first reduction peak (R1) increased as the concentration of benzoic acid increased. This is because protonation of the semiquinone TBAQ^{•-} is very fast and electron transfer primarily takes place on the radical HTBAQ^{•-} to form hydroquinone anion HTBAQ⁻ (species are in **figure 19**). This HTBAQ^{•-} reduction may take place at the same potential as the first TBAQ reduction. According to Hoijtink's calculations for aromatic hydrocarbons (*Hoijtink, 1954; Chambers, Patai, 1964; Given, 1960; Austen, 1958*), the electron affinity of

the protonated quinone radical anion is greater than that for the corresponding quinone. Thus, the second electron reduction of the protonated radical HTBAQ \cdot^- can take place at the potential of the first TBAQ reduction .

Addition of benzoic acid into TBAQ solution results in the shifting of the first TBAQ reduction peak (R1) to more positive potential, the disappearance of the second TBAQ reduction peak (R2), and the appearance of HTBAQ \cdot^- oxidation peak (O3). These results from addition of benzoic acid as protic agent support equations 5-9 and 5-10, which showed the proton transfer to TBAQ \cdot^- and the reduction of HTBAQ \cdot^- . Also, these results are in agreement with the results on anthraquinone reported by Chambers (*Chambers, 1974*).

When benzoic acid is in excess, HTBAQ \cdot^- can be protonated to form H₂TBAQ. The presence of H₂TBAQ can be detected by the appearance of H₂TBAQ oxidation peak. To obtain the evidence of the presence of HTBAQ \cdot^- and the formation of H₂TBAQ from HTBAQ \cdot^- , in situ experiments were conducted.

5.2.5 In situ Generation of Protonated Intermediates

Experiments were conducted by injecting benzoic acid into the equilibrium cyclic voltammetry cell at the first reduction potential and at the second reduction potential of TBAQ in DMF. The mixture had been stirred for 1 hour when the cyclic voltammogram was taken.

The data in **table 14, appendix C** and **figure 27** showed that when benzoic

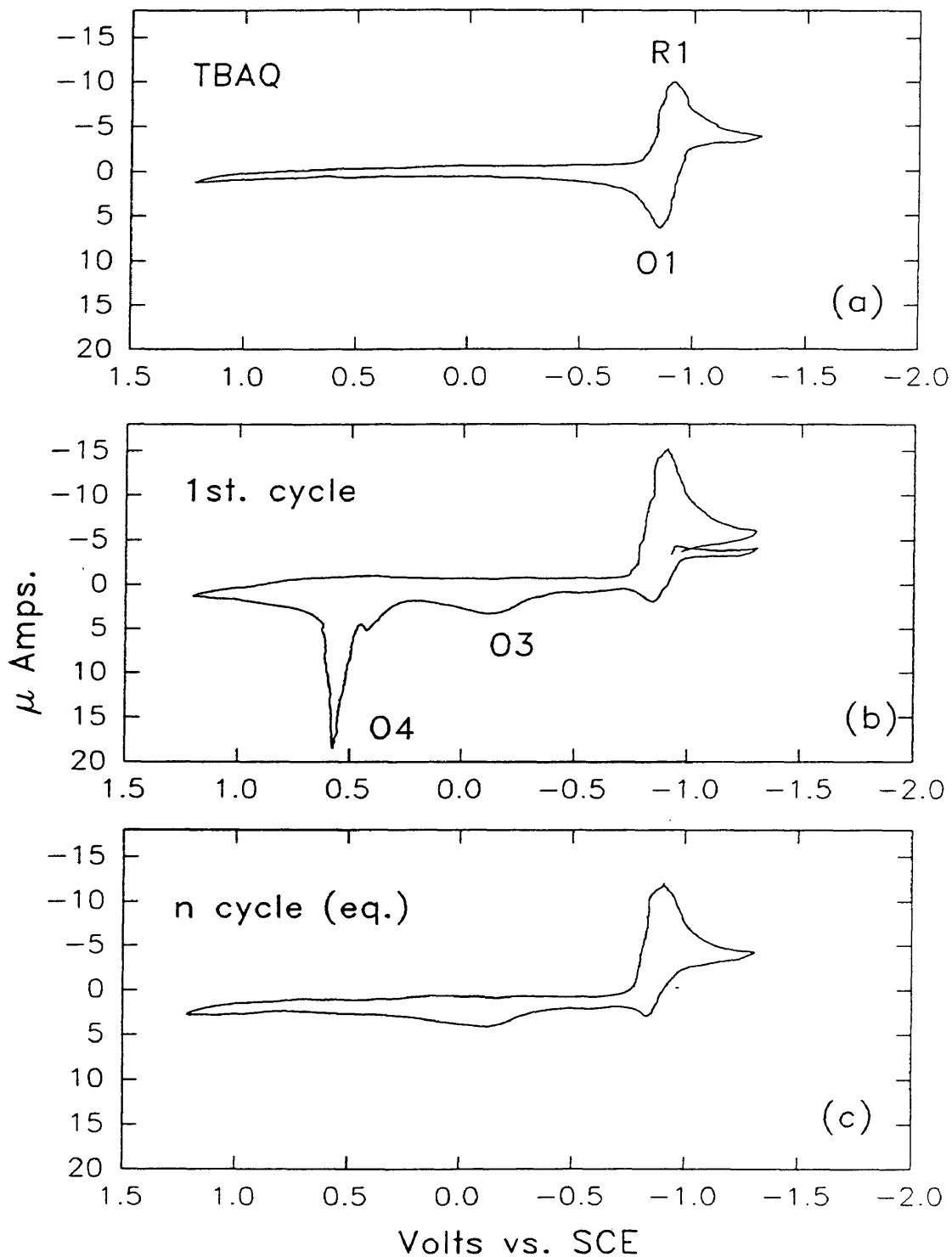


Figure 27. Cyclic voltammogram of TBAQ in DMF with addition of benzoic acid (BA) at the 1st. reduction potential for one hour: 2mM TBAQ, 2mM BA, 0.1 M TBAP, 0.1 V/s.

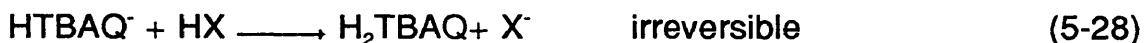
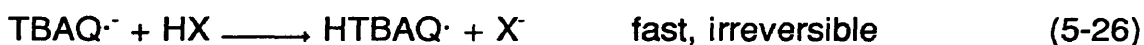
acid was injected and stirred for 1 hour at the first reduction potential, two new oxidation peaks, O3 and O4, appeared and the oxidation peak O1 is shifted to a less negative potential than before. The oxidation peak O4 decreased when the cycle continued, and disappeared after the cyclic voltammetry reached equilibrium. The potential of the oxidation peak O3 was close to the potential of the oxidation peak of the intermediate HTBAQ⁻ in DMF (peak O3 in **table 11, appendix C**). There was also a small oxidation peak as a shoulder at a less positive potential than peak O4, see **figure 27 b**. This shoulder may be due to the unstable intermediate also.

The proposed reaction mechanisms of benzoic acid addition at the first reduction potential of TBAQ (-0.85 Volts) can be written as follow

Before addition of benzoic acid :



During addition of benzoic acid :



Reactions of the first cycle after addition of benzoic acid:

peak O3 and O1 (oxidation):





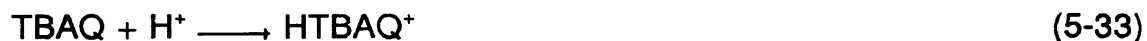
peak O4 (oxidation):



The reduction peak R1 in the first cycle is due to the reaction (5-25). After the first cycle the radical $\text{HTBAQ}\cdot^-$ from reactions (5-26) will be reduced to form intermediate hydroquinone anion HTBAQ^- (5-27), this reduction takes place at the same potential as the first reduction of TBAQ. Hence, the reduction peak R1 after the first cycle is due to reactions 5-25 to 5-27.

The cyclic voltammogram shows that the oxidation peak O4 (equation 5-32) occurs in the first cycle and disappears after several cycles. It appears that the formation of hydroquinone H_2TBAQ by protonation of the intermediate HTBAQ^- (equation 5-28) takes a longer time than the scan time in each cycle, and the amount of hydroquinone H_2TBAQ in the solution decreases after the first cycle.

Another way to produce H_2TBAQ is by the reduction of the preprotonated HTBAQ^+ with a two-electron transfer followed by proton transfer to form H_2TBAQ ; see equations 5-33 to 5-35. A strong acid will protonate the quinone at a positive cell potential. Benzoic acid seems not strong enough to protonate the TBAQ in large amounts, since the peak O4 decreased after the first cycle. The reactions below can explain the mechanisms of hydroquinone formation via quinone preprotonation.



The addition of benzoic acid at the second reduction potential of TBAQ gave almost the same cyclic voltammogram as that of the acid addition at the first reduction potential; **see figure 28 and table 14, appendix C**. In the first cycle, the oxidation peak O1 was still high but was shifted significantly to a more positive potential than the potential of O1 without benzoic acid. After the first cycle, the oxidation peaks O1 and O4 decreased and disappeared. The disappearance of the first oxidation peak O1 was due to the loss of TBAQ^- , since after the first cycle the protonation and reduction of radical anion TBAQ^- was taking place at the first reduction peak potential (see equations 5-26 and 5-27).

As benzoic acid was injected, the cell was maintained at the second reduction potential of TBAQ and stirred for one hour, the reactions that occur can be expressed as below:



The oxidation peak O4 at the first cycle was due to the oxidation of the hydroquinone H_2TBAQ , equation 5-32. This peak was smaller (lower oxidation current)

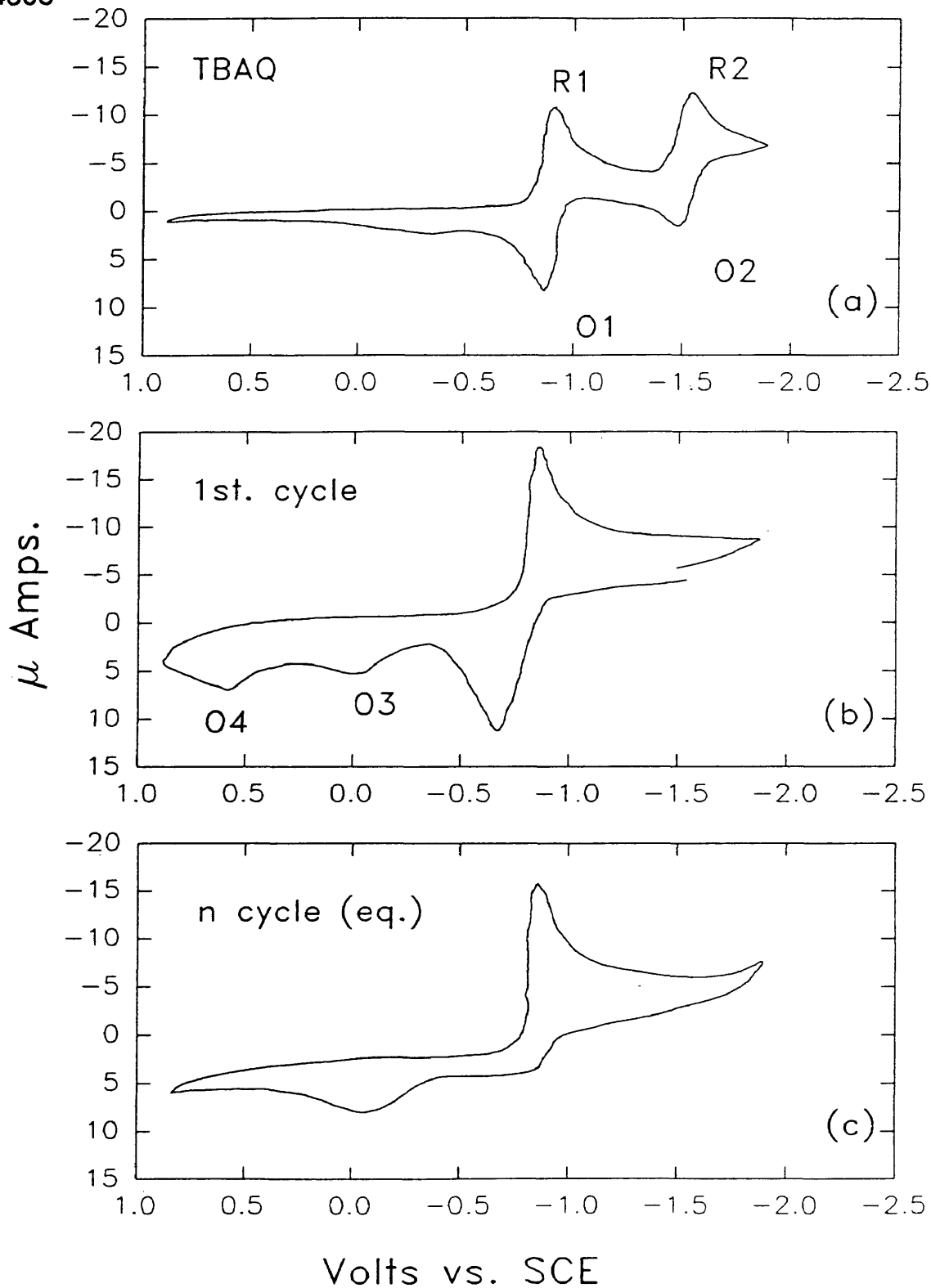


Figure 28. Cyclic voltammogram of TBAQ in DMF with addition of benzoic acid (BA) at the 2nd. reduction potential for one hours: 2mM TBAQ, 2mM BA, 0.1 M TBAP, 0.1 V/s.

than the same peak obtained when benzoic acid was added to a cell maintained at the first reduction potential of TBAQ. This showed that the mechanism to form hydroquinone H_2TBAQ via a protonation of dianion $TBAQ^{2-}$ (equations 5-36 and 5-37) at the second reduction potential is less favorable than reactions via electron and proton transfer at the first reduction potential (equations 5-26 to 5-28).

The fact that TBAQ can be converted to H_2TBAQ by addition of a protic agent such as benzoic acid supports equations 5-9 to 5-11 of the proposed reaction mechanisms of TBAQ reduction in the reactor. This suggests that TBAQ is first reduced by electron transfer, from either H_2S , HS^- or HS_x^- , then it will be protonated by protic agents, such as H_2S or sulfanes H_2S_x .

5.2.6 The Effect of the Protic agent : Benzenethiol

The pK_a 's of benzenethiol (6.5) and H_2S (7.0) are similar. Since it is very difficult to work with H_2S in a conventional electrochemical cell, benzenethiol should be a good substitute for H_2S as a protic agent. The cyclic voltammogram of benzenethiol in DMF has two oxidation peaks and two reduction peaks which do not overlap the redox peaks for TBAQ (**figure 29**).

Addition of benzenethiol as a proton donor to a TBAQ solution gave a complex cyclic voltammogram. The oxidation peaks O1 and O2 of TBAQ almost disappeared after addition of benzenethiol at the peak O2 potential, and new oxidation peaks appeared as O3, O4 and O5 (**figure 30**). Peak O5 was a shoul-

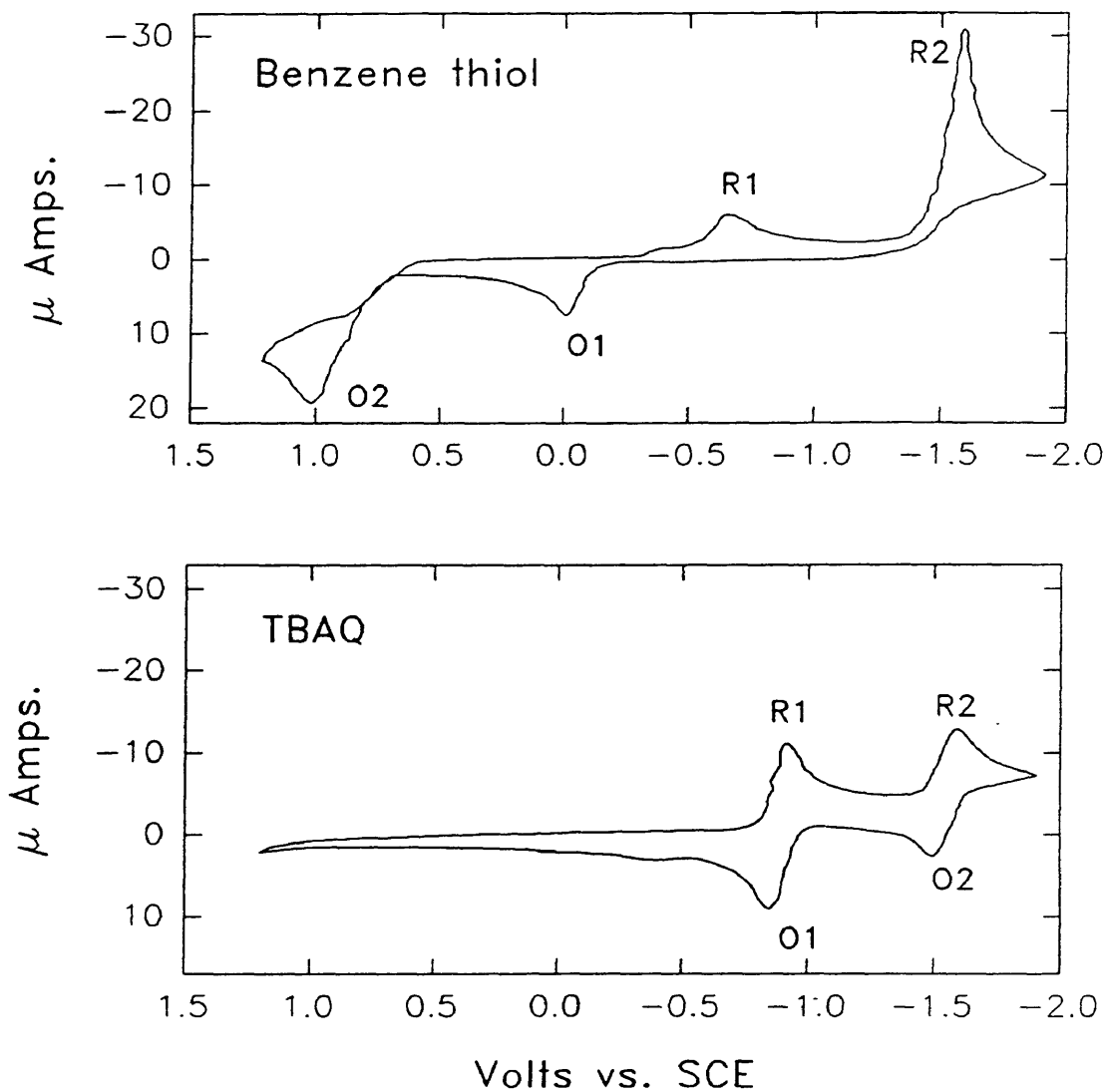


Figure 29. Standard cyclic voltammogram of benzenethiol (a) and TBAQ (b) in DMF: 2mM TBAQ, 2mM benzenethiol, 0.1 M TBAP, 0.1 V/s, 20 °C.

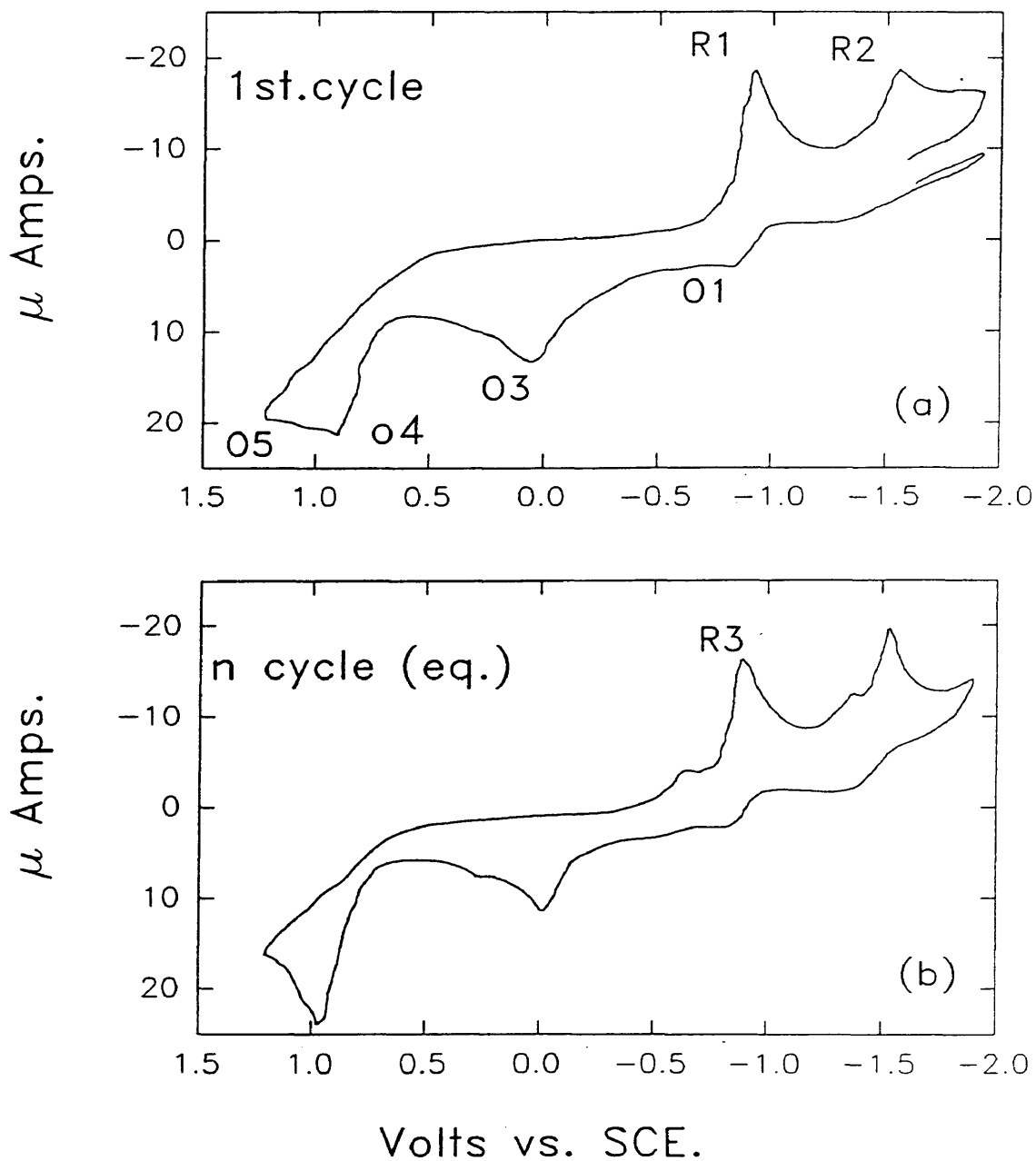


Figure 30. Cyclic voltammogram of TBAQ in DMF with addition of benzenethiol at the 2nd. reduction potential for one hour: 2mM TBAQ, 2mM benzenethiol, 0.1 M TBAP, 0.1 V/s, 20 °C.

der and disappeared at the second cycle. The peak O4 was stable and had a potential which is close to the potential of the second oxidation of benzenethiol itself. These experimental data are presented in **table 15, appendix C**.

It is hard to understand the peak O4, since it overlapped the second oxidation of benzenethiol. The shoulder O5 can come from the oxidation of H_2TBAQ , since this peak also disappeared after the first cycle, as it did in benzoic acid. But this peak was shifted to a more positive potential than that in benzoic acid.

The potential of oxidation peak O3 at the equilibrium cycle is almost the same as the first oxidation potential of benzenethiol itself. The reduction peak R2 was shifted to a less negative potential. This peak may come from the second reduction of $TBAQ^{\cdot-}$ or from the second reduction of benzenethiol.

The cause of the disappearance of peak O2 after the first cycle was the protonation of the dianion $TBAQ^{2-}$ (equations 5-36 and 5-37). The disappearance of peak O1 after the first cycle was due to the protonation of radical anion $TBAQ^{\cdot-}$ at the first reduction potential (equations 5-26 to 5-28). The oxidation peak O3 was stable, but the position was the same as the first oxidation potential for benzenethiol. Therefore, it was difficult to determine whether this oxidation peak (O3) came from the oxidation of the intermediate $HTBAQ^{\cdot-}$ and/or of benzenethiol.

The reduction peaks R2 and R3 were probably due to the reduction of benzenethiol itself because there were no more oxidation peaks of O1 and O2 on the anodic current after the first cycle (**figure 30**). The R1 peak was due to

reactions 5-25. Benzenethiol was not strong enough to preprotonate TBAQ, thus no peak for the reduction of preprotonated HTBAQ⁺ occurred on the first cycle.

The results from addition of benzenethiol support the reaction sequence based on in situ experiments with benzoic acid. The appearance of oxidation peak O5 at the first cycle and the disappearance of TBAQ⁻ oxidation peak (O2) showed that addition of benzenethiol can generate H₂TBAQ. The formation of H₂TBAQ can be represented by equations 5-36 and 5-37. The protonation of TBAQ⁻ which eliminated reduction peak O1 after the first cycle is in agreement with the reactions in equations 5-26 to 5-28. The same as in benzoic acid addition, there was no evidence for the preprotonation of TBAQ by addition of benzenethiol to form HTBAQ⁺. Thus, reactions in equations 5-33 to 5-35 did not occur by addition of benzenethiol.

5.2.7 Correlation of Redox Potentials with HOMO and LUMO Energy Levels

Cyclic voltammetry provides a convenient means of measuring the one-electron redox potential of quinones. It has been known that oxidation and reduction potentials for a series of aromatic hydrocarbons can be related to the theoretically calculated energies of the highest occupied or lowest unoccupied molecular orbitals, HOMO and LUMO respectively (*Matsen, 1956, Hedges, 1958, Peover 1962, Peover nature 1962, 1961, Tani 1970, 1967, Conway, Weinberg ed. 1974*).

Cyclic voltammetry can determine the reduction potential E_c , corresponding to the reaction $\text{TBAQ} + e^- \longrightarrow \text{TBAQ}^-$, and the oxidation potential E_a of the electron donor agent HS^- .

The electron transfer in the reaction takes place between the HOMO of the electron donor molecule and the LUMO of the electron acceptor molecule. The energy of the LUMO can be considered as the electron affinity (EA) of the electron acceptor molecule and the energy of the HOMO as ionization potential (IP) of the electron donor molecule.

The cyclic voltammetry data can be used to investigate the correlation of redox potential with the calculated energies of the LUMO and HOMO and to interpret the effect of solvent on the redox behavior of TBAQ.

For a reversible process, the peak potential in a cyclic voltammogram can be related to the half-wave potential by this expression (*Sawyer, 1974*)

$$E_c = E_{1/2} - 1.11 [(RT)/(nF)] \quad (5-38)$$

where R = gas constant ($8.314 \text{ Joule.mol}^{-1}.\text{K}^{-1}$)

T = absolute temperature (K)

F = Faraday constant ($9.648 \times 10^4 \text{ C.mol}^{-1}$)

n = Number of electron involved

But within experimental error, the potential of a reversible reduction can be

considered as the half wave potential. (*Foster, 1969, Peover, 1962, Bard, 1980*).

Matsen and Hedges (*1956, 1958*) have shown that electron affinity (EA) of aromatic compounds can be related to the reversible one-electron reduction potential, relative to the saturated calomel electrode, by the equation

$$E_c = EA + \Delta E_{\text{sol}} - 5.07 = EA' - 5.07 \text{ (eV)} \quad (5-39)$$

where ΔE_{sol} is the solvation energy change. Similarly, ionization potential can be related to the oxidation potential (E_a) as

$$E_a = IP + \Delta E_{\text{sol}} + \text{constant} \quad (5-40)$$

Since it is difficult to measure or calculate the solvation energy change, the electron affinity cannot be obtained directly from the half-wave potential (reduction potential). Using equation 5-39 and experimental data for the reduction potential, EA' can be calculated as a sum of EA and ΔE_{sol} .

Using molecular orbital theory, electron affinity, which is equal to the energy of the LUMO, can be calculated by equation

$$EA = \epsilon_{\text{lv}} = (\alpha + \chi_{\text{lv}}\beta) \quad (5-41)$$

where ϵ_{lv} is the energy of the LUMO. The ionization potential (IP), which is equal to the energy of the HOMO, is given by the equation

$$IP = \epsilon_{ho} = - (\alpha + \chi_{ho}B) \quad (5-42)$$

where ϵ_{ho} is the energy of the HOMO. α and β are the coulomb and exchange integrals of the 2p atomic orbital of carbon atom respectively, χ_{lv} is the lowest vacant energy level and χ_{ho} is the highest occupied energy level (*Hedges, 1958*).

Tani and Kikuchi (*1967, 1970*) in their research on dye molecules developed an equation for calculating electron affinity, based on molecular orbital theory.

$$EA = 2.78 + 4.07 \chi_{lv} \quad (5-43)$$

Experimental data with selected solvents show that the different values for the reduction potential of TBAQ can be considered as due to changes in solvation energy (ΔE_{sol}).

The reduction potential of some quinones shows a linear relationship with the calculated electron affinity or the energy of LUMO. **Table 16 in appendix C** shows the data (*Peover 1962*) for the plot of reduction potential versus calculated electron affinity in a vacuum (**figure 31**). From the plot in **figure 31** the electron affinity of TBAQ in vacuum can be obtained (0.70 eV).

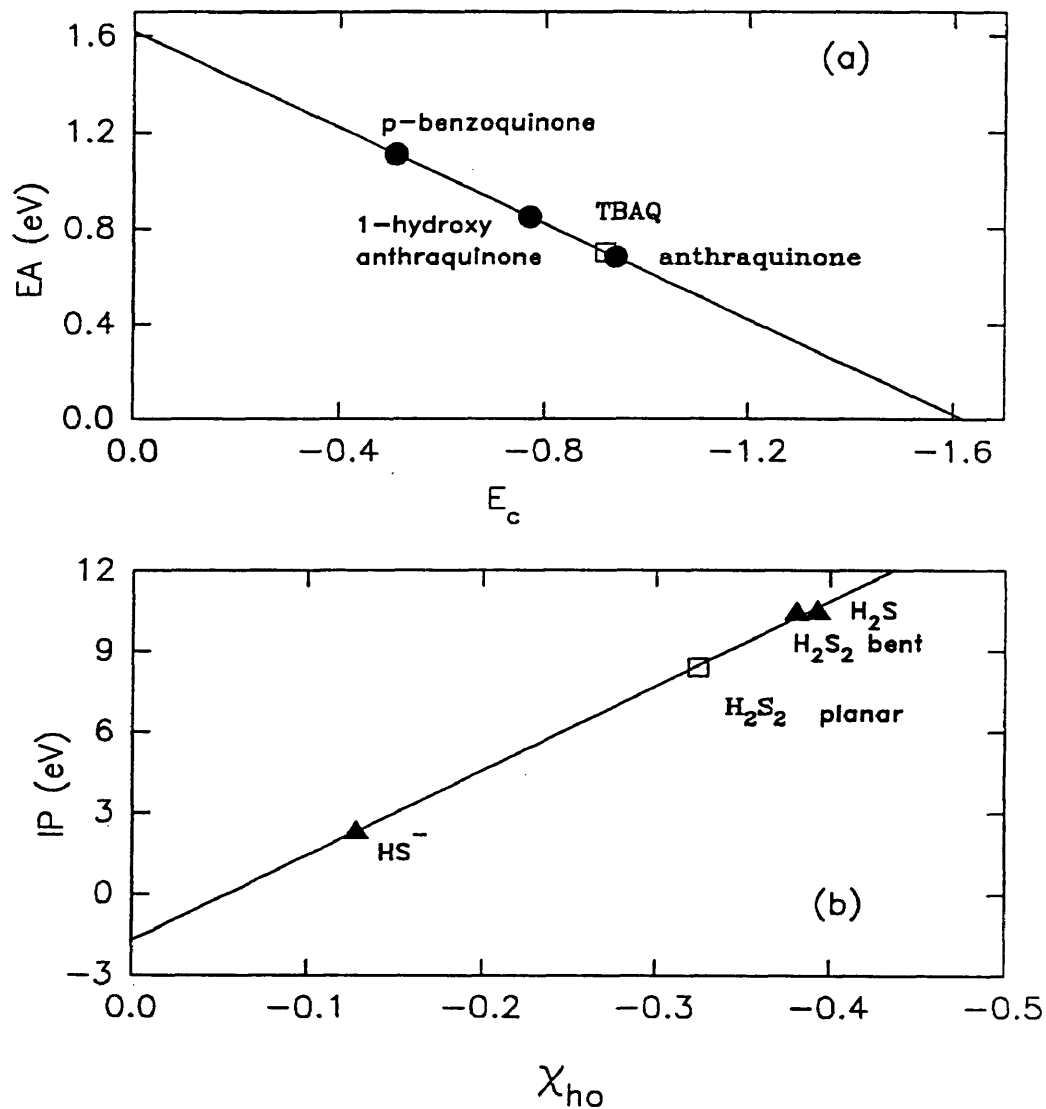


Figure 31. (a) Plot of electron affinity versus reduction potential of quinone; (b) plot of ionization potential versus the HOMO energies of electron donor agents.

Table 17 in appendix C shows the electron affinity of TBAQ in solution (EA'), and the calculated solvation energy (ΔE_{sol}). Using solvents such as NMP, DMAC and DMF, which have high polarity, the solvation energy is about 3.45 eV. This compares to ΔE_{sol} of 2.62 eV for anthracene in 75% dioxane solution (*Hedges, 1958*). Because of their greater polarity, the contribution of ΔE_{sol} for NMP, DMAC and DMF to the electron affinity of TBAQ is expected to be a larger value.

Electron affinity of TBAQ in either DMF, DMAC or NMP solvent is higher (4.15 eV) than the electron affinity of TBAQ in a vacuum (0.70 eV). This means that the energy level of the TBAQ LUMO is raised in these solvents. When the energy of the TBAQ LUMO is raised, then the energy separation between the electron acceptor LUMO of TBAQ and electron donor HOMO of agents such as H_2S or HS^- , will be smaller. The smaller energy gap of LUMO and HOMO increases the probability for electron transfer between TBAQ and the electron donor agent.

The electron affinity of TBAQ is higher in pyridine than in NMP, DMAC and DMF, even though pyridine is less polar than these solvents, probably because pyridine forms a charge-transfer complex with TBAQ. This charge-transfer complex, with pyridine acting as the electron donor, can raise the LUMO energy of TBAQ.

The electron affinity of TBAQ is increased slightly in tetrahydrofuran (THF). As a less polar solvent than pyridine, THF does not form a complex with TBAQ,

and the contribution of solvation energy in this solvent is not important. Hence, with a large HOMO and LUMO energy gap, tetrahydrofuran is not a favorable solvent for reaction between TBAQ and H_2S or HS^- .

The ionization potential can be correlated to the HOMO energy of the electron donor. **Tables 18 and 19 in appendix C** show the data (*Watanabe, 1957, Ansdell, 1962*) used for the plot of ionization potential (IP) in vacuum versus the energies of the HOMO of some electron donor agents. IP of H_2S_2 can be obtained by interpolation in this plot (**figure 31**).

Ionization potentials of H_2S (*Watanabe, 1957*) and H_2S_2 (**table 19, appendix C**) in a vacuum are still higher than the electron affinity of TBAQ in solution. The IP of electron donor agents in solution can not be calculated directly from the experimental data of oxidation potentials, since the solvation energy is unknown. The experimental data on NMR and UV/VIS spectrometry suggested that there is a charge-transfer complex between the solvent and the electron donor agents, such as H_2S , sulfanes (H_2S_x) and HS^- . These charge-transfer complexes can decrease the HOMO energies. The closer the energy gap between the electron affinity of TBAQ and the ionization potential of electron donor agents, the more probable the electron transfer.

From thermodynamic point of view, the probability of the electron transfer between electron donor agents and TBAQ can be determined using the Gibbs free energy (ΔG). The reduction potential of TBAQ (**table 16, appendix C**) and the

oxidation potential of HS^- (**table 19, appendix C**) are known from cyclic voltammetry data. The ΔG of the cell reaction can be calculated using the equation

$$\Delta G = - nFE_{\text{rxn}} \quad (5-44)$$

where n , F and E_{rxn} are the number of electrons transferred, Faraday constant and the cell potential respectively. From data in **tables 16 and 19 (appendix C)** the cell potential E_{rxn} is equal to + 0.55 V. It is known that reactions occur spontaneously when the ΔG of the reactions have negative values. Since E_{rxn} of TBAQ and HS^- is positive, then the reaction of TBAQ and electron donor HS^- occurs spontaneously because ΔG is negative via equation 5-44.

5.3 Ultraviolet and Visible Spectroscopy Analysis

A 219 ultraviolet-visible spectrometer by Varian was used to identify the charge transfer complexes of solvent-TBAQ and solvent-bisulfide anion.

5.3.1 Ultraviolet Spectra of TBAQ in Various Solvents

Since NMR spectra of the TBAQ aromatic protons show chemical shifts that are strongly solvent dependent, it has been suggested that a charge transfer complex forms between solvents NMP and DMAC and TBAQ. Ultraviolet spectra of TBAQ in various solvents was studied to detect this charge transfer complex.

The nonpolar solvents THF and isooctane have large ultraviolet windows,

transparent to 220 nm. Amide solvents such as NMP and DMAC show intense absorption below 260 nm.

The ultraviolet spectrum of TBAQ in either isooctane or THF showed two sharp peaks at 256 nm and 276 nm. There is also a shoulder at 265 nm and a weak, broad doublet at 320 nm and 330 nm. The ultraviolet spectrum of TBAQ in NMP or DMAC did not exhibit peaks below 300 nm, but the absorption at 320 - 330 nm appeared as a single peak at 327.5 nm.

The formation of charge transfer complex is usually identified by a drastic change in the uv/vis spectra. If the collapse of the doublet at 320 nm and 330 nm in the TBAQ spectrum into a singlet in polar DMAC and NMP solvents is the only evidence for a charge transfer complex, then this change is not very significant. Hence, the charge transfer complex may not be formed between TBAQ and DMAC and NMP solvents. However, a possibility is that the charge transfer complex absorption may be in the visible region and be so weak that it was undetected under the conditions of our experiments.

5.3.2 Identification of Charge Transfer Complex between Bisulfide Anion and Amide Solvents

Because mixing H_2S with NMP or DMAC solvent showed a strong color change, it has been suggested that a charge transfer complex forms between the amide solvents (NMP or DMAC) and H_2S . These color changes occurred rapidly,

therefore it is difficult to identify the solvent-H₂S complex. To duplicate the charge transfer complex between amide solvents and H₂S, bisulfide anion from sodium bisulfide was added into the solvents. The ultraviolet spectrum of sodium bisulfide in DMAC showed peaks at 422 nm and 270 nm. Since solutions of sodium bisulfide in amide solvents are blue in color, it was decided to investigate the long wavelength absorption near 600 nm as well as the 422 nm peak (see **table 20**).

Table 20. Long Wavelength Peak of Charge Transfer Complex between Bisulfide Anion and Amide Solvents

Solvent	Wavelength (nm) (maximum peak)	Peak Height Ratio (600 nm / 422 nm)
DMF	617	0.61
DMAC	618.5	0.78
NMP	620	7.4

The wavelength of the 422 nm peak was invariant with solvent type whereas the long wavelength peak showed variations. The long wavelength peak is surely the cause of the blue color in the solutions of amide solvents and sodium bisulfide. Possibly, it represents the existence of a charge transfer complex. Furthermore, the slight variation of the wavelength of the absorption maximum may measure the stability of the complex. The relative intensity of the long wavelength peak and the 422 nm peak showed some variation. This relative intensity variation is probably a measure of the complexed to uncomplexed bisulfide anion. The height peak

ratios of the two absorption peaks are included in the **table 20** .

These data would indicate that the charge transfer complex is more stable in NMP and least stable in DMF since the complexed bisulfide anion appears to be more abundant in NMP. The higher stability of charge transfer complex in NMP probably is due to higher polarity of NMP than DMAC and DMF. Meanwhile, The 600 nm absorption peak may be due to the promotion of an electron from the HOMO of the bisulfide anion to the LUMO of the solvent. This is consistent with the ease of production of the radical derived from bisulfide anion. These data indicate that the promotion of an electron is easiest from the NMP complex.

Chapter 6

CONCLUSIONS

6.1 Role of Solvents

The experimental data showed that solvent polarity is not the primary factor that affects the TBAQ conversion. The ability of the solvent to complex with H₂S and/or TBAQ and alter their respective HOMO and LUMO energy levels may be a requirement.

Tertiary amides, such as NMP and DMAC, appear to be better solvents for TBAQ reduction than secondary amides, cyclic ethers, alcohols, or lactones. The molecular shape of the solvent may also affect the interaction with hydrogen sulfide and TBAQ, as shown by the higher conversion rate in DMAC than in NMP.

From cyclic voltammetry results, it is suggested that solvent polarity can affect the reduction potential of TBAQ. The shifting of the TBAQ reduction potential to more positive value means that TBAQ is more easily reduced. The different values for the reduction potential of TBAQ can be considered as due to changes in solvation energy (ΔE_{sol}). Electron affinity of TBAQ in amide solvents, which is calculated from the reduction potential data, is higher (4.15 eV) than the electron affinity of TBAQ in a vacuum (0.70 eV). This means that the LUMO energy level of the TBAQ is altered in these solvents.

The experimental data on NMR and UV/VIS spectrometry suggested that there is a charge-transfer complex between the solvent and electron donor agents, such as H_2S and HS^- . These charge-transfer complexes decrease the HOMO energies of HS^- or HS_x^- and consequently decrease the ionization potential. The closer the energy gap between the electron affinity of TBAQ and the ionization potential of electron donor agents, the more probable the electron transfer.

6.2 Overall TBAQ Reduction Kinetics

TBAQ reduction rate is first order in H_2S and TBAQ concentration. When the total H_2S pressure is kept constant, the rate expression becomes a pseudo first order reaction with respect to the TBAQ concentration. The data fits a $\ln[\text{TBAQ}]$ versus time (t) plot typical of a first order reaction.

As is expected, the rate constant for TBAQ reduction increased with increasing H_2S pressure. However, the activation energies at different H_2S pressures are identical. Thus the activation energy for TBAQ conversion does not depend on the H_2S pressure as expected.

TBAQ conversion rate increased with increasing temperatures, and it reached maximum at about 60°C (333.1 K). The reaction temperature affects both the reaction rate constant and the hydrogen sulfide solubility. As the temperature increased, the hydrogen sulfide solubility constant decreased. Probably at temperatures above 60°C (333.1 K), the decreasing hydrogen sulfide solubility decreases

the reaction rate.

6.3 Overall Sulfur Formation Kinetics

The sulfur formation process can be represented as first order with respect to the sulfur atoms in solution. The effect of temperature on sulfur recovery appears to be small. The calculated activation energy for sulfur formation of 2.58 kcal/g-mole seems very low, it is much lower than the activation energy for the TBAQ conversion of 22.3 kcal/g-mole.

The sulfur formation is a complex reaction. A large variation in the kinetic data for the effect of H₂S pressure on sulfur formation was observed. At this point there is no correlation that can be made between the sulfur recovery data and the H₂S pressure.

6.4 Detailed Reaction Mechanisms

The mechanism of TBAQ reduction is best explained by the reduction of TBAQ to H₂TBAQ by a sequence of electron and proton transfer steps. The cyclic voltammetry data shows that TBAQ is readily reduced to TBAQ^{•-}. When there is a protic agent in the solution, the TBAQ^{•-} radical anion is rapidly protonated to form HTBAQ[•]. In a second electron transfer step, the HTBAQ[•] radical is reduced to form HTBAQ⁻ and subsequently protonated to form H₂TBAQ. These cyclic voltammetry results support the sequence of reactions in equations 5-8 to 5-11 and

equations 5-14 to 5-17.

It is suggested that TBAQ reduction and sulfur formation involve polysulfane intermediates. Longer chain sulfanes are likely to form complexes with amide solvents more readily than does H_2S , since sulfanes have higher acidity than H_2S .

During TBAQ reduction, the free radicals $\text{HS}\cdot$, $\text{HS}_x\cdot$ and/or $\text{HS}_y\cdot$ are probably generated. The chain growth to form polysulfanes occurs via termination of these free radicals. It is suggested that polysulfanes with sulfur chains greater than nine will decompose to form S_8 and H_2S or H_2S_x (5-19 and 5-20).

Chapter 7

RECOMMENDATIONS

Most of the objectives in this study have been completed. However, some fundamental questions about the reaction mechanism still remain unanswered. Based on the results in this study, the following areas need further investigation.

7.1 Role of HS^- and Solvents in TBAQ Reduction

The role of HS^- in initiating the TBAQ reduction process needs to be studied further. Is HS^- all that is required or must it be complexed with the amide solvent? It is suggested that TBAQ reduction is initiated by an electron donor such as the HS^- ions. Initially, HS^- ions are generated from the complex formed between H_2S and solvent. Although HS^- is consumed during the electron transfer step, it is regenerated during the protonation step (equations 5-8 to 5-11). The amide solvents play a critical role in generating the HS^- species. The possibility exist that other solvents may be successful in the TBAQ reduction as well. The solvents should exhibit the following properties; 1) the ability to complex with H_2S and generate HS^- ; 2) good H_2S and TBAQ solubility; and 3) high polarity.

It is recommended that HS^- in the form of NaHS be added along with H_2S to the TBAQ-amide solvent mixture to determine if reduction of TBAQ is possible.

The reaction should be repeated using solvents other than amides.

Based on the experimental data in which TBAQ failed to be reduced in γ -butyrolactone (GBL), it is recommended that polar oxygenated solvents, such as GBL, be studied further. The failure of TBAQ to be reduced in GBL solvent suggests that GBL is incapable of forming a complex with H_2S . It is predicted that GBL does not have the required resonance structure to make a complex with H_2S . If the HS^- can be independently generated in the TBAQ-GBL solvent mixture by addition of NaHS, TBAQ may be reduced in this mixture. Since GBL has high polarity, good TBAQ solubility and H_2S solubility, TBAQ conversion may be high.

7.2 Mechanism of Sulfane Formation

The mechanism of sulfur formation via polysulfane intermediates is still not clear. More work is required to identify the H_2S_2 and H_2S_3 species in solution and their respective rates of appearance and disappearance relative to the rate of TBAQ conversion. The peaks of H_2S_2 and H_2S_3 in NMR can be observed when no peaks of solvents appeared at the same region. Based on the peaks of sulfane in CS_2 reported by Hyne and Muller (*Hyne, Muller, 1966*), solvents selected should not have peaks at about 3 ppm.

The presence of H_2S_3 in the solution can also be monitored by IR and Raman spectroscopies. Muller and Hyne reported the vibrational spectra of H_2S_3 in CS_2 and CCl_4 solution (*Wieser, et al., 1969*).

7.3 Effect of Substituent on TBAQ Reduction Rate

The quinone reaction rate may be very sensitive to the relative HOMO and LUMO energy levels of the electron donor molecules (H_2S , HS^- , HS_x^-) and the electron acceptor molecules (TBAQ). The presence of electron withdrawing or donating substituents on the quinone ring may accelerate or hinder the reaction progress relative to TBAQ. The effect of these substituents on the reduction potential should be investigated by cyclic voltammetry (CV). The CV data should be correlated to the actual quinone reduction kinetics obtained in the mini-reactor.

REFERENCES CITED

- Ansdell, D.A., Page, F.M., 1962. *Trans. Faraday Soc.*, 58: 1084.
- Austen, D.E., Given, P.H., Ingram, J.E., Peover, M.E. 1958. "Electron Resonance
- Badoz-Lambling, J., Demange-Guerin, G., 1968. *Anal. Letter*, 2:123.
- Bard, A.J., Faulkner, L.R., 1980. Electrochemical Methods, John Wiley & Sons.
- Bloch, J., Huhn, F., Bugge, G., 1910. *J. Prakt. Chem.*, [2], 82:473.
- Bloch, J., Huhn, F., 1908. *Ber.*, 41.
- Brasted, R.C., 1961. Comprehensive Inorganic Chemistry, Vol.8, D.Van Nostrand Co. Inc..
- Burton, K.W.C., Machmer, P., 1968. Inorganic Sulfur Chemistry : Sulphanes, Ed: Nickloss, G., Elsevier.
- Cairns, T.L., Evans, G.L., Larchar, A.W., McKusick, B.C., 1952. "gem-Dithiols", *J.Am. Chem. Soc.*, 74:3982.
- Chambers, J.Q., 1974. The Chemistry of Quinonoid Compounds :Electrochemistry of Quinones, Ed: Patai, S., John Wiley & Sons.
- Conway, B.E., Rudd, E.J., 1974. Technique of Electroorganic Synthesis, Ed.: Weinberg, N.L., Chapter III, Vol.V, Part I, John Wiley & Sons.
- Eggs, B.R., Chambers, J.Q., 1970. "Proton effects in the Electrochemistry of the Quinone Hydroquinone System in Aprotic Solvents", *J. Electrochem. Soc.*, 117:186.
- E.G & G, Princeton Applied Research, Electrochemical instrument group, "Application Note: Cyclic Voltammetry", 4.
- Feher, F., Winkhaus, G., 1956. *Z. Anorg. Allgem. Chem.*, 288:123.
- Feher, F., Berthold, H. J., 1955. *Ber*, 88:1634.

- Feher, F., Berthold, R., 1957. *Z. Anorg. Allgem. Chem.*, 290:251.
- Finley, K.T., 1978. Encyclopedia of Chemical Technology : Quinones, Vol. 19., John Wiley & Sons.
- Foster, R., 1969. Organic Charge-transfer Complexes, Academic Press.
- Fry, A.J., 1989. Synthetic Organic Electrochemistry, 2nd.ed., John Wiley & Sons.
- Gary, Handwork, 1984. Petroleum Refining, Marcel Dekker.
- Given, P.H., Peover, M.E., 1960. "Polarographic Reduction of Aromatic Hydrocarbons and Carbonyl Compounds in Dimethylformamide in the Presence of Proton-donors", *J. Chem. Soc.*, 385.
- Gleicher, G.J., 1974. The Chemistry of Quinonoid Compounds : Theoretical and General Aspects, Ed: Patai, S., John Wiley & Sons.
- Grant, D., Van Wazer, J.R., 1964. "Exchange of Parts between Molecules at Equilibrium", *J. Am. Chem. Soc.* 86: 3012.
- Hayduk, W., Pahlevanzadeh, H., 1987. "The Solubility of Sulfur Dioxide and Hydrogen Sulfide in the associating Solvents", *Can. Chem. Eng.*, 65:299.
- Hedges, R.M., Matsen, F.A., 1958. "Antisymmetrized Huckel Orbital Calculations of Ionization Potential and Electron Affinities of Some Aromatic Hydrocarbons", *J. Chem. Phys.*, 28:950.
- Hojtink, G. J., Van Schooten, J., de Boor, E., Aalbersberg, W. Y., 1954. *Rec. Trav. Chim.*, 13:355
- Hyne, J. B., Derald, G., 1980. "Sulfur Deposition in Reservoirs and Production Equipment: Sources and Solution", Paper at the Annual Gas Conditioning Conference, Univ. Oklahoma, Norman, Oklahoma.
- Kohl, A.L., Riesenfeld, F.C., 1985. Gas Purification, 4th ed., Gulf Publishing Co.
- Koshy, V.J., Swayambunathan, V., Periasamy, N., 1980. "A Reversible Redox Couple in Quinone-Hydroquinone System in Nonaqueous Medium", *J. Electrochem. Soc.*, 127:2761.
- Lowry, T.H., Richardson, K.S., 1987. Mechanism and Theory in Organic Chemistry, 3rd ed., Harper & Row, Publishers, New York.

- Matsen, F.A., 1956. "Electron Affinities, Methyl Affinities, and Ionization Energies of Condensed Ring Aromatic Hydrocarbons", J. Chem. Physics, 24:602.
- Muller, E., Hyne, J.B., 1968. "Hydrogen Bonding in Sulfanes", Can. J. Chem., 46:3587.
- Murieta-Guevara, F., Rodriguez, A. T., 1984., Solubility of Carbon Dioxide, Hydrogen sulfide, and Methane in Pure and Mixed Solvents", J. Chem. Eng. Data, 29: 456.
- Papas, J. A., 1977., "Theoretical Studies of the Reactions of the Sulfur-Sulfur Bond", J. Am. Chem. Soc., 99:2926.
- Peover, M.E., 1961. "Electron Affinity of the Acceptor Molecule in Charge-Transfer Complexes", Nature, 191:702.
- Peover, M.E., 1962., "Electron Affinities of Quinones : Correlation of One-electron Redox Potentials with Quantum-mechanical Calculation", Nature, 193:475.
- Peover, M.E., 1962. "Reduction Potentials and Intermolecular Charge-transfer Spectra of Organic Acceptor Molecules", Part 1. Quinones, Faraday Soc. Trans., 58:1656.
- Peover, M.E., Davies, J.D., 1964. "Reduction Potentials and Intermolecular Charge-transfer Spectra of Organic Acceptor Molecules", Part 3. Solvent Effect on p-Benzoquinone, Faraday Soc. Trans., 60:476.
- Peover, M.E., 1967. Electroanalytical Chemistry : Electrochemistry of Aromatic Hydrocarbons and Related Substances, Ed: Bard, A.J., Vol. 2., Marcel Dekker, Inc..
- Peover, M.E., 1962. "A Polarographic Investigation into the Redox Behavior of Quinones", ****, *:4540.
- Plummer, M.A., 1987. "Gas Processing Developments : Sulfur and Hydrogen from H₂S", Hydrocarbon Proocessing, April:38.
- Plummer, M.A., 1990-5. Confidential Report to the Gas Research Institute, Fifth Quarter.
- Plummer, M.A., 1990-7. Confidential Report to the Gas Research Institute, Seventh Quarter.

- Plummer, M.A., 1991-9. Confidential Report to the Gas Research Institute, Ninth Quarter.
- Pryor, W.A., 1962. Mechanism of Sulfur Reactions, Ch.II, McGraw-Hill.
- Raymont, M.E.D., 1975. "Make Hydrogen from Hydrogen Sulfide", *Hydrocarbon Processing*, July:139.
- Sawyer, D.T., Roberts Jr., J.L., 1974. Experimental Electrochemistry for Chemist, John Wiley & Sons.
- Tani, T., Kikuchi, S., 1967. "Calculation of the Electronic Energy levels of Various Photographic Sensitizing and Desensitizing Dyes in Emulsions", *Photographic Science and Eng.*, 11:129.
- Tani, T., 1970. "Modified Electron Transfer Mechanism Spectral Sensitization IV", *Photographic Science and Eng.*, 14:72.
- Tomilov, E.P., et.al, 1972. Electrochemistry of Organic Compounds, Halsted Press.
- Vetter, K. J., 1967. Electrochemical Kinetics, Academic Press, New York, p 483.
- Wallace, T. J., 1963. "The Base-Catalyzed Oxidation of Mercaptans", *J. Org. Chem.*, 28: 1311.
- Watanabe, K., 1957. "Ionization Potential of Some Molecules", *J. Chem. Phys.*, 26:542.
- Wawzonek, S., Berkey, E., Blaha, E.W., Runner, M.E., 1956. "Polarographic Studies in Acetonitrile and Dimethylformamide", *J. Electrochem. Soc.*, 103:456.
- West, J.R., 1983. Encyclopedia of Chemical Technology : Sulfur Recovery, 3rd. 30ed., John Wiley & Sons.
- Wieser, H., Kruger, P.J., Muller, E., Hyne, J. B., 1969. "Vibrational Spectra and a Force Field for H₂S₃ and H₂S₄", *Canadian Journal of Chemistry*, 47:1633.
- Wiewiorowski, T.K., Touro, F.J., 1966. The Chemistry of Sulfides : The Sulfur-Hydrogen Sulfide System, Ed: Tobolsky, A.V., Interscience Pub..

APPENDIX A

Experimental Procedure for Cyclic Voltammetry

1. Components for Experiment

The components assembled for the cyclic voltammetry studies were obtained from Bioanalytical Systems (BAS) and Princeton Applied Research (PAR).

Electrochemical Cell (BAS)

Electrodes (BAS)

- platinum working electrode
- gold working electrode
- silver/silver nitrate reference electrode
- platinum wire counter electrode

Potentiostat (PAR Model 173)

Universal programmer (PAR Model 175)

X-Y Recorder (PAR)

2. Pretreatment for Platinum/Gold Working Electrode

When operating at a very positive potential, an oxide layer can form on the surface of the platinum or gold working electrode. The reduction of this oxide layer occurs at - 0.8 V with respect to a Ag\AgNO₃ reference electrode and can produce an undesirable signal during the cyclic voltammetric scan as the negative potential

is increased. To eliminate this signal, the platinum or gold working electrode was first immersed in a strong oxidizing solution (chromic acid solution) for 15 minutes to clean the electrode surface and then exposed negative potential of -2.0 V relative to the Ag/AgNO₃ reference electrode for 10 minutes to remove the oxide layer.

3. Potential Setting for Cyclic Voltammetry

- a. The potentiostat (Model 173) was turned on and allow it to warm up for about 15 minutes.

Instrument Settings for Poteniostat:

- Applied Potential/Current : off
- Ext.sig.input : on (right)
- Operating mode : control E
- Meter : potential (2 or 5)
- Ext. cell : off
- reset (Model 179) : 100 μ A

- b. The universal programmer (Model 175) was turned on.

Instrument Settings for Univeral Programmer:

- Settings for the scan potentials : (example for TBAQ in NMP solvent)

Initial Scan Direction : + or - (-)

Initial Potential A : V (-1.0 Volts)

Upper Potential B	: V	(+0.5 Volts)
Lower Potential C	: V	(-2.2 Volts)
Final Potential D	: V	(-1.0 Volts)
End of cycle	: B, C, or D	(D)
Final scan direction	: + or -	(+)

- Operating Mode : sweep
- Multipliers : pos slope (1)
: neg slope (1)
- Scan Rate : mV/sec (100)

* Note: If the tilt indicator lights up, then an unacceptable potential has been selected and the potential must be reset using valid values.

c. Turn on the recorder and attach chart paper to XY recorder:

- Set X Axis Rate : 1 V/in
- Y Axis Rate : 100 mV/in
- Select Chart Scale (in. or cm) : inches

d. A 2.0 millimolar sample of the solution (10 mL) to be studied and a small teflon coated magnetic stirbars were placed into the electrochemical cell. The cap containing the working, counter and reference electrodes was placed on top of the cell. The appropriate wires to the electrometer were attached. The electrometer wires were attached according to the following scheme:

red wire : counter electrode
green wire : working electrode
black wire : disconnected
electrode probe : reference electrode

The cell was placed into a water bath and the cell temperature kept constant using a hot plate attached to an Omega temperature controller.

- f. A 1/16" teflon tube was inserted into the solution and the solution was purged with an inert gas, such as helium, for 15-20 minutes. In these experiments 99.999% helium was prepurified by passing it through a Matheson Deoxy trap.
- g. After purging the solution, the teflon tube was moved to a position above the solution to prevent mixing at the electrode and the helium flow was maintained to prevent air (oxygen) contamination during the scan. The toggle switch on the potentiostat (Model 173) was moved to external cell position and about 1 minute allowed the system inside the cell to stabilize.
- i. The XY recorder power was turned on.
- j. The following settings were selected on the universal programmer (Model 175):
 - one cycle : light on
 - initial : light on
 - activate : light on

- k. Each time the scan rate or potential setting was changed, the external cell was turned off and the solution was stirred using the small teflon coated magnetic stirbar and a magnetic stirrer/hot plate.
- l. After completion of the analysis, the the external cell is turned off (Model 175) and the electrodes were disconnected from the wires. The procedure for removing the oxide layer from the working electrode was repeated.

Experimental Procedure for Micro and Minireactors

1. Preparation of Reaction Solution

- a. The desired solvent was placed into an erlenmeyer flask and weighed.
- b. The weight of quinone needed to make a 15 wt. % solution was calculated and this amount was dissolved in the solvent. This solution became the feedstock for the quinone reduction reaction. The NMR spectrum of the solution was recorded.
- c. The solution (about 30 mL) was placed into the glass minireactor.
- d. A small magnetic stirring bar was placed inside the reactor.
- e. The inlet and outlet valves to the stainless steel reactor manifold were turned off and the glass reactor vessel was attached to the reactor manifold.

2. Quinone Reduction Procedure

- a. The desired temperature setting for the water bath was entered into the digital temperature controller. The water bath was placed on to the hot plate.
- b. The hot plate magnetic stirrer was set to 3.0.
- c. The minireactor was placed in the water bath after the water had reached the desired reaction temperature.
- d. The solution was purged with nitrogen gas for 15 minutes by opening both reactor inlet and outlet valves to remove oxygen which would oxidize hydroquinone.
- e. The solution was purged with hydrogen sulfide for 3 minutes at 15.2 psia to remove residual nitrogen.
- f. After purging with hydrogen sulfide, the reactor outlet line was turned off and the hydrogen sulfide pressure increased to the desired value.
- g. Immediately upon reaching the desired reaction pressure a stopwatch was activated to record the reaction time.
- h. Samples were collected for analysis by opening the valve to the sample syphon tube. After a volume of solution equivalent to the volume of the syphon tube assembly (approximately 1 mL) was removed and discarded, a 1 mL sample was collected in an NMR tube. The samples were collected at 30, 45 and 60 minutes into the reaction.

- i. The samples were analyzed immediately by a Varian EM390 90 MHz NMR.
- j. The following information was recored in the laboratory notebook.
 - reactor temperature and hydrogen sulfide pressure
 - time of sample collection
 - observation of color changes during the reaction and corresponding time
 - time of temperature or pressure changes during experiment
 - time of appearance of sulfur precipitate

3. Sulfur Precipitation Procedure

- a. While the reactor was still in the water bath, the hydrogen sulfide pressure was gradually lowered to 22.2 psia by venting the gas through a train of caustic scrubbers containing 1.0 molar sodium hydroxide.
- b. The glass three-way valve to the scrubbers was turned off to prevent any of the caustic scrubbing solution from entering the reactor.
- c. The reactor outlet line was turned off, the hot water bath was replaced with an ice bath, and the solution was stirred using the magnetic stirring bar.
- d. After 45 minutes under hydrogen sulfide pressure, the reactor was purged with nitrogen gas for 15 minutes at 15.2 psia.
- e. A sample of the solution was collected and it's NMR spectrum recorded.
- f. The reaction mixture was filtered using a 10 μ Milipore filter to collect the

precipitated sulfur, and the filtrate was purged with nitrogen for 10 minutes to remove residual hydrogen sulfide.

- g. The filtered sulfur was washed three times with 25 mL of acetone, dried in air and weighed.
- h. The filtrate was kept under nitrogen overnight. The NMR spectrum of the filtrate was recorded. Additional sulfur was removed by filtration, then washed, dried and weighed.

Experimental Procedure for NMR Reactor

1. Reactor System

a. Reactor Components:

- 1. Gas Reservoir made from 1/2" stainless steel tubing
- 2. Pressure Gauge
- 3. 1/4" Manifold made from 1/4" stainless steel tubing and an VCR fitting containing viton O-rings for attachment of the NMR tube.
- 4. Hydrogen Sulfide Gas Scrubbers
- 5. Thick Walled NMR Tubes
- 6. Liquid Nitrogen Bath

b. Volume of system components:

- total reactor volume = 51.2 mL

- gas reservoir volume = 36.1 mL
- NMR tube and manifold volume = 3.2 ml

2. Solution Preparation :

- a. A 15 wt. % solution of TBAQ in solvent was prepared as the reaction mixture.
- b. The reaction mixture was placed into the NMR tube. Approximately 0.36 mL for medium walled tube (0.77 mm) and 0.095 for thick walled tubes (1.4 mm).

3. Operating Procedure :

- a. The entire reactor volume was evacuated to approximately 10^{-3} torr.
- b. The outlet valve to the gas reservoir was closed and the reservoir was filled with hydrogen sulfide or carbon dioxide gas at 18.2 psia.
- c. The NMR tube was attached to the reactor via the VCR O-ring fitting and evacuated to remove air.
- d. The valve to the vacuum pump was closed and the NMR tube was placed into Dewar flask containing liquid nitrogen.
- e. The valve to the gas reservoir was opened and hydrogen sulfide or carbon dioxide (18.2 psia) was expanded into the evacuated manifold and NMR tube until the pressure of the entire system, including the reservoir, reaches

16.9 or 16.3 psia. The gas reservoir volume and pressure change is recorded.

- f. The NMR tube was removed from the reactor manifold and sealed using a oxygen/methane flame.
- g. An explosion shield was placed in front of the reactor system. The NMR tube was removed from the liquid nitrogen bath placed into a ceramic bowl and allowed to reach room temperature. The final hydrogen sulfide pressure inside the NMR tube at 36°C (NMR probe temperature) was calculated to be 72.2 and 52.2 psia, respectively prior to any H₂S absorption into the solution.

APPENDIX B

Table 2. TBAQ Solubility in Various Solvents

Solvent	Dielectric Constant	Dipole moment (Debye)	TBAQ Saturated ^a Solubility
N-methyl-2-pyrrolidinone (NMP)	32.2	4.09	26.8
Gamma-butyrolactone (GBL)	39	4.12	12.1
N,N-dimethylacetamide (DMAC)	37.8	3.71	24.8
2-pyrrolidinone (PN)	32.2	3.55	8.8
N-methylacetamide (MAC)	191.3	4.27	14.4
tetrahydrofuran (THF)	7.6	1.75	47
dimethylformamide (DMF)	36.7	3.24	15
ethylenediamine (EDM)	12.9	1.90	small
pyridine (PY)	12.9	2.37	37.5
2-nitropropane (2NP)	25.5	3.73	18
ethylacetate (EA)	6.05	1.82	20
acetonitrile (AN)	35.9	3.53	10
3-pentanone (3PN)	17.0	2.82	20

Table 2. (continued)

Solvent	Dielectric Constant	Dipole moment (Debye)	TBAQ Saturated ^a Solubility
N-methylpyrrolidine (NMPY)		2.0	34.3
4-hydroxy-4-methyl-2-pentanone (HMP)	18.2	3.24	10.1
4-methyl-2-pentanol (MPL)		1.7	small

Note : a) at 21 °C (294.1 K)

Table 3. Effect of H₂S Pressure on TBAQ Conversion and Sulfur Recovery

Experiment I.D. Number (Reaction Temperature)	Rxn.time (min.)	mole % H ₂ TBAQ	H ₂ S Press. (psia)	H ₂ TBAQ rate const. (k) ^a	% Sulfur Recovery ^b (at 60 minutes)
DMACTBAQ-M14 (50 °C)	30	39.2	92.2	2.145	76.97
	45	64.6			
	60	79.2			
DMACTBAQ-M15 (50 °C)	30	27.7	52.2	1.125	76.35
	45	41.5			
	60	58.8			
DMACTBAQ-M16 (50 °C)	30	15.9	32.2	0.757	72.89
	45	26.4			
	60	42.4			
DMACTBAQ-M11 (50 °C)	30	17.3	32.2	0.693	58.57
	45	23.9			
	60	41.5			
DMACTBAQ-M12 (50 °C)	30	16.7	32.2	0.745	78.29
	45	27.8			
	60	42.6			
DMACTBAQ-M13 (50 °C)	30	16.4	32.2	0.755	60.68
	45	29.1			
	60	42.7			
DMACTBAQ-M5 (50 °C)	30	32.8	92.2	1.758	
	45	52.1			
	60	72.1			
DMAMCTBAQ-M6 (50 °C)	30	20.98	52.2	0.915	
	45	33.79			
	60	50.00			
DMACTBAQ-M7 (50 °C)	30	17.5	32.2	0.647	
	45	31.56			
	60	40.29			

Table 3. (continued)

Experiment I.D. Number (Reaction Temperature)	Rxn.time (min.)	mole % H ₂ TBAQ	H ₂ S Press. (psia)	H ₂ TBAQ rate const. (k) ^a	% Sulfur Recovery ^b (at 60 minutes)
DMACTBAQ-M8 (50 °C)	30	35.55	92.2	1.983	94.54
	45	58.74			
	60	76.09			
DMACTBAQ-M2 (50 °C)	30	17.9	32.2	0.750	
	45	31.57			
	60	43.6			
DMACTBAQ-M3 (50 °C)	30	17.74	52.2	1.290	
	45	46.15			
	60	62.08			
	89	77.27			
DMACTBAQ-M4 (50° C)	30	31.91	92.2	1.935	
	45	50.81			
	60	74.12			
DMACTBAQ-M22 (50°C)	30	26.7	52.2	0.971	87.02
	45	41.5			
	60	54.9			
NMPTBAQ-M25 (50°C)	30	17.9	92.2	0.578	94.91
	45	26.75			
	60	38.50			
NMPTBAQ-M26 (50°C)	30	22.6	52.2	0.307	47.08
	45	25.4			
	60	33.6			
NMPTBAQ-M27 (50°C)	30	14.8	32.2	0.193	91.66
	45	20.5			
	60	22.1			

Note:

#-M : Minireactor

a) Rate constant (k) = (hour)⁻¹

b) Precipitation Condition

DMACTBAQ-M12,14-16,22 : H₂S Press.= 22.2 psia; Temp.= 0 °C
Time : 45 minutes

DMACTBAQ-M11,13 : H₂S Press.=32.2; 17.2 psia
Temp.= 25 °C; Time : 45 minutes

DMACTBAQ-M2-8 : H₂S Press.= 17 psia; Temp.= 0°C;
Time = 18 minutes

NMPTBAQ-M25-27 : H₂S Press.= 22.2 psia; Temp. = 0 °C
Time : 45 minutes

**Table 4. Effect of Temperature on
TBAQ Conversion and Sulfur Recovery**

Experiment I.D. Number (H ₂ S press.)	Rxn. time ^c (min.)	mole % H ₂ TBAQ	Temp. of rxn (°C)	H ₂ TBAQ rate ^a constant (k)	% S ₈ recovery ^b 60 min.
DMACTBAQ-M18 (52.2 psia)	30	13.8	40	0.360	45.29
	45	19.3			
	60	28.0			
DMACTBAQ-M15 (52.2 psia)	30	27.7	50	1.125	76.35
	45	41.5			
	60	58.8			
DMACTBAQ-M19 (52.2 psia)	30	42.2	60	1.373	78.16
	45	62.2			
	60	70.9			
DMACTBAQ-M20 (52.2 psia)	30	56.6	70	0.308	83.43
	45	61.6			
	60	62.8			
DMACTBAQ-M21 (52.2 psia)	30	17.5	40	0.283 (1.106)	70.14
	45	23.0			
	60	28.4			
	(120)	(76.3)			
DMACTBAQ-M22 (52.2 psia)	30	26.7	50	0.971 (0.203)	87.02
	45	41.5			
	60	54.9			
	(120)	(63.2)			
DMACTBAQ-M23 (52.2 psia)	30	45.2	60	1.416 (0.536)	81.60
	45	63.9			
	60	73.0			
	(120)	(84.2)			

Table 4. (continued)

Experiment I.D. Number (H ₂ S press.)	Rxn. time ^c (min.)	mole % H ₂ TBAQ	temp. of rxn (°C)	H ₂ TBAQ rate ^a constant (k)	% S recovery ^b 60 min.
DMACTBAQ-M24 (52.2 psia)	30	57.0	70	0.301 (0.338)	91.10
	45	59.7			
	60	63.0			
	(120)	(73.6)			
DMACTBAQ-M29 (52.2 psia)	30	43.6	60	1.488 (0.909)	
	45	63.8			
	60	73.2			
	(120)	(89.2)			
DMACTBAQ-M9 (92.2 psia)	30	24.1	40	0.662	85.32
	45	32.9			
	60	45.5			
DMACTBAQ-M5 (92.2 psia)	30	32.8	50	1.758	115.23
	45	52.1			
	60	72.1			
DMACTBAQ-M10 (92.2 psia)	30	43.6	60	1.865	69.66
	45	67.0			
	60	77.8			
DMACTBAQ-Mc10 (15.2 psia)	60	12.4	40	0.230	
	120	24.0			
	180	44.7			
DMACTBAQ-Mc7 (15.2 psia)	60	21.8	50	0.368	59.05
	120	50.5			
	180	62.5			
DMACTBAQ-Mc9 (15.2 psia)	60	26.8	57	0.381	
	120	58.3			
	180	65.9			

Note :

a) Rate constant (k) = (hour)⁻¹

b) Precipitation Condition :

DMACTBAQ-M14-29 : H₂S Press.= 22.2 psia; Temp.= 0 °C

N₂ press. = 15.2 psia; Time = 45 minutes

DMACTBAQ-M11-13 : H₂S Press.=32.2; 22.2; 17.2 psia;

N₂ press.= 15.2 psia; Temp.= 25 °C; Time = 45 minutes

DMACTBAQ-M5-10 ; H₂S Press.= 17 psia; Temp.= 0°C;

N₂ press.= 15.2 psia; Time = 18 minutes

DMACTBAQ-Mc7,9,10 : N₂ pressure = 13.2 psia; Temp.= 25 °C

Time = 48 hours

Calculation based on TBAQ conversion at 60 minutes

c) Numbers in parentheses are mole % H₂TBAQ after sulfur precipitation and filtration and TBAQ rate constant during sulfur precipitation at 0 °C respectively.

**Table 5. Effect of Temperature on Sulfur Recovery
at 52.2 psia H₂S Pressure**

Experiment I.D. Number	Reaction Temperature (°C)	Sulfur (S _g) Recovery (mole %) at 60 minutes	Sulfur (S _g) Recovery Rate Constant (hr ⁻¹)
DMACTBAQ-M15	50	76.35	1.442
DMACTBAQ-M21	40	70.14	1.209
DMACTBAQ-M22	50	87.02	2.042
DMACTBAQ-M23	60	81.60	1.693
DMACTBAQ-M24	70	91.10	2.419
DMACTBAQ-M18	40	45.29	0.603
DMACTBAQ-M19	60	78.16	1.521
DMACTBAQ-M20	70	83.43	1.797

Note : Rate constant of sulfur recovery is calculated using equation:

$$\text{rate} = - d[S]/dt = k [S]$$

where [S] is the sulfur concentration in the solution

Precipitation Condition :

H₂S Pressure = 22.2 psia , Time = 45 minutes

N₂ (Purge) Pressure = 15.2 psia, Time = 15 minutes

Temperature = 0 °C

**Table 6. Effect of H₂S Pressure on Sulfur Recovery
in DMAC at 50°C**

Experiment I.D number	H ₂ S Pressure (psia)	% Sulfur Precipitation at 60 minutes
DMACTBAC-Mc7	15.2	59.05
DMACTBAQ-M12	32.2	78.29
DMACTBAQ-M14	92.2	76.97
DMACTBAQ-M15	52.2	76.35
DMACTBAQ-M16	32.2	72.89
DMACTBAQ-M22	52.2	87.02
DMACTBAQ-M8	92.2	94.54
DMACTBAQ-M11	32.2	58.57
DMACTBAQ-M13	32.2	60.68

Table 7. Effect of Solvent on TBAQ Conversion

Solvent [Experiment I.D. Number]	Dipole moment (Debye)	Rxn. time (hr.)	TBAQ Conv. (mole%)
N-methyl-2-pyrrolidinone [NMPTBAQ Mc02] TBAQ Conc.=25 % (w.f)	4.09	1.0	28.64
		2.0	28.95
		3.0	43.92
		4.0	52.94
		6.0	64.95
		42	90.05
N,N-dimethylacetamide [DMACTBAQ Mc03] TBAQ conc.=15 %(w.f)	3.71	1.1	16.34
		2.0	48.46
		3.0	62.5
		5.3	72.94
		6.3	74.54
		42	90.38
Gamma-butyrolactone [GBLTBAQ Mc04] TBAQ conc.=10 %(w.f)	4.12	1.0	0
		2.0	0
		3.0	0
		4.0	0
2-pyrrolidine [PNTBAQ Mc 05] TBAQ conc.= 7.9 % (w.f)	3.55	1.0	?
		2.5	?
		3.5	small
		4.5	small
		5.5	small
N-methylacetamide [MACTBAQ Mc06] TBAQ conc.=11.5 % (w.f)	4.27	1.0	small
		2.0	>10.0
		3.0	29.8
		4.0	35.3
		5.0	36.6
N-methylpyrrolidine [NMPYTBAQ Mc 11] TBAQ conc.= 14.5 % (w.f)	2.0	0.3	?
		1.0	?
		3.0	?

Table 7. (continued)

Solvent [Experiment I.D. Number]	Dipole moment (Debye)	Rxn. time (hr.)	TBAQ Conv. (mole%)
N,N-dimethylacetamide + Thiophenol (as H ₂ S substitute) [DMACTHP Mc12] TBAQ conc.=21.9%(wt)	3.71	0.05 2.0 3.0	no rxn
Methanol+ THF (1:1) mole [METTHF-M28] TBAQ conc. = 15 %(wt)	2.87	0.5 0.75 1.0	no rxn

Note:

a) at 57 °C (330.1 K) and H₂S pressure of 13.2 psia

b) at 21 °C (294.1 K) and N₂ pressure of 13.2 psia

* wt = weight basis

** Reaction temperature = 57°C; H₂S pressure = 13.2 psia

APPENDIX C

Table 8 Cyclic Voltammetry Data of Solvents

Group	Solvent	moment dipole (Debye)	dielectric constant	TBAQ solubility ^c	Pot.(V) /NaClO ₄ ^a	Pot.(V) /TBAP ^b
t-amide	N-methyl pyrrolidinone (NMP)	4.09	32.2	26.8	0 → -1.8	+0.5 → -1.5
t-amide	N,N-dimethylacetamide (DMAC)	3.71	37.78	24.8	-1.8 → 0. (*)	+2 → -1.0
t-amide	Dimethylformamide (DMF)	3.24	36.71	15	-.3 → -1.6	+8 → -2.0
s-amide	2-pyrrolidinone (PN)	3.55	?	8.8	+5 → -5	+8 → -0.5
t-amine	Pyridine (PY)	2.37	12.91	37.5	+5 → -1.0	+5 → -1.6
t-amine	Acetonitrile (AN)	3.53	35.95	10	+1. → -1.5	+9 → -8
t-amine	N-methyl pyrrolidine (n-MPY)	2.0	?	34.3	undiss.	undiss
alkoxy ketone	4-hydroxy-4 methyl-2 pentanone (HMP)	3.24	18.20	10.1	+5 → -1.3	0.5 → -1.5
ester	Ethylacetate (EA)	1.82	6.053	20	+1.5 → -1.0	1.0 → -1.3
ester (cyclic)	gamma butyrolactone (GBL)	4.12	39	12.1	-.5 → +.5 (*)	+5 → -.7

Table 8 (continued)

Group	Solvent	moment dipole (Debye)	dielectric constant	TBAQ solubility ^c	Pot.(V) /NaClO ₄ ^a	Pot.(V) /TBAP ^b
ether	tetrahydrofuran (THF)	1.75	7.58	47	+1.0 → 0.0	0 → 0.8(*)
ether	1,2-dimethoxyethane	1.71	7.20	-	-1.6 → +0.5(*)	0.6 → -1.8
ketone	3-pentanone	2.82	17.00	20	+1. → 0.	0 → 0.7(*)
nitro	2-nitropropane(2NP)	3.73	?	18	undiss	.9 → -0.3

Note: All measurement in cyclic voltammetry use negative scan direction except (*) use positive scan direction
a) using NaClO₄ as the electrolyte
b) using tetrabutylammoniumperchlorate (TBAP) as the electrolyte
c) Solubility in mol fraction at 21°C
d) Potential is measured versus Ag/AgNO₃ reference electrode
e) Ag/AgNO₃ reference electrode is +0.426 versus Saturated Calomel Electrode (SCE)

**Table 9 . Effect of Polarity of Solvent
on Reduction/Oxidation Peaks of TBAQ.**

Quinone	solvent/di pole moment	diel. const	Red.peak (Volt)		Oxidat. peak (Volt)	
			R1	R2	O1	O2
TBAQ	NMP/ 4.09	32.2	-0.92	-1.72	none	-0.82
	DMF/ 3.24	36.71	-0.92	-1.72	-1.52	-0.85
	PY/ 2.37	12.91	-0.89	-1.41	-1.52	-0.79
	DMAC/ 3.71	37.78	-0.92	-1.72	none	-0.83
	p-Xyle- ne 0.0	2.70	none	none	none	none
	dioxane 0.45	2.21	none	none	none	none
	THF/ 1.75	7.58	-1.12	none	none
	THF/NMP (50:50) ^a	20.0	-0.92	none
	NMP/PY ^b (50:50)	22.55	-0.99	-1.59	-1.44	-0.87

Note :

NMP : N-methyl-2-pyrrolidinone

DMF : N,N-dimethylformamide

PY : Pyridine

DMAC : N,N-dimethylacetamide

THF : Tetrahydrofuran

DME : N-dimethoxyethane

a) mixture of NMP and THF in 50/50 mol ratio

b) mixture of NMP and PY in 50/50 mol ratio

* dipole moment in Debye

* potential is measured versus Saturated Calomel Electrode

**Table 10. Potential Proton Donor for Use in
Cyclic Voltammetry Studies**

Potential Proton Donor (example)	Approximate pK_a
carboxyl acids (benzoic acid)	4-5 (4.2)
benzenethiol hydrogen sulfide	6.5 7.0
aromatic alcohol (phenol)	8-11 (9.99)
alkylthiol (ethanethiol)	10-11 (10.5)
water	15.7
alkylalcohol (butanol)	16 (16.0)

Table 11. Effect of Proton Donor on Cyclic Voltammetry of TBAQ-Solvent Mixture

mixture	scan mV/s	Reduction (Volt)		Oxidation (Volt)		
		R1	R2	O2	O1	NP
TBAQ-DMF +BU(xs)	100	-0.92 -0.92	-1.72 -1.70	-1.52 -1.37	-0.85 -0.85	none none
TBAQ-NMP +BU(xs)	100	-0.92 -0.92	-1.72 -1.62	none none	-0.82 -0.82	none none
TBAQ-PY +BU(xs)	100	-0.89 -0.89	-1.41 -1.37	-1.27 -1.25	-0.79 -0.79	none none
TBAQ-DMF +BA(1:1)* +BA(2:1)	100	-0.92 -0.89 -0.89	-1.72 -1.62 none	-1.52 none none	-0.85 -0.85 -0.81	none -0.22 NO/O3 -0.32 (NO)
TBAQ-NMP +BA(1:1) +BA(2:1)	100	-0.92 -0.92 -0.92	-1.72 -1.69 ** -1.69 **	none -1.42 *** -1.42 ***	-0.82 -0.82 -0.82	none none -0.27 NO/O3
TBAQ-PY +BA(1:1) +BA(2:1)	100	-0.89 -0.89 -0.89	-1.41 -1.42 ** -1.42 ***	-1.27 -1.29 none	-0.79 -0.79 none	none -0.27 NO/O3 -0.27 NO/O3
TBAQ- DMAC +BA (2:1) +BA (4:1)	100	-0.89 -0.92 -0.92	-1.62 (@) (@)	none none none	-0.85 none none	none -0.02 (NO) -0.07 (NO)

Table 11 (continued)

mixture	scan mV/s	Reduction (Volt)		Oxidation (Volt)		
		R1	R2	O2	O1	NP
TBAQ- DMAC +PH (2:1) +PH (4:1)	100	-0.92 -0.92 -0.92	-1.62 -1.59 none	none none none	-0.83 -0.83 -0.83	none none none
TBAQ-DMF +PH (2:1) +PH (4:1) +PH (6:1)	100	-0.92 -0.92 -0.92 -0.92	-1.72 -1.67 -1.67 none	-1.52 none none none	-0.85 -0.85 -0.85 -0.85	none none none none
TBAQ-DMF +BT (9.7 :1) +BT(19.4:1) +BT(29.1:1)	100	-0.89 -0.87 -0.87 none	-1.57 -1.53 none none	-1.50 none none none	-0.85 -0.83 none none	none +0.88 (NO) -0.57 (NR) +0.98 (NO) -0.59 -1.35 -1.77 (NR) -0.62 (NR)

Table 11. (continued)

Note :

Electrolyte : tetra butyl ammonium perchlorate (TBAP)
Potential is measured versus SCE
Reference electrode :
Ag/AgNO₃ (0.1M)/TBAP(0.1M)/NMP = + 0.426 V vs SCE
TBAQ concentration : 2mM in solvent(TBAP 0.1M)

TBAQ: t-butyl anthraquinone
NMP : N-Methyl pyrrolidinone
DMF : dimethyl formamide
PY : Pyridine
BA : Benzoic acid
BU : Butanol
PH : Phenol

* : molar ratio
** : shoulder peak
*** : wide and small peak
@ : peak from donor proton
R1 : first reduction peak
R2 : second reduction peak
O1 : first oxidation peak
O2 : second oxidation peak
NP : New Peaks
NO : New Oxidation Peak
NR : New Reduction Peak
mV/s : milivolts/seconds

**Table 12. Oxidation and Reduction of TBAQ in DMAC
in the Presence of Benzoic Acid (BA) as Proton Donor**

mixture	Reduction peaks (Volt)			Oxidation peaks (Volt)		
	R1	R2	R3	O1	O3	O4
BA	-1.31			-0.66		
TBAQ	-0.93	-1.57		-0.834		
+BA 2:1	-0.92	disapp.	-1.32	disapp.	-0.01	
+BA 4:1	-0.89	disapp.	-1.32	disapp.	-0.01	-0.61
+BA 6:1	-0.86	disapp.	-1.28	disapp.	-0.12	-0.63
	Current (μ Amps.)			Current (μ Amps.)		
TBAQ	12.09	6.64		9.37		
+BA 2:1	16.86		1.05		2.80	
+BA 4:1	17.62		3.71		2.74	2.09
+BA 6:1	18.58		4.30		2.32	3.43

Note :

Concentration of TBAQ = 2mM; electrolyte TBAP = 0.1 M;

TBAP = tetrabutylammoniumperchlorate;

scan rate = 0.1 Volts/sec.

BA = Benzoic acid

Potential is measured versus SCE

**Table 13. Oxidation and Reduction of TBAQ in DMF Solvent
in the Presence of Benzoic Acid (BA) as Proton Donor**

	Reduction peaks (Volt)			Oxidation peaks (Volt)		
	R1	R2	R3	O1	O2	O3
BA	-1.12			-0.80		
TBAQ	-0.94	-1.74		-0.86	-1.50	
+BA 1:1	-0.90	-1.66		-0.86	disapp.	-0.19
+BA 2:1	-0.90	disapp.	should.	-0.82	disapp.	-0.31
+BA 4:1	-0.90	disapp.	-1.18	-0.79	disapp.	-0.35
	Current (μ Amps.)			Current (μ Amps.)		
TBAQ	10.61	6.94		10.56	4.06	
+BA 1:1	14.21	1.78		6.46		2.38
+BA 2:1	20.01			9.25		5.16
+BA 4:1	22.26		3.47	15.50		6.21

Note :

Concentration of TBAQ = 2mM; electrolyte TBAP = 0.1 M;

TBAP = tetrabutylammoniumperchlorate

scan rate = 0.1 Volts/sec; temperature = 20 °C

TBAQ = t-butylanthraquinone

BA = benzoic acid

should. = shoulder peak

Potential is measured versus SCE

**Table 14. Oxidation and Reduction Potential of TBAQ
in DMF Solvent in the Presence of Benzoic Acid as Proton Donor
Added at the First and Second Reduction Potential**

	Reduction		Oxidation	
	potential (Volt)	current (μ Amps)	potential (Volt)	current (μ Amps)
TBAQ	R1=-0.91 R2=-1.54	R1=10.26 R2= 8.20	O1=-0.87 O2=-1.48	O1=9.87 O2=6.22
TBAQ + BA, addition at 2nd.red.pot -1st. cycle	R1=-0.88 R2=disapp.	R1=17.27 R2=disapp	O1=-0.67 O3=-0.00 O4= 0.60 O2=disapp.	O1=12.96 O3=2.17 O4=2.04 O2=disapp
-n cycle (eq.)	R1=-0.86	R1=18.08	O3=-0.01 O1,O4,O2= disapp.	O3=3.41
TBAQ	R1=-0.92	R1=9.69	O1=-0.85	O1=9.06
TBAQ+BA, addition at 1st.red.pot -1st.cycle	R1=-0.89	R1=14.09	O1=-0.84 O3=-0.13 O4=0.56 O5=0.44	O1=4.09 O3=2.05 O4=16.59 O5=shoul.
-n cycle (eq.)	R1=-0.91	R1=14.16	O1=-0.83 O3=-0.12 O4,O5=dis- appear	O1=4.65 O3=2.06

Table 14. (continued)

Note : BA = Benzoic acid

Concentration of TBAQ = 2mM; concentration of BA= 4mM;

electrolyte TBAP = 0.1M; TBAP = tetrabutylammoniumperchlorate

scan rate = 0.1 Volts/sec;

temperature = 20 °C

Potential is measured versus SCE

Table 15. Oxidation and Reduction Potential of TBAQ in DMF Solvent in the Presence of Benzenethiol as Proton Donor Added at the Second Reduction Potential

	Reduction		Oxidation	
	potential (Volt)	current (μ Amps)	potential (Volt)	current (μ Amps)
BT	R1=-0.64 R2=-1.59		O1=-0.01 O2=1.02	
TBAQ	R1=-0.92 R2=-1.59	R1=10.60 R2=8.09	O1=-0.85 O2=-1.50	O1=10.23 O2=7.40
+BT(1:1), addition at 2nd.red.pot - 1st.cycle	R1=-0.92 R2=-1.55 R5=should.	R1=16.96 R2=8.75	O1=-0.84 O4=-0.90 O3=0.05 O5=should. O2=disapp.	O1=small O4=12.85 O3=7.30
- n cycle (eq.)	R1=-0.89 R2=-1.53 R3=-1.38 R4=-0.64 R6=should.	R1=16.55 R2=11.15 R3=small R4=small	O1=-0.80 O3=-0.02 O4=0.97 O6=shoul. O5=disapp.	O1=small O3=7.01 O4=17.97

Note :

BT = Benzenethiol
 concentration of TBAQ = 2mM; concentration of BT = 2mM;
 concentration of electrolyte TBAP = 0.1M;
 TBAP = tetrabutylammoniumperchlorate
 scan rate = 0.1 Volt/sec; temperature = 20 °C
 Potential is measured versur SCE
 Ref. electrode = Ag/AgNO₃ = +0.426 V vs. SCE
 should. = shoulder peak

Table 16. Reduction Potential, Electron Affinity, and Solvation Energy of TBAQ

Solvent			Electron acceptor (TBAQ)			
Name	Dipole moment (Debye)	Dielectric constant	E_c (V)	(eV)		
				EA' ^a	EA_{calc}	ΔE_{sol} ^c
NMP	4.09	32.2	-0.92	4.15	0.70 ^b	3.45
DMAC	3.71	37.78	-0.92	4.15		3.45
DMF	3.29	36.71	-0.92	4.15		3.45
PY	2.37	12.91	-0.89	4.18		3.48
THF	1.75	7.58	-1.12	3.95		3.25

Note: a) EA' is calculated using equation (5-42)
 b) EA_{calc} is in vacuum (from figure 31)
 c) E_{sol} is calculated using equation (5-42)

Table 17. Reduction Potential and Electron Affinity of Quinones

Species	$E_{1/2} = E_c$ (V)	EA_{vac} (eV)
Anthraquinone	-0.94 ^b	0.68 ^b
p-benzoquinone	-0.51 ^b	1.11 ^b
1-hydroxyanthraquinone	-0.77 ^b	0.85 ^b
TBAQ	-0.92 ^c	0.70 ^a

Note: a) EA is from figure 31
 b) from Peover, M.E, Nature, 191, 702, 1961.
 c) from experimental data in table 19

Table 18. Oxidation Potential and Ionization Potential of HS⁻ as Electron Donor Agents

Solvent			HS ⁻	
Name	Dipole moment	Dielectric Constant	E _a =oxid.pot. ^a	IP _{cal} (eV) ^b
NMP	4.09	32.2		2.3
DMAC	3.71	37.78	-0.26	
DMF	3.29	36.71	-0.19	
PY	2.37	12.91		
THF	1.75	7.58		

Note :

- a) $E_a = IP + \Delta E_{sol} + \text{constant}$ (5-43)
 b) IP_{cal} in vacuum (Ansdell, Page, 1962)
 * Dipole moment in Debye

Table 19. Ionization Potential and the Highest Occupied Molecular Orbital Energies of Electron Donor Agents

Species	HOMO(χ_{ho}) eV	IP (vac) eV
H ₂ S	-0.3928	10.47 ^a
HS ⁻	-0.1279	2.30 ^b
H ₂ S ₂ (planar)	-0.3245	8.4
H ₂ S ₂ (bent, 90°)	-0.3808	10.13

Note : a) Watanabe, 1957
 b) Ansdell and Page, 1962